university of groningen

Synthetic Developments Towards BODIzy, a new Photolabile Protecting Group

Emmanuel Vrionakis

Stratingh Institute for Chemistry,

University of Groningen

1st Examiner: Prof. Dr. B.L. Feringa, Stratingh Institute for Chemistry

2nd Examiner: Prof. Dr. W.C. Szymanski, University Medical Centre Groningen

Daily supervisor: Dr. G. Alachouzos, Stratingh Institute for Chemistry

BSc. Research Project

Feringa Group

26-11-2021

Table of Contents

1. Abstract 4

2. Introduction 4

2.1 Development of the field of PPGs 5

2.2 Prominent classes of PPGs 6

2.3 Background and application of BODIPY derivatives 7

2.4 Photochemistry of BODIPY and BODIzy 8

2.5 Previous attempts from the group and new strategy for the synthesis of BODIzy 8

3. Results and discussion 10

3.1 Attempted synthetic route 1: Regioselective zincation 10

3.1.1 Protecting indazole at N1 using MOM group 11

3.1.2 Synthesis of $(TMP)_2Zn{\cdot}2MgCl_2{\cdot}2LiCl$ from commercial TMPMgCl·LiCl 12

3.1.3 Attempted zincation of MOM-indazole at C3 position 12

3.1.4 Attempted zincation and transmetalation of MOM-indazole 13

3.1.5 Synthesis $(TMP)_2Zn{\cdot}2MgCl_2{\cdot}2LiCl$ from TMP and iPrMgCl·LiCl 14

3.1.6 Attempted zincation and transmetalation of MOM-indazole with improved TMP_2Zn 14

3.1.7 Conclusion Strategy 1 14

3.2 Attempted synthetic route 2: Lithium/Halogen exchange and Turbo Grignard 15

3.2.1 Bromination of indazole using NBS 16

3.2.2 Attempted lithium/halogen exchange 3-bromoindazole and deuteration studies 17

3.2.3 Synthesis of *N*1-benzyl-3-bromoindazole 18

3.2.4 Attempted metalation of *N*1-benzyl-3-bromoindazole 19

3.2.5 Conclusion Strategy 2 20

3.3 Attempted synthetic route 3: Stepwise lithiation 20

3.3.1 Synthesis of 3-acetyl-2*H*-indazole via stepwise lithiation of 3-bromoindazole 22

3.3.2 Nucleophilic attack of phenyllithium on 3-acetyl-2*H*-indazole 23

3.3.3 Nucleophilic attack of lithiated indazole on 3-acetyl-2*H*-indazole 24

3.3.4 Conclusion Strategy 3 25

3.4 Attempted synthetic route 4: N2 SEM protection for Directed *ortho*-Metalation 25

3.4.1 N2 SEM protection of indazole 26

3.4.2 Lithiation and BzCl electrophile trapping of *N*2-SEM-indazole 27

3.4.3 Attempted one-pot synthesis of BODIzy dye 2 from *N*2-SEM-indazole 27

3.4.4 Nucleophilic attack of phenyllithium on *N*2-SEM-3-benzoyl indazole 28

3.4.5 Conclusion Strategy 4 28
4. Conclusion 28
5. Experimental Procedures 30
5.1 General remarks 30
5.2 Attempted synthetic route 1: Regioselective zincation 31
5.2.1 Synthesis of 1-(methoxymethyl)-indazole 31
5.2.2 Synthesis of $(TMP)_2Zn{\cdot}2MgCl_2{\cdot}2LiCl$ from commercial TMPMgCl·LiCl 31
5.2.3 Synthesis of CuCN·2LiCl 32
5.2.4 Attempted zincation, transmetalation and electrophile trapping of MOM-indazole 32
5.2.5 Synthesis of $(TMP)_2Zn{\cdot}2MgCl2{\cdot}2LiCl$ from TMP and iPrMgCl·LiCl 32
5.3 Attempted synthetic route 2: Lithium/Halogen exchange and Turbo Grignard 32
5.3.1 Synthesis of 3-bromoindazole through bromination of indazole using NBS 32
5.3.2 Attempted lithiation of 3-bromoindazole, deuteration studies 33
5.3.3 Attempted synthesis of *N1*-benzyl-3-bromoindazole 33
5.3.4 Synthesis of *N1*-benzyl-3-bromoindazole 33
5.3.5 Attempted lithiation of *N1*-benzyl-3-bromoindazole using butyllithium 33
5.3.6 Attempted magnesiation of *N1*-benzyl-3-bromoindazole using Turbo Grignard 33
5.4 Attempted synthetic route 3: Stepwise lithiation 34
5.4.1 Synthesis of 3-acetyl-2*H*-indazole via stepwise lithiation of 3-bromoindazole 34
5.4.2 Synthesis of 20 via nucleophilic attack of phenyllithium on 3-acetyl-2*H*-indazole 34
5.4.3 Nucleophilic attack of lithiated indazole on 3-acetyl-2*H*-indazole 34
5.5 Attempted synthetic route 4: N2 SEM protection for Directed *ortho*-Metalation 35
5.5.1 Synthesis of *N*2-SEM-indazole via SEM protection of indazole 35
5.5.2 Synthesis of 24 via lithiation and BzCl electrophile trapping of *N*2-SEM-indazole 35
5.5.3 Attempted one-pot synthesis of BODIzy dye 2 from *N*2-SEM-indazole 35
5.5.4 Attempted synthesis of 25 via nucleophilic attack of phenyllithium on *N*2-SEM-3-benzoyl-indazole 36
6. References 37
7. Appendix 42

Abstract

Photolabile protecting groups, or PPGs, can be bound to a substrate (the payload, PL) and cleaved from the PL by irradiating them with light of a specific wavelength. This is of great interest for applications in the body, such as the delivery of drugs, as drugs can be deactivated with a PPG, injected into the body, and be activated with high spatiotemporal control *only at the desired site*, greatly enhancing its efficacy. However, to be activated *through* tissue, PPGs need to absorb NIR light, which has good tissue penetration and does not show phototoxicity. The best performing PPGs are currently based on scaffolds that absorb around 500 nm, 200 nm shy of the NIR range. In the search for a new PPG scaffold that performs well as PPG and absorbs in the NIR without extensive derivation, computational analysis was done in our lab on derivatives of one of the current state-of-the-art PPG, BODIPY. This revealed a new PPG, BODIzy, which has been calculated to have $\Delta\lambda_{max}$ = +96 nm compared to the parent BODIPY chromophore. However, BODIzy has never been synthesized and as such, a synthetic route must be developed to confirm these calculations. Successful single addition of C3 metalated indazoles to model acid chloride electrophiles was achieved via a Directed *ortho*-Metalation (DoM) strategy and a stepwise lithiation strategy. Stepwise lithiation also showed a second addition to the electrophile, clearing the first and second hurdle towards the synthesis of BODIzy. These results pave the way towards obtaining and characterizing BODIzy, with the ultimate goal of providing a PPG scaffold that can be tailored to many different *in vivo* applications with simple derivatives.

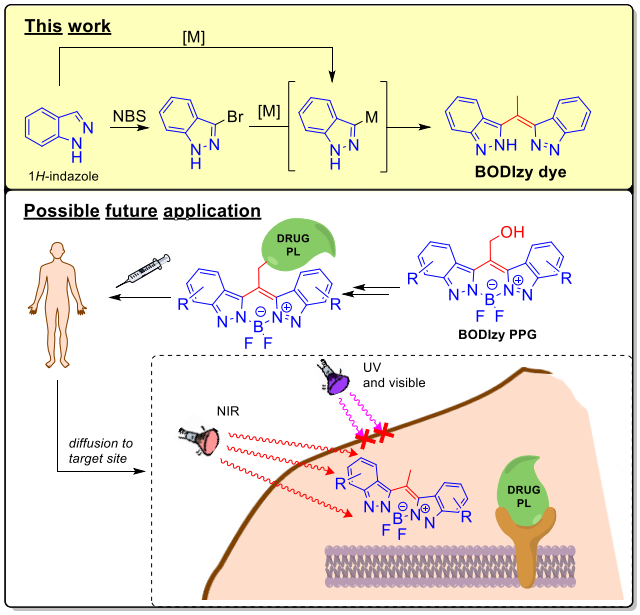

Figure 1: Summary of this work and possible future application.

1. Introduction

The field of photochemistry is of increasing importance for a plethora of applications in biological systems.[1,2] Light can be used to activate target molecules, providing high spatiotemporal control, down to millisecond and submicron resolutions.[3] Possible benefits of applying this technology to local drug activation pharmacology are decreased side effects and potentially significantly improving a drugs therapeutic index.[1,4] A prominent category of such biological photoresponsive tools are photocages, also known as photolabile protecting groups (PPGs). While PGGs are often referred to as “photocages”, it could be considered more akin to locking a molecule using a padlock (the PPG) and unlocking it using a key (light of a wavelength specific to the PPG). When bioactive molecules are bound to a PPG, they are rendered inactive, or “caged”. Upon irradiation with light of the appropriate wavelength, the bond between the molecule and the PPG irreversibly cleaves, restoring the activity of the molecule, “uncaging” it.

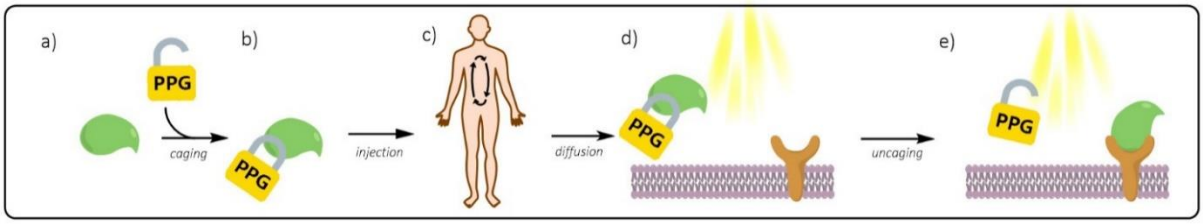

Figure 2: A diagram schematically showing the use of a photocage. a) an uncaged bioactive molecule, b) the molecule is caged by a PPG, c) the inactive molecule is injected into the body and diffuses to the target site d) at the target site the molecule is irradiated with light of the appropriate wavelength, initiating photocleavage, e) the molecule is uncaged, and its bioactivity is restored, it reacts only at the target site.

Biological photoresponsive tools such as PPGs offer high orthogonality to biological processes, making it ideal means for externally controlling biological systems.[5] While biological applications of PPGs such as drug delivery are the focus of this thesis, they also show promise in other fields like DNA chip technology [6], polymer science [7] and synthetic organic chemistry. [8–10] Initially, one might have the impression PPGs are inferior versions of photoswitches, which can *reversibly* undergo photoisomerization to change a molecules' chemical and/or biological properties. However, structural changes following the cleavage of a PPG are generally notably more significant, making PPGs a better fit for many purposes.[11] Specific to our purposes, rendering a molecule virtually completely biologically inactive is an example of something that requires such significant structural changes, and is quite challenging to do with photoswitches.[12]

1.1 Development of the field of PPGs

Photolabile protecting groups have been around for a long time, starting with a publication by Barltrop and Schofield in 1962, covering the liberation of glycine after irradiating benzyloxycarbonylglycine with UV light.[13,14] Towards the end of the 1970's, Kaplan and Engels published papers researching *in situ* photolytic release of bioactive compounds and introduced the term "caging", from which point the field has continued to grow.[14–16] In recent years the field has received much attention. Interesting developments include the design of orthogonal systems with multiple functional levels,[11] two photon absorption PPGs,[17] organelle-targeted PPGs, [18] and much more.[1,9,19,20] Additionally, requirements and desirable properties were composed, particularly for biological applications, most importantly: [9]

1. A PPG requires good absorption in the NIR region, between 650 nm and 950 nm.[21] Lower wavelength photon possesses three considerable downsides. Firstly, low wavelength photons do not penetrate tissue sufficiently for appreciable *in vivo* applications and require invasive procedures to achieve target irradiation. Such photons are also more susceptible to interact with biological substances, possibly causing two issues. Firstly, autofluorescence is more prevalent at wavelengths of light lower than NIR, which can interfere with molecular imaging applications of chromophores. Also photons in the UV region cause phototoxicity, harming the organism's cells.[22,23]
2. When photocleavage occurs after irradiation with photons of the appropriate wavelength, the $\Delta\lambda_{max}$ of the PPG, the subsequent process of uncaging must possess a high rate constant. Assuming a first order reaction, the rate constant $k_{uncaging}$ is given by *equation 1*, showing a proportionality to the quantum yield, Φ, and the molar absorptivity, ε. This is referred to as the efficacy of the PPG. [9,11]

$$k_{uncaging} \propto \varepsilon \cdot \Phi \qquad (1)$$

   a. As such, the PPG should possess a high quantum yield (Φ), given by (2).[24]

$$\Phi = \frac{number\ of\ uncaged\ payload\ molecules}{number\ of\ absorbed\ photons} \quad (2)$$

b. In addition, the molar absorption coefficient, or molar absorptivity, ε should be high, given by the rearranged Lambert-Beer Law (3), where *A* is the absorbance, *c* is the molar concentration and *l* is the path optical length.[24]

$$\varepsilon = \frac{A}{cl} \quad (3)$$

3. The PPG should be soluble in the target medium/media. In the case of biological applications this is water, but it can also be advantageous to tailor this property to more specific environments such as particular cells or cell membranes.
4. By-products of the uncaging should not interfere with the photochemistry (i.e. should not show significant absorption at the same wavelength the photocage does) and should not be toxic to the organism.

1.2 Prominent classes of PPGs

The library of photocage scaffolds is extensive and varied, each of these have a unique set of properties making them suitable for particular purposes. *Table 1* shows an overview of popular photocage scaffolds and how well-suited they are for biological applications according to the previously defined criteria. Note that the properties of each photocage can often be fine-tuned through derivatization to a certain extend.

Photocage	**1. Wavelength**	**2. Rate**	**3. Solubility**	**4. Toxicity**
p-Hydroxyphenacyl	<380 nm	✓	X	✓[25]
Bimane	<380 nm	~[26]	✓	✓[27]
o-Nitrobenzyl group	<443 nm	✓	✓	X
Nitro stilbene	<430 nm	✓	✓	-[i]
(Coumarin-4-yl)-methyl group	<515 nm	✓	X	~
Quinones	<500 nm	X	~	~[28]
Si-Phthalocyanines	<690 nm	✓[29]	X	✓
BODIPY	<700 nm	~	✓	✓

Table 1[30,31]: Overview of suitability of several notable PPG classes for applications in complex biological systems. Note that this table is only meant to give an impression of the current PPG library. Under "Wavelength" the $\Delta\lambda_{max}$ of the derivative with the highest bathochromic shift is reported. The other ratings are based on general descriptions of the PPG found in literature, though these may differ between derivatives, see text below. Competitive processes caused by photolysis products is included under "Toxicity".

From this *table 1*, it is abundantly clear that the ideal photocage scaffold for use in tissue is yet to be developed. However, this is not to say no promising *in vivo* experiments have taken place yet. Through significant derivatization, there are many examples of effective utilization of photocages for the delivery of bioactive molecule in mice, including for the treatment of tumours.[32–35] Such developments are fantastic examples of the fields progress since Barltrops initial publication and why further improvements are still highly desirable. Extensive derivatization is complex and limited in scope as tuning one property may inadvertently influence another. For example, placing sizable ligands on the

[i] Insufficient literature available.

scaffold PPG to yield a bathochromic shift may come at the cost of the compounds solubility in water or its quantum yield.[31] As such, it can be troublesome to improve on such PPGs. Creating a new scaffold with favourable properties *and* a higher wavelength absorption compared to the current top performers would allow for significantly more adaptability and absorption even further into the therapeutic window. This thesis explores the synthesis of BODIzy, a new class of PPGs based on BODIPY.

1.3 Background and application of BODIPY derivatives

BODIPY, short for boron-dipyrromethene (IUPAC: 4,4-difluoro-4-bora-3a,4a-diaza-s-indacene), was first synthesized by Treibs and Kreuzer, albeit accidentally, in 1968.[36] Since then, its derivatives have been well-utilized in a plethora of applications, including the labelling of biomolecules for cellular imaging,[37,38] LED's,[39] photodynamic therapy,[40] dye-sensitized solar cells,[41,42] and more.[43,44] In recent years the popularity of BODIPY derivatives as visible light/NIR photocages has also grown significantly.[43] This popularity is for good reason. BODIPY derivatives generally have a good stability under physiological condition, are resistant to photobleaching and are stable in a relatively broad pH range. They possess a sharp fluorescent peak with high quantum yields and good molar extinction coefficient. What gives rise to these photochemical properties is that the potential energy surfaces of the S_0 and S_1 states of this molecule are quite similar due to the molecule's rigid, planar structure.[31] However, this also results in a small Stokes shift, which can be problematic for application such as intracellular fluorescence imaging and molecular probes.[45,46] The BODIPY scaffold are easily modified on the α and β position, allowing for facile modification of electronic or solubility properties.[30,47] BODIPY derivatives have had successes such as allowing transition-metal-free *in vivo* delivery of CO [33], the first organic NIR-photocontrolled NO donors for photoacoustic tomography [48], and organelles specific targeting for the delivery of bioactive molecules.[18]

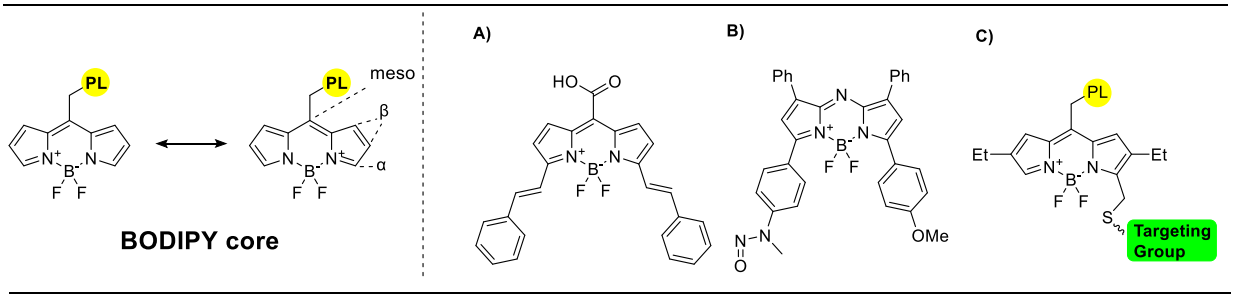

Figure 3: Left: BODIPY core with indications of the α and β substituent sites and the payload (PL). Right: Various BODIPY derivatives. A) CO delivery photocage by Palao et al.[33] B) NO donor by Zhou et al. [35]c) organelles specific delivery photocage by Kand et al.[18]

These properties and the progress made with BODIPY derivates make it a particularly interesting class of photocages, which, if the scaffold could be improved, would me more impressive still. Opposed to only placing substituents on the α and β positions, there are also BODIPY derivatives where the heterocycles have been adapted, giving rise to electronically more favourable products. These have been developed for other applications of BODIPY, such as organic photovoltaics [49], yet these derivates have not been well-investigated to function as photocages. According to our groups unpublished computational exploration, the "bis-indazole" BODIPY derivative is predicted to have a $\Delta\lambda_{max}$ = +96 nm compared to the BODIPY PPG. This alternate heterocycle BODIPY derivative is called BODIzy; its synthesis the focus of this thesis.

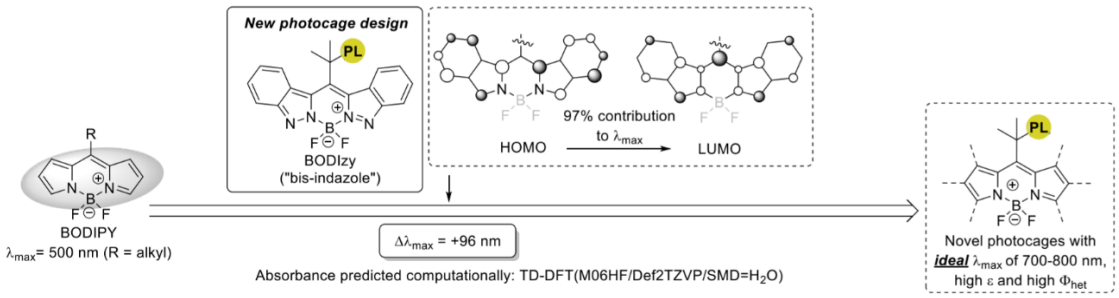

Figure 4: Overview of the computational findings suggesting BODIzy as novel photocage scaffold. Adapted from G. Alachouzos for the use in this thesis.

1.4 Photochemistry of BODIPY and BODIzy

The photocleavage of BODIzy derivatives is expected to work similarly to those of BODIPY derivatives. The chromophore is excited by a photon corresponding to the energy difference between its S_1 and S_1 excited state. From this point, intersystem crossing can take place, yielding the triplet excited state T_1. In both excited states, there is an increased electron density on the *meso* carbon of the molecule. This mixes with the σ* antibonding orbital of the BODIPY-PL bond, enabling bond cleavage. The resulting intermediate is a carbocation with a multiplicity corresponding to the preceding excited state. The quantum yield, and therefore the efficacy of photocleavage is limited by fluorescence, phosphorescence, nonradiative decay and recombination of the formed ion pair. It has been found that for BODIPY, most effective heterocleavage takes places from the T_1 state.[5] Singlet excited state cleavage is thought to be heavily affected by the aforementioned undesirable processes.[5]

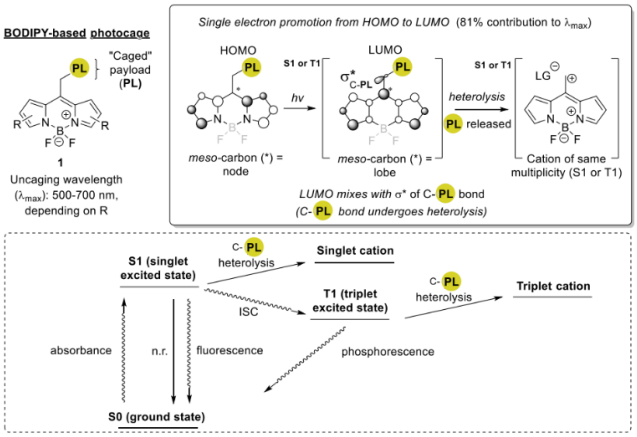

Figure 5: The reaction mechanism and Jablonski diagram of BODIPY-PL photoinduced heterocleavage adapted from G. Alachouzos for use in this thesis.

1.5 Previous attempts from the group and new strategy for the synthesis of BODIzy

The Feringa group has made previous attempts at synthesizing BODIzy, mostly based on Friedel-Crafts acylation or the aldehyde variation thereof with indazole[ii], sadly to no avail. The recurring issue was insufficient nucleophilic behaviour from the C3 site, a notorious synthetic challenge.[50,51] Either no reaction was seen at all, or N1 showed better reactivity. *Vide infra* for a summary of the attempts thus far.

[ii] In this thesis "indazole" always refers to *1H*-indazole, unless otherwise stated.

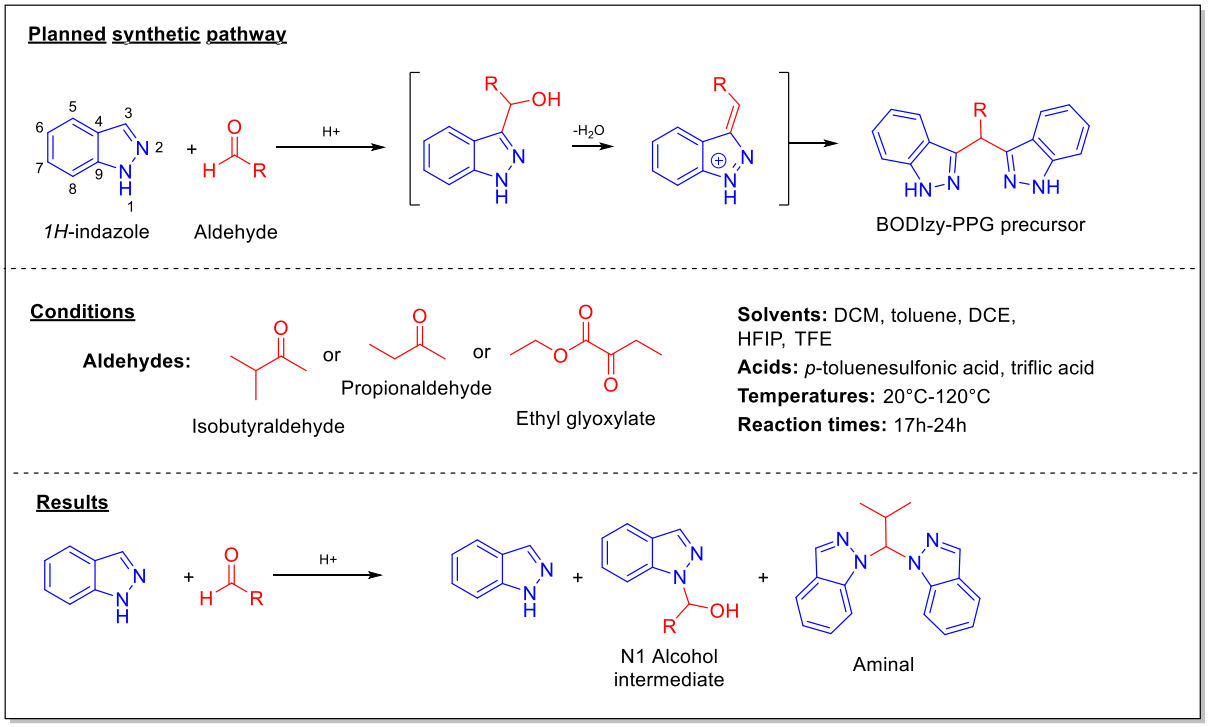

Figure 6: Overview of previous attempts at synthesizing BODIzy PPG precursors from our group.

The strategy followed in this thesis focuses on improving C3 reactivity, either through activation by means of halogenation and various organometallic reagents and/or the protection of the competing functionality, N1. The starting point of the exploration of these options is displayed below. It should be noted that for the purposes of developing the synthetic route towards BODIzy PPG 1, model reactions are used. For simpler purification and as there is more literature available, benzoyl chloride and acetyl chloride are used as electrophiles, which would yield a dye as final product not a PPG.

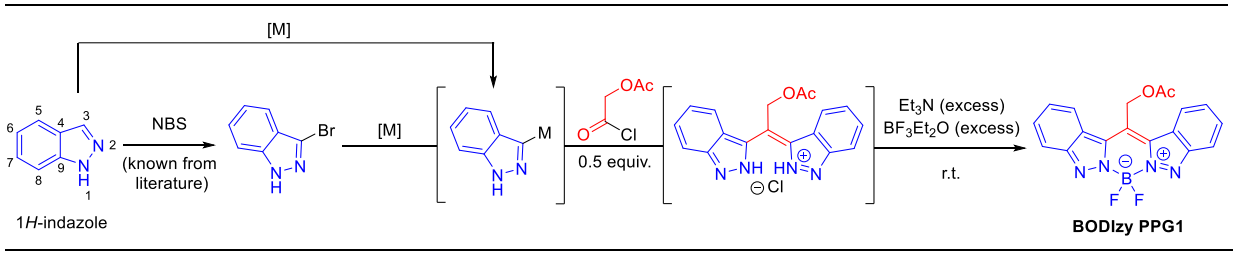

Figure 7: The synthetic pathway suggested to improve C3 reactivity of indazole.

Element	*Electronegativity*
Lithium	0.98
Magnesium	1.31
Zinc	1.61
Copper	1.90
Carbon	2.55
Nitrogen	3.04

Table 2: An excerpt of the Pauling scale showing the electronegativity of metals used this in thesis, carbon, and nitrogen.[52]

A variety of different organometallic reagents are explored, to solve the challenges of **low C3 activity, competing N1 pathways and, fragility of the starting material**.[53] An important factor to keep in mind is the electronegativity of the metal in question, data relevant to this thesis is shown in *table 2*. Metals with higher electronegativities are increasingly mild organometallic reagents, resulting in lower reactivity and higher selectivity.

2. Results and discussion

The results have been categorized and divided into four sections. Each section is introduced with an outline of the planned strategy and the expected advantages and disadvantages. Next, the individual steps of the strategy and the experimental results are discussed in subsections. At the end of each section, the results are summarized, and the strategy's performance is evaluated, with particular attention for the challenges described in the introduction of this thesis.

2.1 Attempted synthetic route 1: Regioselective zincation

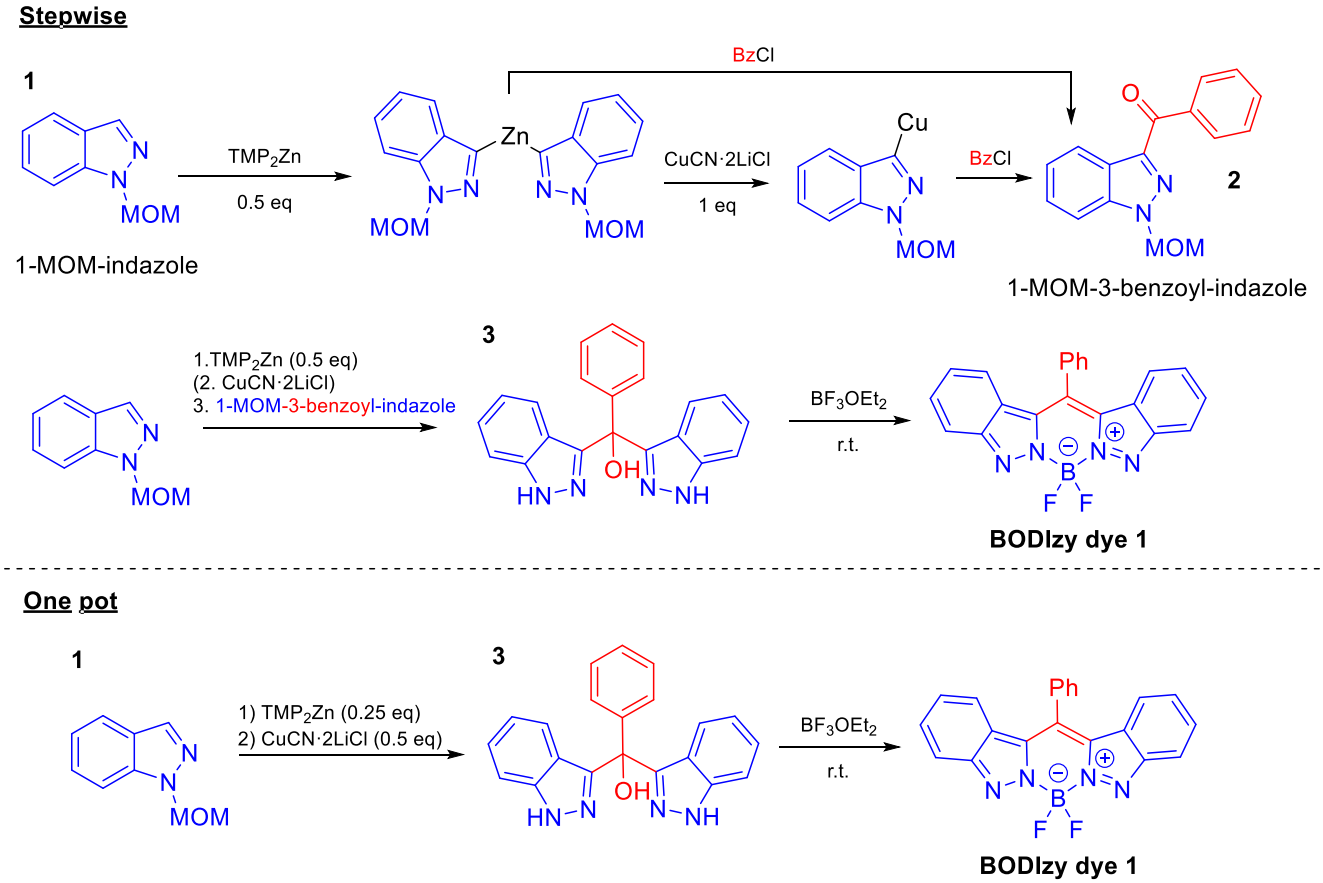

*Figure 8: Planned synthetic strategy towards synthesizing BODIzy dye 1 via regioselective zincation. The synthesis of **2** is adapted from literature, where "TMP_2Zn" refers to $(TMP)_2Zn{\cdot}2MgCl{\cdot}2LiCl$.[51] The second step seeks to expand on this literature to determine whether for synthetic progress towards BODIzy. If the stepwise synthesis proofed successful, attempting a one pot strategy could be attempted. This exciting prospect could pave the way to a facile synthesis of BODIzy.*

This planned synthetic strategy, as shown in *figure 8,* is reliant on use of TMP_2Zn for the metalation of N1 MOM protected indazole. These are then expected to perform a nucleophilic attack on benzoyl chloride, and again to **2** yielding the *bis*(indazole) **3**. This method uses mild conditions to create a *bis*-indazolylzinc species which can selectively react at the C3 position with various electrophiles or be used for Negishi coupling with aryl iodides.[51] It can also be transmetalated with CuCN·LiCl to create an even milder reactive intermediate, see *table 2*. This method deals with the aforementioned challenges in the following ways:

1) While zinc organometallic reagents are relatively mild compared to alternative organometallics reagents, if successful zincation takes place the activity of the C3 site is expected to be considerably increased, and there is literature precedent showing TMP_2Zn possesses high metalation activity.[51,54,55] Moreover, the procedure followed reported a 71% yield for the synthesis of **2,** suggesting the reactivity of the *bis*-indazolylzinc species should be sufficiently high for our purposes.[51] Do note in the literature reaction a Boc protecting group is used opposed to the MOM group used here.
2) As the starting material is notoriously fragile, the relatively mild conditions should help prevent side reactions resulting from the degradation of the substrate.
3) A MOM protecting group on N1 prevents processes where N1 nucleophilic activity competes with C3 reaction pathways, as was problematic in the Friedel-Crafts attempts.

The experiments to explore this method were based on the strategy shown in *figure 7*. First, 1-MOM-indazole was synthesised using NaH and MOMCl. From this point, attempts were made to replicate the literature procedure for the synthesis of **2**, both only using TMP_2Zn and combined use of TMP_2Zn and copper reagent. A similar reaction can then be attempted, using **2** as electrophile. If **3** is generated successfully, it is expected BF_2 chelation using BF_3OEt_2 would proceed relatively smoothly, as it does in the synthesis of BODIPY.[56] An attempt was made at performing these three steps in one pot for convenient synthesis of **BODIzy dye 1**.

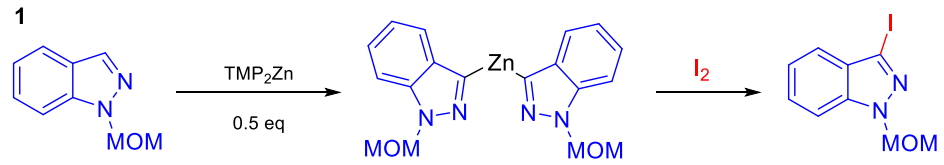

Figure 9: Iodine quench of the bis-indazolylzinc species to determine the degree of metalation.

To monitor the degree of zincation in the reaction mixture, aliquots were taken and quenched in a solution of iodine in THF. This sample was then analysed using ^{1}H-NMR and the degree of metalation was determined by comparing the integration of the C3-H signal to a well-defined aromatic signal of the substrate. The degree of diminishment of the C3-H signal corresponds to the degree of zincation in the sample.

2.1.1 Protecting indazole at N1 using MOM group

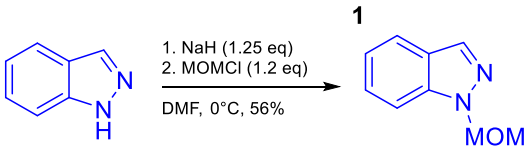

Figure 10: Reaction scheme for the N1 MOM protection of indazole.

To attempt a new synthetic route for the linkage of two indazole units at their C3 positions, the synthesis of 1-(methoxymethyl)-indazole, from here on referred to as MOM-indazole, was required.[51] The N1 position is deprotonated using NaH, increasing its nucleophilicity, allowing it to attack MOMCl, displacing the chloride ion. The first synthesis of MOM-indazole was performed at a 5 mmol scale and gave a 20% yield. The product has been reported to be a colourless oil, but ^{1}H-NMR analysis showed slightly yellow fractions were also of high purity. TLC analysis of the crude product showed two major spots, one of which corresponding to indazole, which helps explain the low yield. Some product may

also have been lost in the separation of the product from other compounds. The yield may be improved by adding more NaH and MOMCl and/or performing the reaction at a higher temperature. A second synthesis was done under the same conditions, except at a 20 mmol scale, and gave 56% yield. This product was also of high purity judging by ^{1}H-NMR analysis.

2.1.2 Synthesis of $(TMP)_2Zn{\cdot}2MgCl_2{\cdot}2LiCl$ from commercial TMPMgCl·LiCl

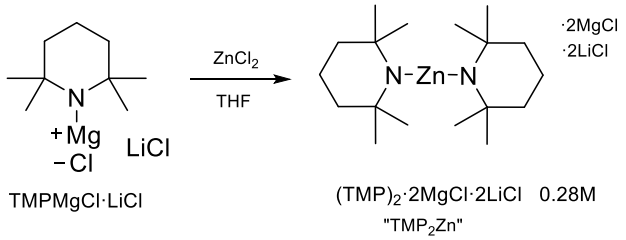

Figure 11: Reaction scheme for the synthesis of TMP_2Zn from commercial TMPMgCl·LiCl.

$(TMP)_2Zn{\cdot}2MgCl{\cdot}2LiCl$ (TMP short for 2,2,6,6-Tetramethylpiperidyl), in this thesis abbreviated to TMP_2Zn, was synthesized from commercial TMPMgCl·LiCl and $ZnCl_2$. It has been reported that with a TMPMgCl·LiCl solution of 1 M, TMP_2Zn with a concentration of 0.4 M is obtained.[51] It should be noted 1 mL of 0.4 M TMP_2Zn is sufficient to deprotonate 0.8 mmol of substrate. In the product of the first synthesis, a grey powder settles to the bottom of the vessel holding the product, suggesting a significant excess of $ZnCl_2$ remains. The product was titrated, giving a concentration of 0.28 M, significantly lower than expected. The commercial TMPMgCl·LiCl was titrated also, which turned out to be 0.757 M instead of 1 M, explaining the discrepancy in product concentration. The second batch was produced from the same TMPMgCl·LiCl source and also had a final concentration of 0.28 M. Both concentrations have a margin of error of ±3% due to the accuracy of the syringe used.

2.1.3 Attempted zincation of MOM-indazole at C3 position

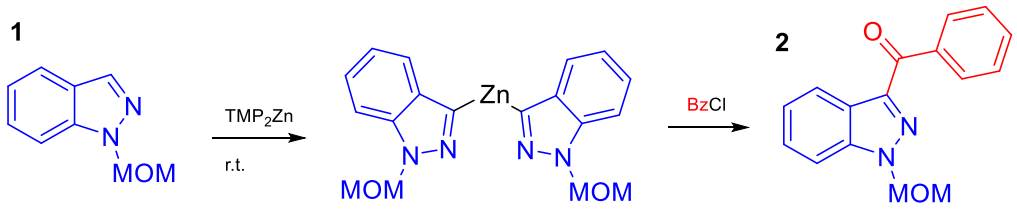

*Figure 12: Synthetic plan scheme for the synthesis of **2** via zincation, which does not correspond with results, see table 3.*

MOM-indazole was stirred at room temperature with TMP_2Zn. As the TMP_2Zn was of lower concentration than what is used in the procedure, no additional THF was added. The effective concentration of TMP_2Zn used in literature is 0.21 M as the TMP_2Zn (2.2 mL, 0.4 M) is diluted with 2 mL of THF, meaning our TMP_2Zn should be sufficient in concentration. Aliquots were taken and quenched with iodine, this allows using the integration of the ^{1}H-NMR C3-H signal to determine the degree of metalation of the substrate. Both attempts showed little conversion at room temperature, around 10%. In entry 2, the mixture was then heated to 50 °C for 72 h, which showed a minor increase in conversion, to approximately 23%, though this was not as significant as was hoped. This outcome is noteworthy as diorganozinc compounds have been reported to show good reactivity.[57] It should also be noted that

Entry	Temperature	Results
1	r.t., 1 h	<10% metalation
2	r.t., then 50 °C 16 h, then 72 h	~23% metalation ~45% deprotection

*Table 3: Summary of the attempted synthesis of **2** via zincation.*

significant deprotection of the N1 MOM group took place after heating the reaction from which can be inferred that prolonged heating is not the solution to the issue of low reactivity. The results are summarized in *Table 3*.

2.1.4 Attempted zincation and transmetalation of MOM-indazole

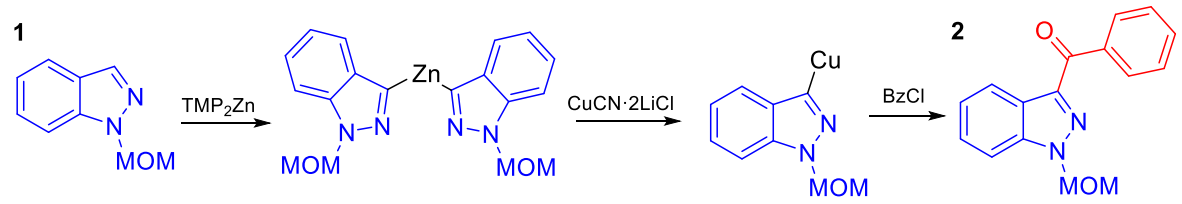

*Figure 13: Synthetic plan for the synthesis of **2** via zincation and copper transmetalation, which does not correspond with our results, see Table 4.*

More attempts were made successfully performing zincation at the C3 position of indazole. In these instances, copper reagent CuCN·2LiCl was added 1 h after addition of the TMP_2Zn, its purpose being to transmetalate the *bis*-indazolylzinc to even milder organometallic reagent using copper see *table 2*. The addition of this reagent serves no purpose if the zincation step does not first occur, which it does not, deduced from the results of the attempted synthesis shown in *figure 12*. Nevertheless, to ascertain the lack of the copper reagent is not the cause for the poor results, these reactions were attempted still. *Table 4* displays the results. In entry 1, it is noticeable the C3-H singlet has disappeared entirely in the ^{1}H-NMR spectrum of the crude product, suggesting full conversion. However, at least 3 different products containing a MOM group were formed (7:5:2 by comparison of CH_2 signal integration) and a significant portion was deprotected, as indicated by the N1-H signal at 8.65 ppm. The ratio between deprotected indazoles and the various MOM-indazoles combined is 20:15. Entry 2 and 3 also created a complex mix of starting materials and various products. The most abundant product from entry 2, listed in *table 4* as **6**, was isolated and analysed by ^{1}H-NMR and LCMS, no structure that would satisfy the outcomes of both methods of analysis could be determined, see Appendix.

Entry	Temperature	Degree of Metalation	Time	Results (1:4:5:6:7)
1	r.t., then 50 °C	0%[a]	10 min, 2 h	See text
2	-40 °C, then r.t.	36%[a]	10 min, 72 h	1:1:3:3:0
3	-40 °C, then r.t.	23%	10 min, 16 h	1:0:3:3:3

Products 026, 028

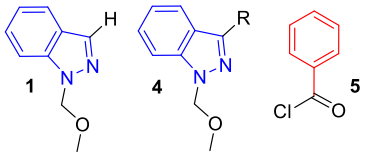

6 unknown structure

7 unknown product

Table 4: Results of the 3 attempted synthesis as shown in figure 14 and the structures of the products. Results column shows ^{1}H-NMR ratios of the products. a) note that during the I2 quench of entry 1 and 2, the formation of a side product could be identified as another set of CH2 and CH3 MOM signal could be observed.

2.1.5 Synthesis $(TMP)_2Zn{\cdot}2MgCl_2{\cdot}2LiCl$ from TMP and iPrMgCl·LiCl

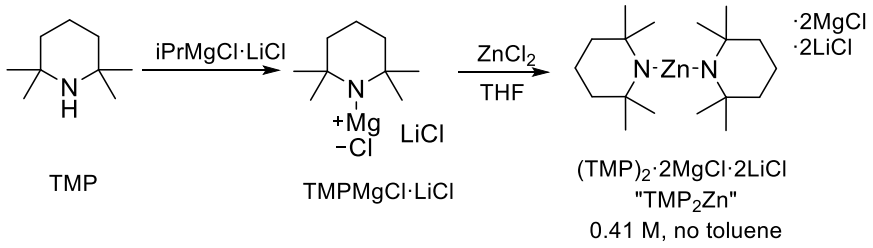

Figure 14: Reaction scheme of the synthesis of TMP_2Zn of a higher concentration than before and absent of toluene.

Following the advice of prof. Knochel, who was contacted about the encountered issues with reproducing his synthesis, an attempt was made to make an improved TMP_2Zn that was both of a higher concentration and did not contain any toluene, which is present in one of the starting materials previously used. TMP_2Zn of low concentration and the presence of toluene would significantly negatively affect the reaction rate. The new TMP_2Zn (see *figure 14* for information on the synthesis) was titrated to have a concentration of 0.41 M ±5%, slightly higher than what was used in the literature.

2.1.6 Attempted zincation and transmetalation of MOM-indazole with improved TMP_2Zn

With the improved TMP_2Zn, the reactions as shown in *figure 13* were attempted. As the TMP_2Zn was now of the correct concentration, in this attempt, additional THF was added to the reaction mixture to follow the procedure as closely as possible.[51] The TMP_2Zn was added and after 16 h and an iodine quench as shown in *figure 9* was performed with an aliquot of the reaction mixture, showing approximately 25% metalation, no significant improvement over what was seen with the different TMP_2Zn and certainly far from literature, where a final yield of 72% was obtained with 2 h reaction time for the zincation step.[51] The product ratio in the crude product was 1:2:1 of 1-MOM-indazole, indazole, and an unknown product respectively.

2.1.7 Conclusion Strategy 1

Despite various efforts and advice from prof. Knochel, the literature procedure could not be reproduced. TMP_2Zn, even when of good concentration and without retarding toluene present, was unable to effectively metalate the C3 position of indazole. Attempting to heat the reaction mixture for extended time periods, showed slightly improved metalation when using the low-quality TMP_2Zn, however this also caused significant deprotection, ~45%, and is therefore no viable solution. Entries 2 and 3 of the attempted zincations, **6** was present, as determined from ^{1}H-NMR. It was isolated from the product of but its structure could not be determined, though its ^{1}H-NMR signals and LCMS peaks do not correspond to any desired products or expected intermediates.

Looking back on the established challenges of this synthesis, we can conclude the following:

1) Despite promising literature findings, the TMP_2Zn did not show significant metalation in any of the performed experiments. Heating the reaction mixture improved metalation but degraded the substrate to a much greater extent. The addition of CuCN·2LiCl seemed to improve metalation slightly, up to 36% percent at best, though the desired product was still not obtained. Moreover, our observed metalation of 36% percent is far less than the metalation reported in literature, where 72% yield was obtained in a 2 h reaction time.[51] In the literature by Unsinn *et al.* Boc, MOM, and SEM were used. In the instance of using benzoyl chloride as electrophile with metalated indazole as nucleophile, a Boc protecting group was used instead of

MOM. It is unlikely the poor results are a consequence of protecting group choice as these are not expected to have a significant effect on C3 reactivity.

2) No competing N1 products were observed, also after the MOM groups were removed due to prolonged heating.
3) The substrate did not degrade under the conditions as reported in the followed procedure. Only after prolonged heating, deprotecting of N1 took place.

From these results, it is evident that stronger metalating reagents are needed. The TMP_2Zn does not seem to cause issues with N1 side reactions or cause degradation of the substrate, but this is to be expected of the mild and soft TMP_2Zn. The next synthetic route therefore explored more reactive metalating agents at the risk of increased side reactions or substrate degradation.

2.2 Attempted synthetic route 2: Lithium/Halogen exchange and Turbo Grignard

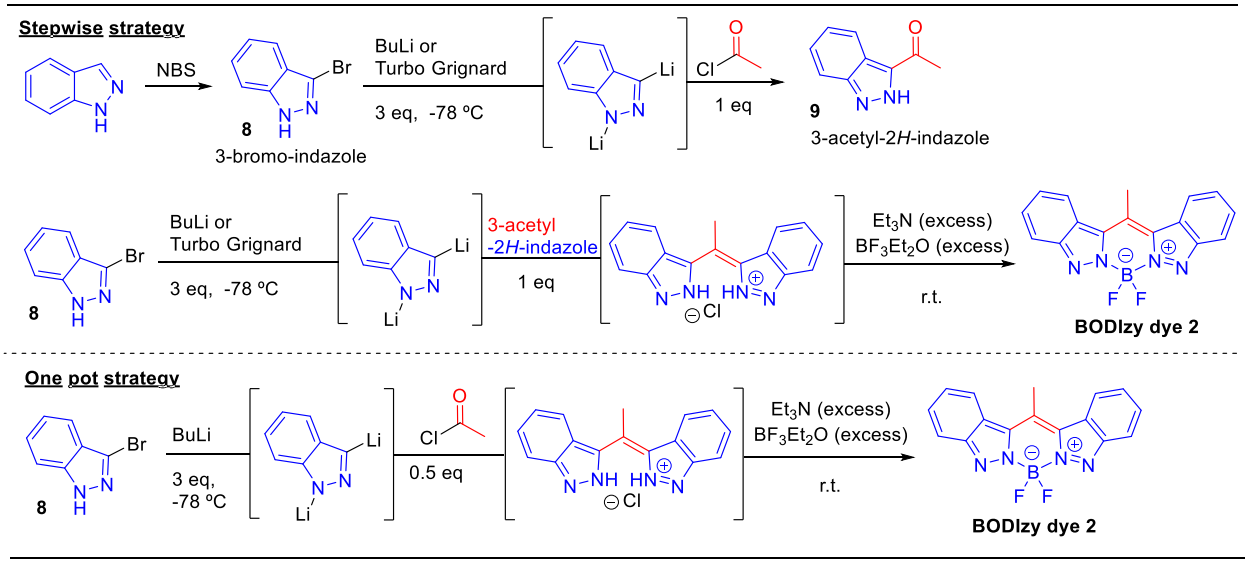

*Figure 15: Planned synthetic strategy towards **BODIzy PPG1**, showing both a stepwise strategy and a one pot process. The stepwise process also shows the synthesis of **8**, though it should be noted this compound is also commercially available. BuLi and Turbo Grignard reagent were used for the attempted metalation of **8**.*

This planned synthetic strategy is uses *n*-BuLi, *t*-BuLi, and iPrMgCl·LiCl, also known as Turbo Grignard reagent, for metalation. As would be expected from *table 2*, these reagents, in particular BuLi, are significantly more reactive than zinc organometallics. As such, **in these cases C3 metalation is likely to be successful, but there is an increased chance of side products via different pathways and product degradation.**

Similarly to the zincation strategy, in the stepwise strategy the electrophilic intermediate product, in this case **9**, is synthesized and worked up, then added to a second reaction vessel containing lithiated indazole. This is opposed to the one pot strategy, where **9** would be generated *in situ*, and would then react with remaining lithiated indazole. If the generation of the *bis*(indazole) intermediate is successful, chelation with BF_2 can be attempted, yielding **BODIzy dye 2**.

The experimental exploration started with the synthesis of 3-bromoindazole from indazole, though 3-bromoindazole was later obtained from a commercial source. Lithiation of 3-bromoindazole was

attempted and aliquots were quenched with D_2O. Similar to the iodine quench in *figure 9*, this allows for the determination of the degree of metalation of the substrate, from the diminishment of the C3-H signal compared to other 3-bromoindazole signals. See *figure 17* for the reaction scheme. This method of monitoring the reaction also enables the observation of potential side reactions.

2.2.1 Bromination of indazole using NBS

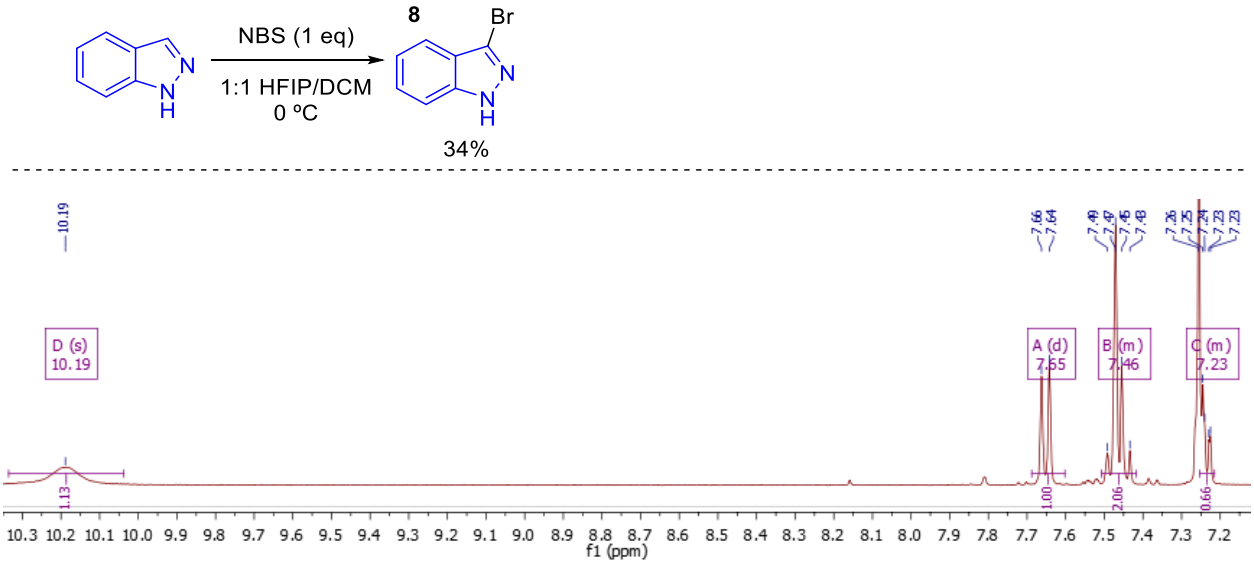

Figure 16: Top: The reaction scheme of the bromination of indazole using NBS. Bottom: The aromatic region of the ^{1}H-NMR spectrum of the purified product in $CDCl_3$, see appendix for full spectrum.

A literature procedure from Tang *et al.* was followed.[58] Said procedure was scaled up 10x and a 1:1 mix of HFIP/DCM was used as solvent, opposed to pure HFIP, as it was believed this should not influence the catalytic effect of HFIP significantly. The obtained yield was of the experiment was 334 mg, 33.9%, significantly lower than the 84% reported in literature. From TLC analysis of the flash column chromatography fractions, it appeared that significant amounts of product were present in fractions also holding a side product. The mass of these mixed fractions amounts to 469 mg, meaning the total conversion into the desired product lies between 33.9% and 81.6%. The product, **8**, could be characterized though ^{1}H-NMR spectroscopy. A doublet and a triplet overlap to form a multiplet integrating to 2, a triplet partially overlaps with the residual solvent peak, a clear doublet can be seen at 7.64 ppm and the distinct N1-H peak can be seen at 10.21 ppm. Moreover, the spectrum lacks the C3-H signal characteristic of the starting material. In future attempts the yield could be improved by using a less polar eluent for the flash column chromatography purification step. Also, using only HFIP will increase its catalytic effect and may therefore increase the yield.

2.2.2 Attempted lithium/halogen exchange 3-bromoindazole and deuteration studies

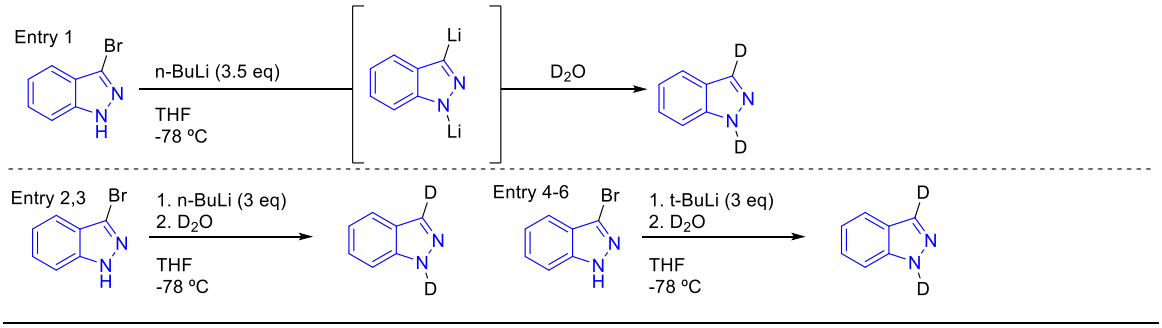

Figure 17: Expected reaction mechanism and schemes of the deuteration studies performed on 3-bromoindazole using n-BuLi and t-BuLI in the case of full lithiation, which did does not correspond with the results, see table 5.

Several attempts were made to perform a lithium/halogen exchange with 3-bromoindazole, which, if successful, could allow for facile linkage of 2 indazole units at C3. Entry 1, with the conditions as shown above, resulted in a 2:5 ratio of products. It should be noted that the N1 position was fully deuterated, as the corresponding signal in the ^{1}H-NMR spectrum had disappeared entirely. The solutions of *n*-BuLi and *t*-BuLi were titrated and more lithiation attempts were done to investigate if higher conversion could be obtained via this method. In the ^{1}H-NMR spectra of the crude products of entries 2,3 and 4, a signal characteristic of N1-H can be found around 10-12 ppm, suggesting these experiments were contaminated with a source of ^{1}H, likely water. The results are summarized in *table 5.* The formation of **12** is elaborated on the in next subsection. The ^{1}H-NMR spectrum of the crude product of entry 5 can be seen in *figure 18,* showing the ratio of products as indicated in *table 5*.

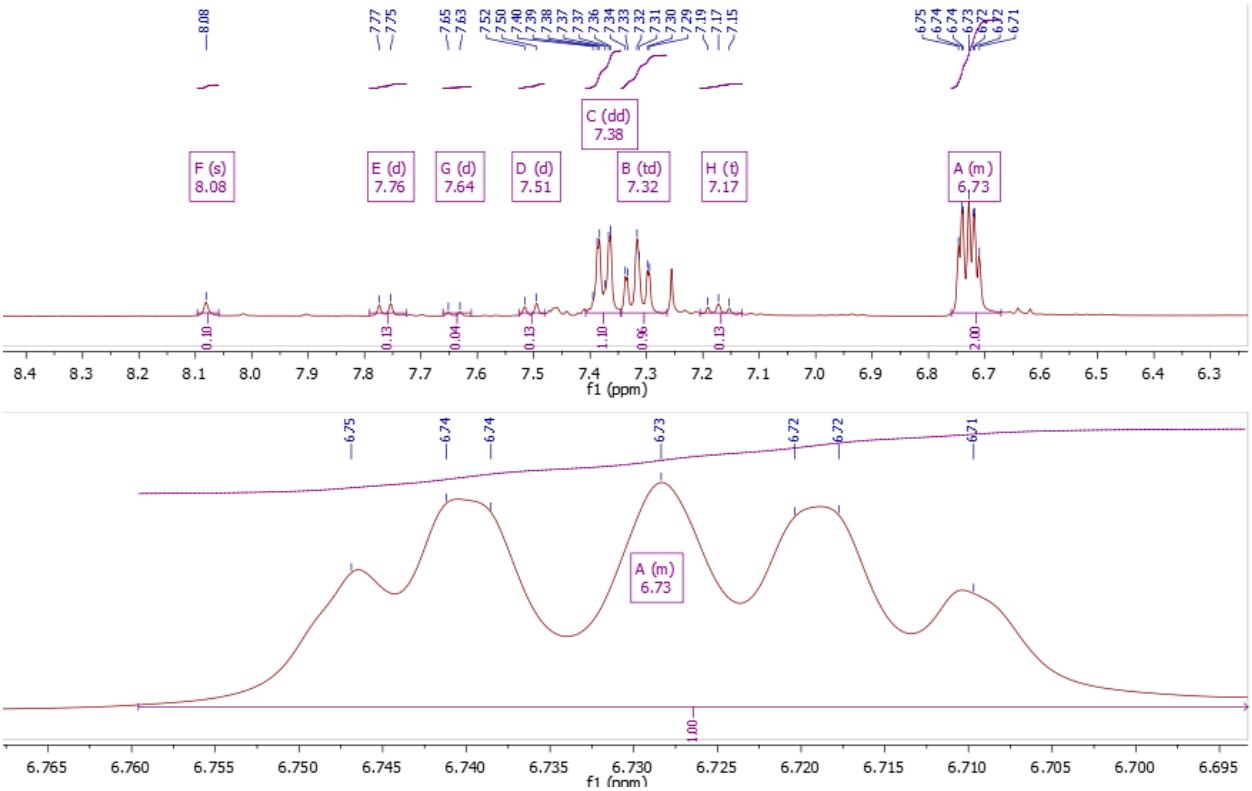

Figure 18: ^{1}H-NMR spectrum of the crude product of entry 5 in $CDCl_3$, showing the ratio of products and the expansion of the 6.73 ppm multiplet.

The C3-H signal at 8.08 ppm integrates to 4 while the doublet at 7.76 and 7.51 ppm integrate to 5. These doublets are shifted differently from those seen in 3-bromoindazole (see Appendix) and correspond well with literature on indazoles ^{1}H-NMR spectrum.[59] As the C3-H signal is diminished by 20% and no NH signal was observed, we can deduce that **10** and **11** exist in a 5:4 ratio. In the next subsection, it was discovered that ring opening, the cause of the formation of **12**, results in an aromatic triplet and doublet being shifted upfield to around 6.7 ppm. At this shift, a multiplet integrating to 2x the doublet at 7.38 ppm or the triplet at 7.32 ppm is found in the spectrum of the product of entry 5, which, upon closer inspection, is a triplet and a doublet overlapped. This is evidence for the formation of product **12**.

Entry	Reagent	Eq	Temp	Reaction Time	Results (10:11:12:13)
1	*n*-BuLi	3.5	-78 °C	1 h	1:10:25:0
2		3		15 min	1:1:3:0
3				2 h	1:0:4:8
4	*t*-BuLi			15 min	1:5:15:0
5				2 h	5:4:55:0
6				3 h	1:0:0:5

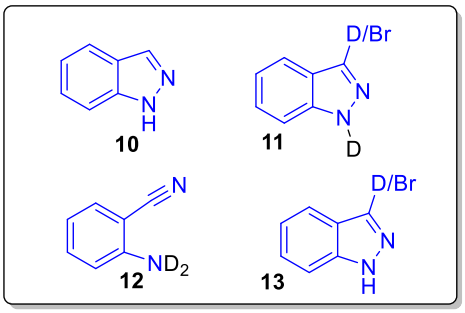

Table 5: The reaction conditions, results, and structure of the products of the attempted deuteration reactions as shown in figure 17. The results column shows the ratios of products by ^{1}H-NMR analysis.

2.2.3 Synthesis of *N*1-benzyl-3-bromoindazole

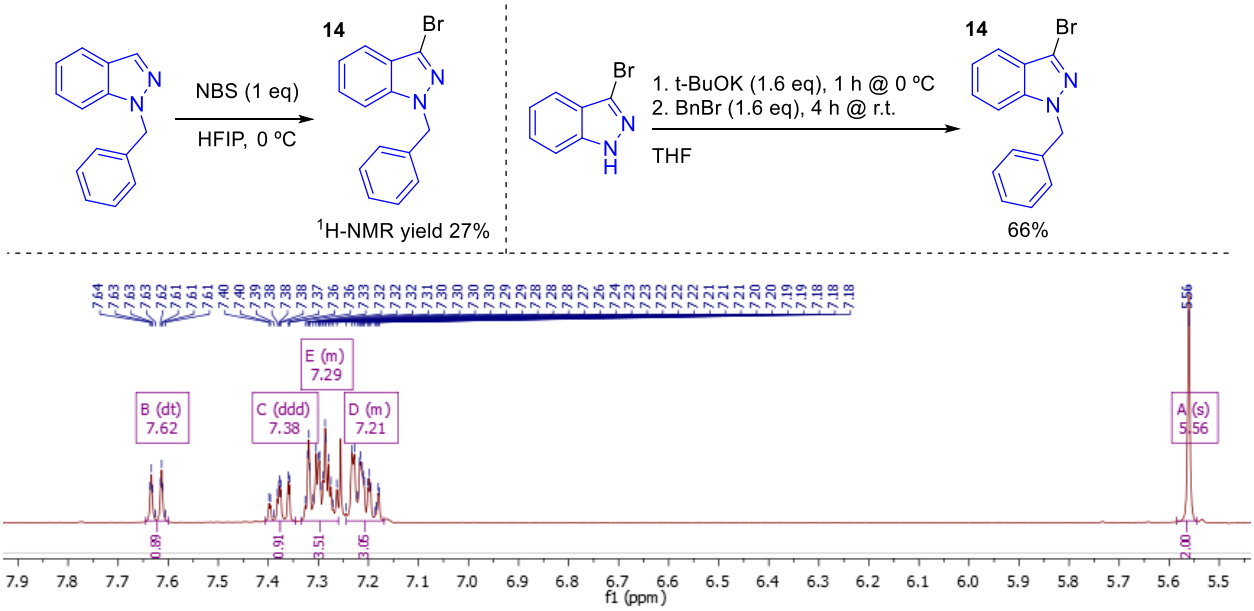

*Figure 19: Top: Reaction schemes for the two attempted synthetic pathways toward N1 benzyl protect 3-bromoindazole. Bottom: ^{1}H-NMR spectrum of **14** resulting from the benzylation of 3-bromoindazole in $CDCl_3$.*

The target molecule of this reaction, N1 benzyl protected 3-bromoindazole, was synthesized to be used as a substitute for **8** as shown in the reaction mechanism in *figure 15*. First, the bromination of *N*1-benzylindazole was attempted using NBS. The attempted bromination of *N1*-benzylindazole, the same procedure was followed as was done for the bromination of indazole, only using *N1*-benzylindazole as starting material. ^{1}H-NMR analysis shows a mix of products was formed, and the ratio between the

desired product and side products was 4:11. Instead, the N1 benzylation of 3-bromoindazole was attempted. Literature and previously obtained, unpublished results from our group have shown that while the C3 position has a relatively low reactivity, the N1 position will react quite readily, of which this new approach takes advantage.[60] Commercially obtained 3-bromoindazole was treated with potassium *tert*-butoxide, then benzylated using benzyl bromide, adapting a procedure for the benzylation of 3-iodoindazole and at one fourth the scale, 0.259 mmol.[61] While assigning individual signals is difficult due to significant overlap, the ^{1}H-NMR spectrum of the obtained product as shown in *figure 19*, corresponds with what was reported by Xiao *et al.*[61]. From the spectrum can be determined that conversion to the 95% of the substrate was converted to N1 benzylated product, compared to the N2 benzylated by product, through comparison of the CH_2 peaks to literature.[61] Their relative integrations can be found in *figure 19* around 5.55 ppm. The yield was 66%, lower than the reported 95%. The second time this procedure was followed, a scale of 2.59 mmol was used and a 73% yield was achieved, a slight improvement over the first attempt.

2.2.4 Attempted metalation of *N*1-benzyl-3-bromoindazole

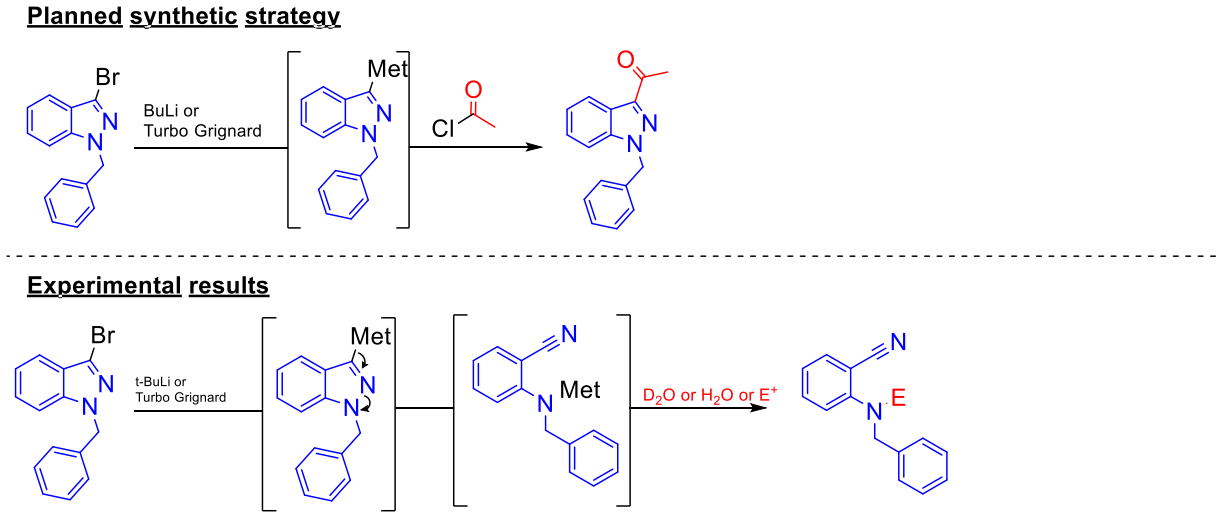

Figure 20: Diagram showing the planned synthetic strategy and experimental results for the attempted metalation of *N1*-benzyl-3-bromoindazole. ***Planned synthetic strategy:*** *The reaction scheme for the metalation of N1-benzyl-3-bromoindazole where 3 eq of t-BuLi or 2 eq of Turbo Grignard reagent (iPrMgCl·LiCl) is used.* ***Experimental results:*** *shows the experimental product observed in aliquots and the mechanism proposed by Welch et al.*[62] *See Table 6 for all results.*

Several attempts of metalating the C3 position of *N*1-benzyl-3-bromoindazole were done. As *t*-BuLi had shown slightly better conversions compared to *n*-BuLi in the experiments shown in *figure 20*, *t*-BuLi was used for the N1 protected lithiation experiments. After adding the base, aliquots were taken and quenched with D_2O, and analysed using ^{1}H-NMR. Using *t*-BuLi at both -78 °C or -98 °C, and using the Turbo Grignard reagent at room temperature, all showed the formation of an unexpected product on ^{1}H-NMR. A curiosity found in entry 3 was that starting the Turbo Grignard reagent at -78 °C showed no reaction, even after heating the mixture to 50 °C. This was possibly the result of a leak in the Schlenk system. The unexpected product was isolated from the reaction ran in entry 1 and was analysed further using APT, COSY, HSQC, and gHMBC NMR. This analysis confirmed ring opening between N1 and N2 took place, see **17** in the overview below. Similar results have been obtained in literature before and the mechanism in *figure 20* has been suggested in several publications.[51,62,63] The results are summarized in *table 6.*

Entry	Reagent	Eq	Temp	Reaction Time	Results (15:16:17:18)
1	*t*-BuLi	2	-78 °C	1 h	1:20:0:0
2	*t*-BuLi	2	-98 °C, r.t.	30 min, 18 h	7:2:1, then 7:2:1
3	iPrMgCl·LiCl	1.1 + 1.1	-78 °C, 0 °C, r.t., 50 °C	3 h, 16 h, 24 h, 3 h	No reaction
4	iPrMgCl·LiCl	1.1	r.t.	1 h, 1 h, 1 h	1:0:10:7

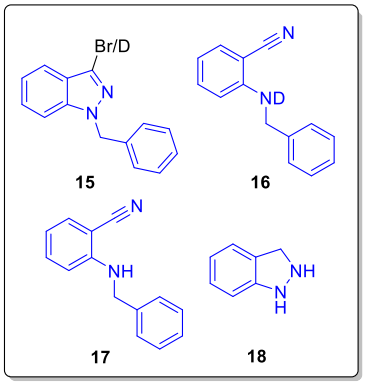

Table 6: Reaction conditions, results, and structure of the products of the attempted reactions as shown in figure 20.

2.2.5 Conclusion Strategy 2

Straightforward lithiation proves to be no viable pathway for the purpose of improving the nucleophilicity of the C3 site of indazole. For both N1 substituted and unsubstituted 3-bromoindazole, the major product is generally the corresponding benzonitrile when lithiated or magnesiated at C3, in line with literature findings.[60,62,64] Evaluation against our previously determined challenges is as follows:

1) The C3 position was certainly metalated, so while this point could be considered a success, though degradation of the substrate makes this improved reactivity inapplicable to our purposes.
2) The N1 position did not compete with C3 reactivity, as was seen in the Friedel-Crafts attempts, though the N1 did react in the form of N-N bond cleavage. Placing a benzyl substituent on N1 seemed to be of little effect to this process.
3) Ring opening was seen in every experiment aside from two reactions which are expected to have been contaminated by water and are therefore not as relevant. Even at -98 °C, with *t*-BuLi, the first product that is formed was determined to be **17**. Using an organometallic somewhat gentler than *t*-BuLi, the Turbo Grignard reagent, did not improve the results either.

A synthetic method is required that is more reactive than the TMP_2Zn, but does not result in ring opening, as was seen in the case of straight forward lithiations and magnesations. As the ring opening process has been a known issue for decades, there are solutions that have been developed.[62] Two of these have been attempted and the results will be discussed in the next two subsections.

2.3 Attempted synthetic route 3: Stepwise lithiation

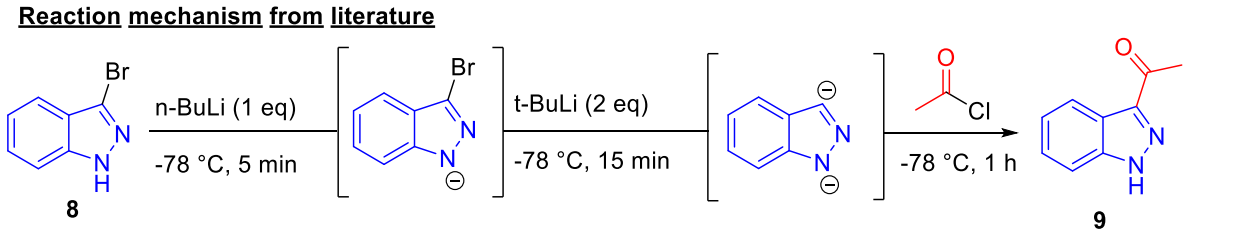

Figure 21: Reaction mechanism of the stepwise lithiation of 3-bromoindazole from Welch et al.[62] Note that N1 and C3 are lithiated rather than fully anionic, though this simplification is helpful in illustrating the mechanism.

This planned synthetic strategy is identical to *figure 15,* with one crucial difference. Fundamental to this approach from Welch *et al.* is the formation of the anionic intermediates in a controlled fashion by adding BuLi in two instances opposed to one.[62] First, 1 eq of *n*-BuLi is added, and the solution is stirred

for 5 min. This serves to deprotonate the N1 position, creating an increased electron density at this position. This disables the pathway to ring opening, as observed in previous lithiation and magnesiation approaches, see *figure 20*, since the mechanism involves placing a negative charge on the N1 position after C3 metalation takes occurs. With the N1 position now fully deprotonated, we are free to metalate the C3 position, without fear of ring opening if the lithiated nucleophile is used sufficiently quickly. The resulting dianion can then be trapped with an electrophile, such as acetyl chloride, creating 3-acetyl-2*H*-indazole, **9**. This process is then repeated using 3-acetyl-2*H*-indazole as electrophile, or it could be attempted to perform this reaction in one pot, simply by adding only 0.5 eq of acetyl chloride. The dimeric intermediate can then be chelated with BF_2, yielding **BODIzy dye 2**. This deals strategy deals with the challenges in the following ways:

1) If the dianion is formed, the C3 position will be a strongly nucleophilic. It is likely this lithiation will occur, as can be deduced from the results of previous lithiation experiments.
2) In this strategy, the N1 position will also be lithiated and could therefore participate in reaction pathways competing with C3. However, negatively charged secondary amines, such as N1, are generally significantly less reactive than negatively charged secondary carbons, such as C3, as can be deduced from their relative positions on the Pauling scale, see *table 2*. Therefore, it is expected the N1 position will be the first to be lithiated but second to perform a nucleophilic attack of the electrophile. Competing reactions can therefore be avoided by simply using 1 eq of electrophile.
3) Resultingly, when the first equivalent of BuLi is added, the first intermediate will be the N1 anion, preventing ring opening as previously discussed. To what extend formation of the ring opening product can still be observed will depend on the exact relative reactivities of N1 and C3 in the lithiation step.

Experimentally, first the literature reaction yielding **9** via stepwise lithiation of **8** and trapping with acetyl chloride was performed. In subsequent reactions, **9** can then be used as electrophile. A model reaction was performed using commercially obtained phenyllithium as nucleophile and **9** as electrophile, to serve as a proof-of-concept electrophilic activity for indazole with a carbonyl substituent on C3. The reaction in *figure 21* was also attempted with **9** as electrophile.

2.3.1 Synthesis of 3-acetyl-2*H*-indazole via stepwise lithiation of 3-bromoindazole

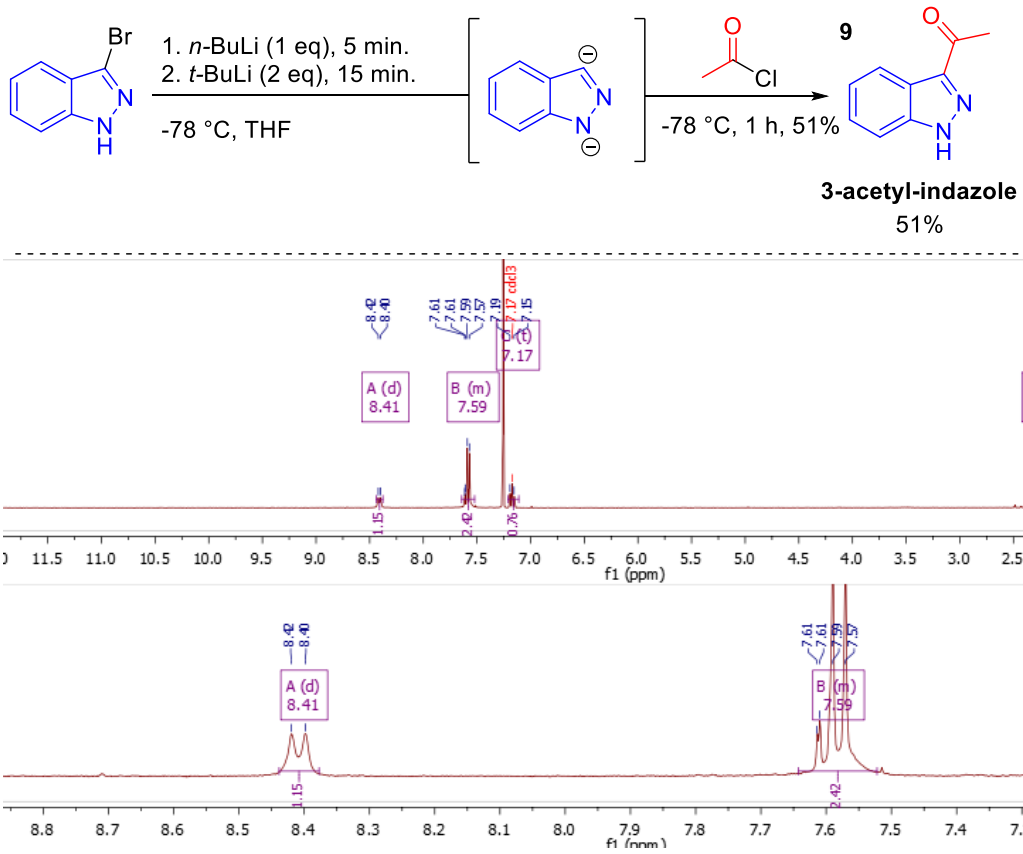

Figure 22: Top: Synthesis of 3-acetyl-2H-indazole from indazole via stepwise BuLi addition. Bottom: full ^{1}H-NMR spectrum of the product of the reaction as shown above in $CDCl_3$ and a magnification of the aromatic region thereof.

The experiment was performed twice, at a 1 mmol and 4 mmol scale respectively. In the 1 mmol scale attempt, a mass corresponding to 18% yield was obtained, though the product seemed to be only 70% pure from its ^{1}H-NMR spectrum, suggesting the yield is closer to 13%. Some product was not successfully purified and remained in a mixture contaminated with indazole and solvent. Approximately 50% percent of the 59 mg the contaminated fraction consists of the desired product, bringing the total conversion to the desired product to approximately 25%.

In a second synthesis, 51% yield was obtained. This yield, being significantly higher than that obtained before and what is reported in literature,[62] 20%, is likely due to an increased scale, as the aforementioned reactions were run at a 4 mmol and 0.2 mmol scale respectively. Running the reaction on a smaller scale results in minor water contamination or leaks in the Schlenk system to have more pronounced effects on the yield. This is also supported by the crude ^{1}H-NMR ratios between 3-acetyl-2*H*-indazole in the 1 mmol scale synthesis, ratio of 5:3, and in the 4 mmol scale synthesis, ratio of 4:1. The ^{1}H-NMR spectrum of the purified product of the 4 mmol scale synthesis very clearly shows the 4 aromatic 1H signals (where one doublet and one triplet overlap) and a 3H singlet at 2.27 ppm corresponding to the acetyl CH_3. LMCS results are as follows: 160 (5), 118 (100), the former corresponding to **9** and the latter to indazole, in line with literature findings.[62] A mass of 261 was also detected, possibly suggests ionization caused dimerization to form **22**, *see figure 24*, as masses correspond. This compound also shows strong absorption at 365 nm, as would be expected from **22**.

2.3.2 Nucleophilic attack of phenyllithium on 3-acetyl-2*H*-indazole

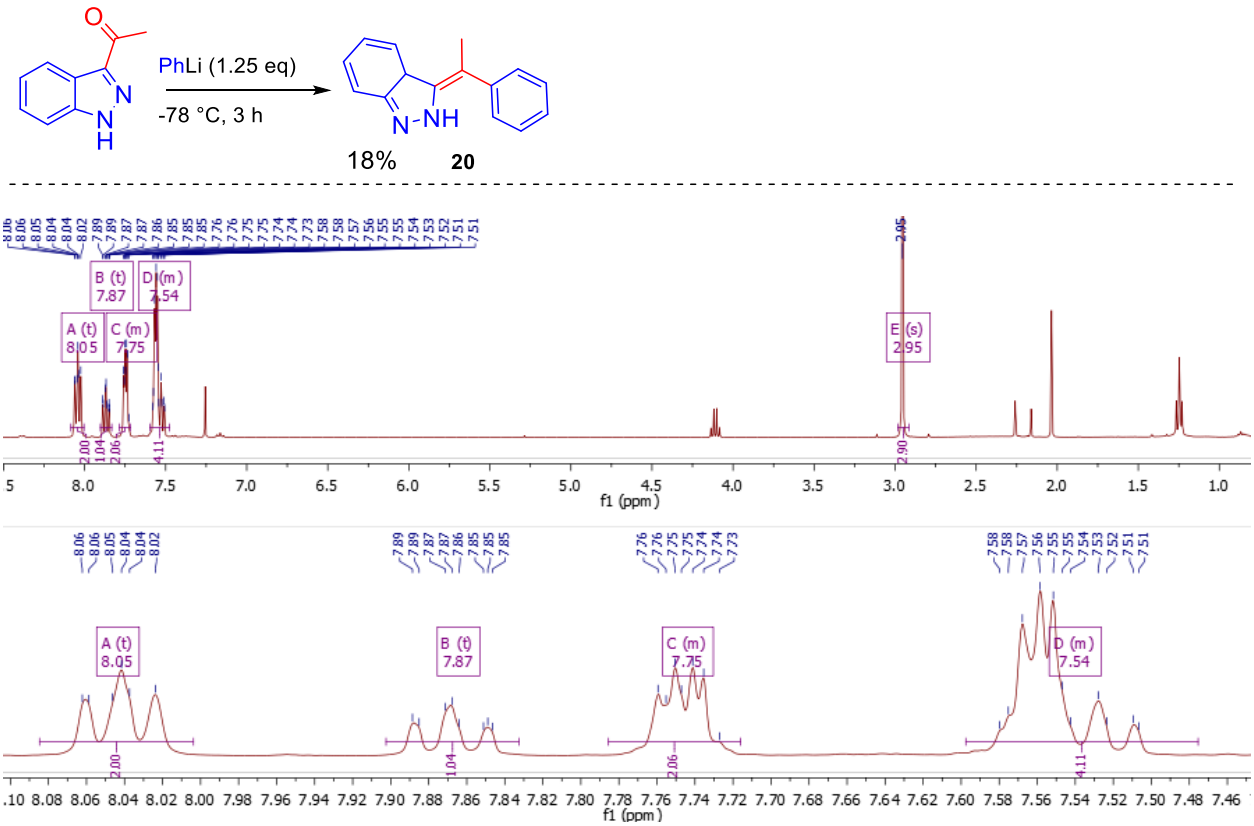

*Figure 23: Top: Reaction scheme of the nucleophilic attack of 3-acetyl-2H-indazole on phenyllithium, resulting in **20**. Bottom: ^{1}H-NMR spectrum of the product of the reaction above in $CDCl_3$ and a magnification of the aromatic region thereof. The sample shows ethyl acetate contamination, identifiable by the characteristic quartet, singlet and triplet around 4.10, 2.01, and 1.26 ppm respectively.*

This experiment explores the reactivity of 3-acetyl-2*H*-indazole as an electrophile by using commercially obtained phenyllithium as a model for lithiated indazole attack this position. The recovered yield after flash column chromatography was 18%, with minor contamination of EtOAc and acetone. In the crude product, a ratio of 4:1 was determined between the desired product and a different acetyl-indazole side product via ^{1}H-NMR. No starting material was present, suggesting 80% conversion into the correct product. The ^{1}H-NMR spectrum clearly shows an aromatic triplet integrating to 2H, an aromatic triplet integrating to 1H and 2 multiplets integrating to 2H and 4H respectively, together corresponding to the 4 aromatic indazole protons and the 5 phenyl protons. Additionally, a singlet integrating to 3H is found at 2.95 ppm, slightly downshifted from where the acetyl CH_3 is found in the ^{1}H-NMR spectrum of **9**, supporting the notion of extended conjugation in the product, as shown in **20**. The suggested structure was confirmed with HRMS, showing an m/z of 221.10745 (Calcd. 221.10732). Though TLC analysis, the presence of benzene was confirmed, the product of phenyllithium and water, which could have resulted from the quenching step or minor water contamination in the system. Considering the small scale and the moisture present in the starting material, 80% conversion into the desired product with only a small excess of phenyllithium this model reaction can be considered a promising proof-of-concept.

2.3.3 Nucleophilic attack of lithiated indazole on 3-acetyl-2*H*-indazole

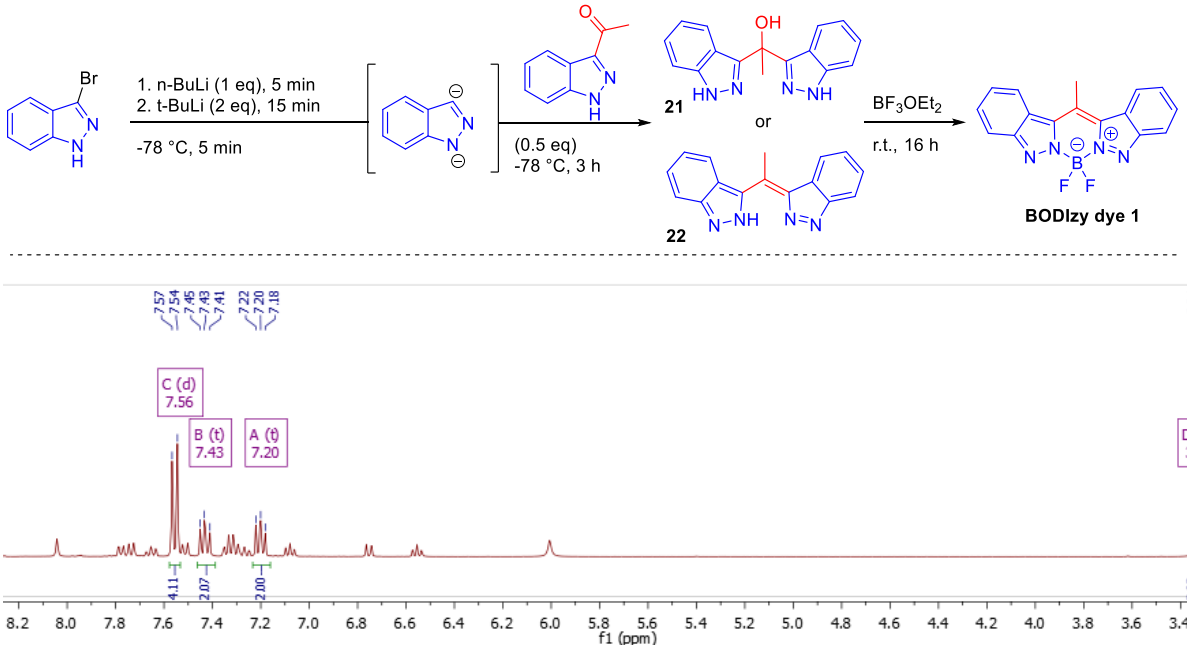

*Figure 24: Top: Expected reaction scheme for the nucleophilic attack of lithiated indazole on **9**, see figure 25 for the results. Bottom: ^{1}H-NMR spectrum of the product of the reaction above in $CDCl_3$ with product ratios as shown in figure 25. Only product signals are analysed here, for full analysis see the appendix.*

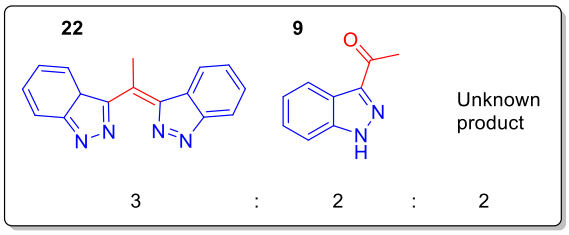

Figure 25: Ratio of products and their structures from the reaction as shown in figure 24.

An attempt at the synthesis of **BODIzy dye 1** was made by using the same 2 step addition of BuLi to generate the dianionic species and using 0.5 eq of 3-acetyl-2*H*-indazole to trap it, resulting in either alcohol, **21,** or the elimination product, **22**, as shown in *figure 25*. In the case of **22**, the addition of BF_3OEt_2 was proposed to result in the formation of **BODIzy dye 1** akin to its function in the synthesis of BODIPY.[56] With the hydroxy-bis(indazole) a similar chelation is expected to take place, with the resulting electron rearrangement resulting in the elimination of the hydroxyl group. As **22** is symmetrical due to its conjugation, it would be expected that the aromatic signals overlap, giving 2 triplet and 2 doublets integrating to 2 in the aromatic region and a singlet integrating to 3 further upfield. This is exactly what can be found in *figure 24,* except the two doublets happen to overlap also, giving a doublet integrating to 4. However, due to the lability of the OH proton it is not possible to tell whether **21** or **22** formed from only the crude product ^{1}H-NMR spectrum, however the product could not be purified due to time constraints. As **BODIzy dye 1** is expected to be a dye with high molar absorptivity in the visible light region, and such strong coloration was not observed, it is likely this product did not form. LCMS analysis indicated a m/z of 261 with strong absorption at 365 nm, confirming **22** as the product. The ratio of products is determined to be 3:2:2 by ^{1}H-NMR, with the corresponding structures as shown in *figure 25.* This low yield may be partially explained by the presence of acetic acid in the starting material, as it can be observed in the ^{1}H-NMR of the product also, (see Appendix).

2.3.4 Conclusion Strategy 3

Stepwise lithiation seems to be a simple, yet effective strategy for the synthesis towards BODIzy. For all attempted reactions, the desired product was obtained, including two compounds that have not been synthesized before, **20** and **22**, the latter of which could not be purified due to time constraints. The formation of these was confirmed with ^{1}H-NMR, and HRMS or LCMS respectively. The synthesis of 3-acetyl-2*H*-indazole was produced a significantly higher yield than expected from literature, likely due to an increased scale. This could mean the modest yields of **20** and **22** may be improved when performed at a larger scale also. Due to time constraints, the one pot synthesis could not be attempted, though considering the results thus far, this is a promising concept. While the synthesis of **22** was successful, chelation with BF_2 in the same pot seemed to be ineffective. The next step for this synthetic pathway is investigating this by performing this reaction in a separate reaction vessel with purified **22**.

The solutions stepwise lithiation was expected to offer for the issues encountered in straightforward lithiation are effective. **The C3 position was successfully lithiated, afterwards showing good nucleophilicity, no competing N1 reactions were observed, and ring opening was fully suppressed.**

2.4 Attempted synthetic route 4: N2 SEM protection for Directed *ortho*-Metalation

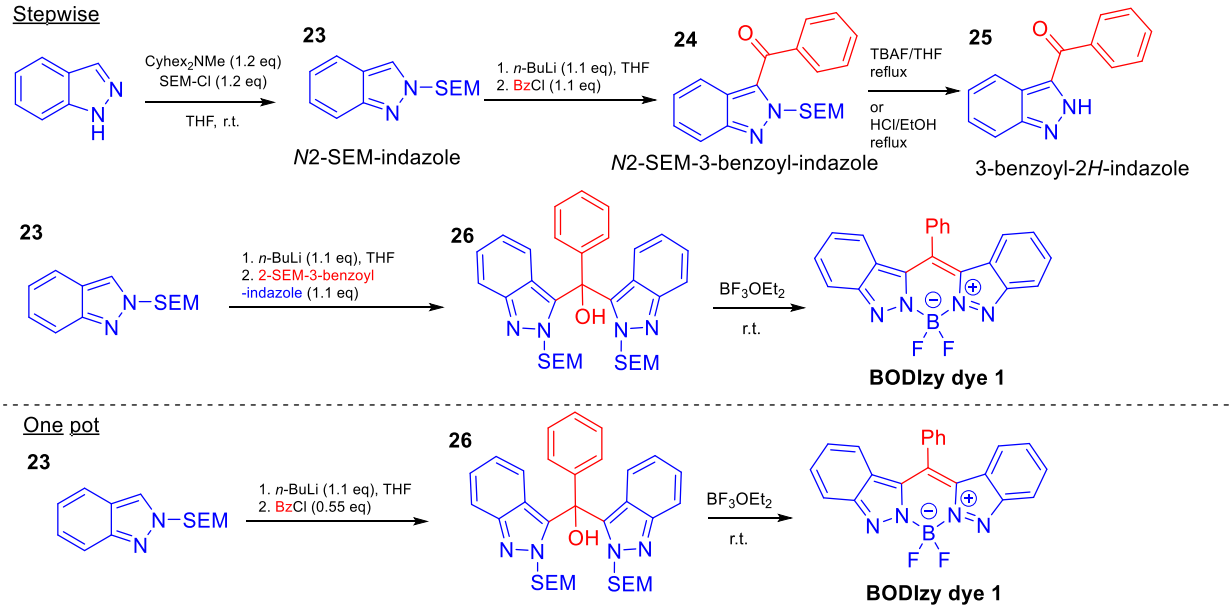

Figure 26: Planned synthetic strategy towards 3-benzoyl-2H-indazole and the corresponding BODIzy dye. The synthesis of 3-benzyol-indazole is reproduced from research by Luo et al, the synthesis of the BODIzy dye is an adaptation of this method.[60] *Note that a deprotection step may be required between before the addition of BF_3OEt_2, see "Attempted one-pot synthesis of BODIzy dye 2 from N2-SEM-indazole" below.*

The following strategy is based on placing a trimethylsilylethoxymethyl (SEM) protecting group on the N2 position of indazole. This serves three purposes:

1) The SEM group has long been a well-known Directed Metalation Group (DMG), for aryls, pyridyls, pyrroles, and indoles alike.[65–67] In short, the oxygen of the SEM group interacts with stabilizes lithium at the *ortho* position, facilitating the lithiation of these sites, see *figure 27*, this is referred to as Directed *ortho*-Metalation (DoM).[60] This should help to resolve the issue of limited metalation at this site, as encountered in previous experiments.

2) Secondly, the SEM group binding to the N2 position causes a rearrangement of electrons in the molecule, resulting in the loss of the labile *N*1-H, and this N1 electron is now engaged in a stable double bond, delocalized over the conjugated system. This serves to prevent competing reactions via the N1 pathway.
3) Thirdly, the creation of the *N*2-SEM bond results in the breaking of the N2=C3 double bond, hereby blocking the path to the formation of the benzonitrile as shown in *figure 20* and therefore also the ring opening of the heterocycle. This improves the molecules tolerance of harsh conditions.

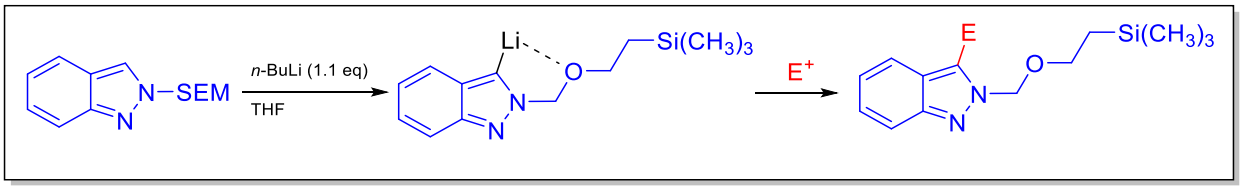

Figure 27: Reaction scheme showing the Directed ortho-Metalation effect with SEM as Directed Metalation Group.

It should be noted that the aforementioned benefits of this strategy closely correspond to the issues faced in the development of this synthesis so far, competition of N1 pathways in Friedel-Crafts attempts, the lack of reactivity found with TMP_2Zn, and the ring opening caused by straightforward lithiation or magnesiation.

The experimental examination of the planned synthetic strategy starts with the synthesis of *N*2-SEM-indazole from indazole. From this point, a stepwise synthesis can be followed, where **24** is purified before being added to lithiated indazole as an electrophile. Similar to what was done in the reaction shown in *figure 23*, a model reaction using phenyllithium was performed to confirm nucleophilic behaviour **24** with a reagent similar to lithiated indazole. Lastly, a one pot strategy was attempted to investigate a facile and quick synthetic route to **BODIzy dye 1**.

2.4.1 N2 SEM protection of indazole

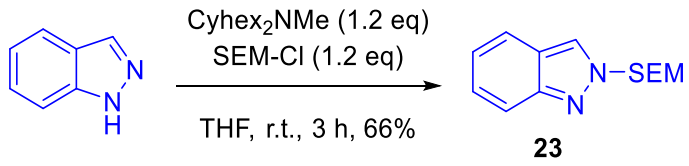

23

Figure 28: Reaction scheme for the synthesis of N2-SEM-indazole.

The synthesis as shown above was performed at a 10 mmol scale and a yield of 1.661g, 66%, was recovered. Literature reports purifying the product by flash column chromatography using 0-50% hexanes:EtOAc as eluent.[60] In this experiment, the product was also purified by flash column chromatography, but a gradient of 0%-10% pentane:EtOAc was used. However, still fractions containing two products were obtained and these were analysed using ^{1}H-NMR, from which could be determined these fractions were composed of **23** and impurities in a 4:1 ratio. The mass of the contaminated product was 577 mg, suggesting and additional 462 mg *N*2-SEM-indazole was synthesized but not recovered. Conversion to the desired product is therefore 85%. The recovered yield could be improved by further lowering the polarity of the gradient of eluent used in the flash column chromatography purification step.

2.4.2 Lithiation and BzCl electrophile trapping of *N*2-SEM-indazole

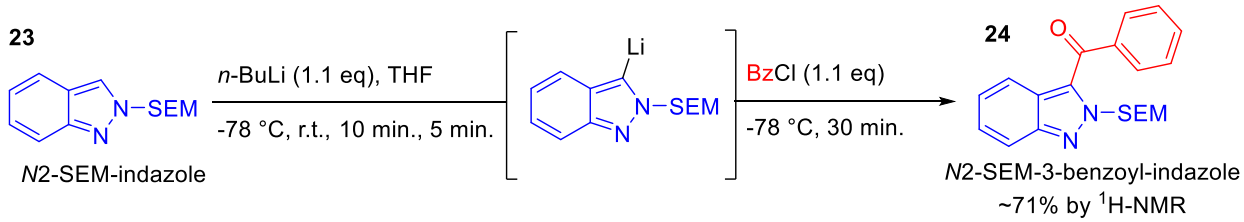

Figure 29: Reaction scheme for the lithiation of indazole and the trapping of the intermediate with benzoyl chloride.

The experiment was performed as described in the *figure 29*. The product was not purified due to time constraints, however there were certainly significant impurities present as a crude yield of 401 mg was obtained, which would correspond with 113%, was obtained. From the ^{1}H-NMR signals of the major project correspond well to what is reported for the desired product in literature procedure followed, though there cannot be absolute certainty due to signal overlap with impurities.[60] In the ^{1}H-NMR spectrum between 6.2 and 5.5 ppm, 1 major and 4 minor singlet signals are found. The major singlet at 6.16 ppm is attributed to the CH_2 from the SEM group, the other, minor signals are thought to result from 4 minor SEM-indazole side products. As such, the ratio of products was determined to be 12:2:2:2:1. As all starting material was converted, this suggests an approximate conversion to the desired product of 71%.

2.4.3 Attempted one-pot synthesis of BODIzy dye 2 from *N*2-SEM-indazole

A one-pot synthesis of the **BODIzy dye 2** was attempted by following the same procedure as was done in in the reactions as shown in *figure 29*, but only adding 0.55 eq of benzoyl chloride. In theory, ~0.5 eq of the lithiated *N*2-SEM-indazole reacts with benzoyl chloride, forming *N*2-SEM-3-benzoyl-indazole, **24**. The remaining 0.5 eq of lithiated *N*2-SEM-indazole, assuming complete lithiation, may then react with the carbonyl of **24**, creating the alcohol intermediate as shown in *figure 26* and then **BODIzy dye 2** after addition of BF_3OEt_2. Deprotecting SEM-pyrroles using BF_3OEt_2 is a known process, but unlike in our experiment this is generally followed by treatment with a base such as Triton-B or sodium acetate.[65] **BODIzy dye 2** is expected to be a high ε dye, and while the product did have a distinct red color, it was not as strongly absorbing in the visible light region as a BODIzy would be expected to be, and as such, significant formation of this product is unlikely.

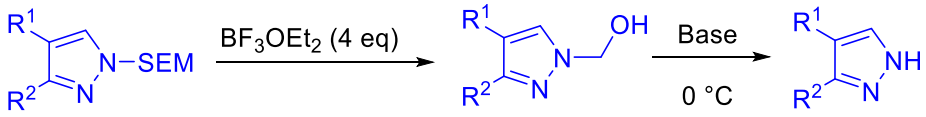

Figure 30: General reaction mechanism for SEM deprotection using BF_3OEt_2 and a base as described by Muchowski et al.[65]

The procedure was followed as shown in *figure 26* and the crude product was analyzed using ^{1}H-NMR. The SEM Si-$(CH_3)_3$ singlet can clearly be observed and is slightly shifted downfield. The CH_2 signal cannot be observed in the region of 2.5-7 ppm, where it would be expected. As such, it is unlikely that the SEM protecting group is still bound to N2 or that the process as shown in *figure 30* took place. Hence, it is expected that the *N*2-SEM bond was cleaved, and the SEM Si-$(CH_3)_3$ singlet is caused by the presence of free SEM in the crude product. The products of the reaction are difficult to identify by the ^{1}H-NMR spectrum as there is a complicated overlap of signals in the aromatic region.

2.4.4 Nucleophilic attack of phenyllithium on *N*2-SEM-3-benzoyl indazole

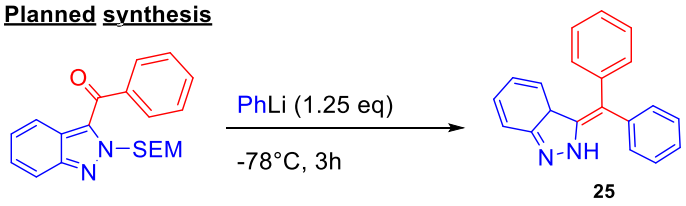

*Figure 31: Reaction scheme for the planned synthesis of **25**. The structure of the product could not be confirmed due to lack of analytical data and time constraints.*

The second step in stepwise process, as shown in *figure 26*, was attempted. For this reaction crude **24**, *N*2-SEM-3-benzoyl-indazole, was used as starting material. The product was analyzed using ^{1}H-NMR analysis, but due to complicated overlap of signals and a low concentration of product in the sample, making definitive statements on the structure of the formed products remains difficult. HRMS analysis shows 283.12298 (M^{+}, 1), 212.11851 (100). While the mass of **25** is detected, its relative abundance is quite low, and unlike the case of the reaction in *figure 22*, there is no literature to compare this data to. This makes drawing conclusions on this basis alone difficult.

2.4.5 Conclusion Strategy 4

The DoM strategy was confirmed to work well for the first step of the synthesis, reacting the indazole C3 site with an acid chloride electrophile. Synthesis of the starting material, *N*2-SEM-indazole was straightforward and it is expected the yield can be improved significantly with minor adjustments to the procedure. Lithiation and nucleophilic activity of this starting material was good, showing a conversion to the desired product of 71% in ^{1}H-NMR analysis of the crude product. The products of nucleophilic attack of phenyllithium on **24** and of the attempted one pot synthesis towards **BODIzy dye 1** could not be determined. The effectiveness of this strategy regarding the established challenges is as follows:

1) The indazole C3 position was successfully activated and was able to perform a nucleophilic attack on benzoyl chloride. The conversion to the desired product was determined to be 71% in the crude product, which, while lower than the 99% yield reported in literature, can still be considered good. Whether **24** is a sufficiently good electrophile to undergo nucleophilic attack by a second equivalent of lithiated *N*2-SEM-indazole could not be confirmed due to a lack of analytic data.
2) No competing N1 reactions were observed, suggesting the electron rearrangement caused by the SEM protection of N2 was an adequate method for stabilizing the N1 position.
3) No ring opening could be observed meaning the SEM protection of N2 was also an effective method for preventing the formation of the benzonitrile side product.

As it was not possible to collect sufficient data on **24** as electrophile, more research is required on these reactions. Since lithiation of *N*2-SEM-indazole and subsequent nucleophilic attack on benzoyl chloride worked well, it is expected that the reactivity of this lithiated species should be sufficient to attack the carbonyl on **24** proceed also.

3. Conclusion

Photolabile protecting groups could be of tremendous value for applications in complex biological systems. However, currently, there is no photocage that can fulfill all four strict requirements for such

applications, namely NIR absorbance, high efficacy of uncaging, high solubility in water, and low toxicity of the PPG and its cleavage products.[9,30] One of the best performing PPGs in these requirements is BODIPY, reaching $\Delta\lambda_{max} \approx 700$ nm after heavy derivation. However, not only is placing all these derivatives synthetically challenging and laborious, there is also a limit to the performance of a particular PPG scaffold and its derivatives. Our proposed BODIzy PPG scaffold is predicted to have $\Delta\lambda_{max}$ = +96 nm compared to the parent chromophore BODIPY, possibly capable of opening many doors in the application of PPGs in tissue.

Various synthetic routes towards BODIzy PPG precursors were explored through model reactions. It was determined that straightforward lithiations or magnesiation were ineffective, with or without an N1 protecting group, as lithiation of the C3 position resulted in N-N bond cleavage, yielding nitriles instead of lithiated heterocycles as reaction intermediates. A synthetic route through the usage of a milder base, $(TMP)_2Zn{\cdot}2MgCl{\cdot}2LiCl$ on 1-MOM-indazole, was also attempted, based on promising literature results, though these could not be successfully replicated.[51] This method showed poor metalation, even after reaction times significantly longer than reported. This could be slightly improved by heating the reaction mixture to 50 °C for extended time periods, however this also caused considerable deprotection of the MOM group. TMP_2Zn is a soft, mild base, by our results too much so to activate the C3 position and harsher conditions are not tolerated by the MOM-indazole reactant. It is therefore deemed unlikely methods will be found to improve the effectiveness of this synthetic route.

The stepwise lithiation strategy gave good results. It differs from straightforward lithiation only by first adding 1 eq of BuLi so only the N1 position is lithiated, significantly increasing electron density at this position. This negative charge prevents the N-N bond cleavage, meaning the C3 position can now safely be lithiated without risking ring opening.[62] A yield of 51% was obtained when reacting lithiated 3-bromoindazole with acetyl chloride to give 3-acetyl-2*H*-indazole, 30% higher than was reported in literature, likely due to the reaction being run at a larger scale, 4 mmol instead of 0.2. A model reaction using phenyllithium and 3-acetyl-2*H*-indazole was successful, confirmed by ^{1}H-NMR and HRMS, acting as a proof-of-concept. Moreover, the synthesis of a bis(indazole) was attempted by using 3-acetyl-2*H*-indazole as electrophile, was confirmed to be successful by ^{1}H-NMR and LCMS analysis of the product.

The DoM strategy also shows promise. In theory it should: stabilize lithiation at C3, prevent competing N1 reactions due to electron rearrangement and prevent ring opening, all of which seem to hold true in our experimental results. Nucleophilic attack of lithiated *N*2-SEM-indazole on benzoyl chloride yielded the desired product *N*2-SEM-3-benzoyl-indazole, supported by ^{1}H-NMR analysis of the crude product, however it could not be purified due to time constraints. Two attempts to use this product as electrophile were made, with lithiated phenyllithium and *N*2-SEM-indazole, however the formation of the desired products could not be confirmed due to lack of analytic data, although for the former the correct mass was detected by HRMS, albeit at a low relative abundance.

Both the stepwise lithiation and DoM routes have proven to be effective solutions to the first step of the total synthesis as shown in *figure 7*. If after further development, either route shows too little reactivity for the second step, the effect of two possible solutions can be explored. Firstly, as both reactions are performed at -78 °C, performing

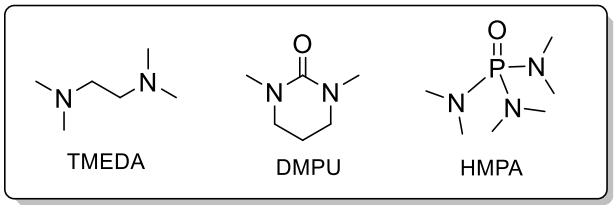

Figure 32: Structures of the disaggregating additives that could improve reactivity.

them at -40°, 0 °C or r.t. could be attempted. Secondly, disaggregating additives, such as TMEDA, DMPU or HMPA could be used to improve the effectiveness of lithiation, as numerous literature examples have successfully demonstrated.[68] As a *bis*(indazole) product could already be produced via stepwise lithiation, chelation with BF_2 needs to be investigated with this product.

Once the first two steps show good results and the chelation with BF_2 is also performed successfully, corresponding BODIzy dye, can be obtained. The photochemical properties of this dye can be measured and whether the calculations were accurate can be confirmed. If these properties show promise, the developed procedure(s) can be attempted with and optimized for an electrophile that will yield a PPG, such as acetoxyacetyl chloride. Finally, at that stage, the PPGs performance with regards to the aforementioned four requirements can be explored.

4. Experimental Procedures

4.1 General remarks

Synthesis and purification

All compounds were obtained from commercial suppliers and were used without further purification unless otherwise stated. Dry solvents were obtained from a Demaco Pure Solve MD5 solvent dispenser with the exception of acetonitrile, which was produced by drying reagent grade acetonitrile for 24 h over 3 Å molecular sieves (10% w/v). For thin layer chromatography (TLC) analysis, aluminium foils with a silica gel matrix (Supelco, silica gel 60) was used. The compound spots were visualized using UV (254 nm or 366 nm) irradiation or by staining using a phosphomolybdic acid (PMA) solution. Flash column chromatography purification was performed using silica gel (Supelco, silica gel 60), particle size 40-64 µM, eluding with technical grade solvents.

All reactions were performed under air unless otherwise stated. Standard Schlenk techniques using N_2 gas the inert gas and a membrane pump to apply a vacuum were utilized for reactions performed under inert atmosphere.

Characterization

Nuclear magnetic resonance (NMR) spectra were measured on an Agilent Technologies 400-MR (400/54 Premium Shielded) spectrometer (400 MHz for ^{1}H, 101 MHz for ^{13}C) at room temperature. The deuterated solvents utilized for these measurements, $CDCl_3$ and *d6*-DMSO were obtained from Sigma-Aldrich. For every spectrum, it is indicated which solvent is used in the figure description and the chemical shift of compound resonances relative to the residual solvent signal (δ) is given in parts per million (ppm). The ^{1}H-NMR data are reported as follows: chemical shift, multiplicity (s = singlet, d = doublet, t = triplet, q = quartet, m = multiplet, dd = doublet of doublets, td =triplet of doublets), coupling constant (J) given in Hz, and integration, proportional to the number of protons. ^{13}C-APT spectra are reported as follows: chemical shift (δ), number of attached protons (CH, CH_2, CH_3, C).

High Resolution Mass Spectra (HRMS) was performed using a Thermofisher LTQ Orbitrap XL with eluent MeOH (0.1% TFA) and flow rate of 0.15 mL/min in positive (ACPI/ESI) mode. UPLC–MS (LCMS) analysis was performed using a ThermoFisher Scientific Vanquish UPLC System (Waltham, MA, USA) with a reversed phase C18 column (Acquity UPLC HSS T3 1.8 µm, 2.1 × 150 mm; eluents: water and acetonitrile, both with 0.1% v/v formic acid added; the gradient was established from 5% to 95% organic phase over 17 min) in combination with an LCQ Fleet mass spectrometer and UV–vis detector at 254 nm, 360 nm, 530 nm and 680 nm.

General procedures

General aliquot procedure: 0.1 mL of the reaction mixture was quenched with D_2O in a 20 mL vial. NH_4Cl (aq) (3 mL) and chloroform (1 mL) was added. The organic layer was separated using a Pasteur pipette and the solvent was removed *in vacuo*. The sample was analyzed using ^{1}H-NMR spectroscopy.

Titrating bases with diphenylacetic acid: A 10 mL round bottomed flask, a magnetic stirring bar and a rubber septum was connected to a Schlenk line. The system was flame dried and flushed with nitrogen 3 times. The flask was charged with DPAA (212 mg, 1.00 mmol, 1.00 eq) and dry THF (10 mL). The solution was cooled to 0 °C. Once cooled, *n*-BuLi (or *t*-BuLi) in hexane (2.00 eq) was added to the stirred solution dropwise until a color change is observed. The expelled volume of the respective BuLi solution was recorded and the molarity of these solution were determined to be 1.42 M for *n*-BuLi and 1.6 M for *t*-BuLi. Note that DPAA is deprotonated twice before color change is observed.

Titrating bases with benzoic acid and 4-(phenylazo)diphenylamine [69]: A 10 mL round bottomed flask, equipped with a magnetic stirring bar and a rubber septum, was connected to a Schlenk line. The system was flame dried and flushed with nitrogen 3 times. The flask was charged with benzoic acid (110 mg, 0.900 mmol, 1.00 eq) and 4-(phenylazo)diphenylamine (2 mg, 0.007 mmol, 0.008 eq). Dry THF (1.5 mL) was added, and the resulting orange solution was cooled to 0 °C. The analyte was added dropwise to the solution until the solution changed to a persistent, deep red color. The titration volume was noted, and the concentration of the analyte was calculated. The following concentrations of commercial reagents were determined phenyllithium (1.48 M), iPrMgCl·LiCl (1.18 M), TMPZnCl·LiCl (0.78 M).

4.2 Attempted synthetic route 1: Regioselective zincation

4.2.1 Synthesis of 1-(methoxymethyl)-indazole [51]

A round bottom flask was equipped with a magnetic stirring bar and charged with indazole (591 mg, 5.00 mmol, 1 eq) and *N,N*-dimethylformamide (12.5 mL). The mixture was cooled to 0 °C, followed by the addition of sodium hydride (250 mg, 6.25 mmol, 60% in oil, 1.25 eq). The mixture was stirred for 30 min. To the reaction mixture was added chloromethyl methyl ether (483 mg, 6.00 mmol, 1.20 eq) followed by stirring at r.t. for 30 min. To the reaction mixture water was added and the aqueous layer was extracted with ethyl acetate for two times. The organic layer was washed with brine, dried over anhydrous $MgSO_4$ and the solvent was evaporated. The residue was purified and separated by silica gel flash column chromatography (10:1 pentane:diethyl ether), to give 1-(methoxymethyl)-indazole, 162 mg, 20.0%, as colourless oil. ^{1}H-NMR (400 MHz, Chloroform-*d*) δ 8.05 (s, 1H), 7.76 (d, J = 8.2 Hz, 1H), 7.58 (d, J = 8.4 Hz, 1H), 7.44 (t, J = 7.6 Hz, 1H), 7.22 (t, J = 7.5 Hz, 1H), 5.73 (s, 2H), 3.31 (s, 3H). ^{1}H-NMR data matches that of the literature report.

4.2.2 Synthesis of $(TMP)_2Zn{\cdot}2MgCl_2{\cdot}2LiCl$ from commercial TMPMgCl·LiCl [51]

In a 20 mL pressure flask, $ZnCl_2$ (1.084 g, 7.93 mmol, 1 eq) was dried *in vacuo* at 140 °C overnight. After warming to room temperature under positive nitrogen pressure, dry THF (3.8 mL) and TMPMgCl·LiCl (15 mL, 0.78 M, 11.7 mmol, 1.48 eq) was added slowly. If replicating, using 2 eq of TMPMgCl·LiCl is recommended. The resulting mixture was stirred for 15 h at r.t.. The freshly prepared $(TMP)_2Zn{\cdot}2MgCl_2{\cdot}2LiCl$ solution was titrated prior to use at 0 °C with benzoic acid using 4-(phenylazo)diphenylamine as indicator, yielding a concentration of 0.28 M.

4.2.3 Synthesis of CuCN·2LiCl [51]

In a 20 mL pressure flask with rubber septum, LiCl (2.29 g, 54.0 mmol, 1.00 eq) was dried *in vacuo* at 150 °C overnight. The reaction flask was cooled to room temperature and under positive nitrogen pressure, the septum was removed briefly to add copper cyanide (2.318 g, 27 mmol, 0.5 eq) to the flask. Dry THF (10 mL) was added, and the mixture was stirred at room temperature for 15 min., yielding a green solution.

4.2.4 Attempted zincation, transmetalation and electrophile trapping of MOM-indazole [51]

A 10 mL round bottomed flask equipped with a Teflon stirring bar and a rubber septum was connected to a Schlenk line. The system was flame dried and flushed with nitrogen 3 times. The flask charged with MOM-indazole (324 mg, 2.00 mmol, 1.00 eq). The TMP_2Zn (1.2 mmol, 0.28 M, 4.3 mL, 0.6 eq) was added at r.t. dropwise and the mixture was stirred for 22 h. To determine the degree of metalation, aliquots were quenched with I_2 in THF, sodium thiosulfate was added, followed by work up and analysis via the general aliquot procedure, showing 23% metalation. The reaction mixture was cooled to -40 °C and CuCN·2LiCl (1.6 mL, 2.2 mmol, 1.1 eq) and benzoyl chloride (0.28 mL, 2.4 mmol, 1.2 eq) were added. The reaction mixture turned dark red brown while stirred for 2h. The reaction mixture was quenched with a sat. aq. NH_4Cl solution (10 mL), extracted with diethyl ether (3 × 20 mL) and dried over anhydrous $MgSO_4$. After filtration, the solvent was evaporated *in vacuo*. The crude product was purified by silica gel flash column chromatography (pentane:diethyl ether = 3:2). The product as a colourless solid, a yield of 20 mg, 7.5%. Note that only the product of entry 1 of *table 4* was purified as crude as ^{1}H-NMR spectra of the other experiments showed no formation of the desired product. ^{1}H-NMR (400 MHz, DMSO-d6) δ 8.13 (d, J = 7.2 Hz, 2H), 7.99 – 7.88 (m, 2H), 7.79 (t, J = 7.5 Hz, 1H), 7.65 – 7.57 (m, 3H), 7.48 (t, J = 7.7 Hz, 2H), 7.28 – 7.09 (m, 3H).

4.2.5 Synthesis of $(TMP)_2Zn·2MgCl2·2LiCl$ from TMP and iPrMgCl·LiCl [51]

A 10 mL round bottomed flask equipped with a Teflon stirring bar and a rubber septum was connected to a Schlenk line. The system was flame dried and flushed with nitrogen 3 times. The flask was charged with iPrMgCl·LiCl (8.6 mL, 1.18 M, 10 mmol, 1 eq) and TMP (1.7, 10 mmol, 1.0 eq). The reaction mixture was stirred for 16 h. $ZnCl_2$ (692, 5.1 mmol, 0.5 eq) was dried at 140 °C overnight and the iPrMgCl·LiCl and TMP solution was added to this. The resulting mixture was stirred overnight. was titrated prior to use at 0 °C with benzoic acid using 4-(phenylazo)diphenylamine as indicator, yielding a concentration of 0.41 M.

4.3 Attempted synthetic route 2: Lithium/Halogen exchange and Turbo Grignard

4.3.1 Synthesis of 3-bromoindazole through bromination of indazole using NBS [58]

Commercial *N*-bromosuccinimide (NBS) was recrystallized from water. To a stirred solution of indazole (590 mg, 5.00 mmol, 1.00 eq) in HFIP (10 mL) and DCM (10 mL) was added recrystallized NBS (890 mg, 5.00 mmol, 1.00 eq) under air. The reaction mixture was stirred at 0 °C for 1 h, during which the solution turned from orange to yellow. After, the solvent of the reaction mixture was evaporated under reduced pressure and the crude product was purified by silica gel flash column chromatography (step gradient 0-20% ethyl acetate : pentane) to give the product; 334 mg (33.9% yield) of 3-bromoindazole, as white solid. In 20% EtOAc : pentane the product has an Rf of 0.6. ^{1}H-NMR (400 MHz, Chloroform-*d*) δ 10.19 (s, 1H), 7.65 (d, *J* = 8.2 Hz, 1H), 7.51 – 7.42 (m, 2H), 7.25 – 7.21 (m, 1H). ^{1}H-NMR data matches that of the literature report.[58]

4.3.2 Attempted lithiation of 3-bromoindazole, deuteration studies

A 10 mL round bottomed flask equipped with a Teflon stirring bar and a rubber septum was connected to a Schlenk line. The system was flame dried and flushed with nitrogen 3 times. The flask was charged with 3-bromoindazole (39 mg, 0.20 mmol, 1.0 eq) and dry THF (2 mL) and the mixture was cooled -78 °C. Once cooled, *n*-BuLi (0.42 mL, 1.42 M, 0.60 mmol, 3.0 eq) or *t*-BuLi (0.38 mL, 1.60 M in hexane, 0.61 mmol, 3.1 eq) was added to the stirred solution. Aliquots were taken according to the general procedure. These were analyzed by ^{1}H-NMR and no product was isolated. See *table 5* for the results.

4.3.3 Attempted synthesis of *N1*-benzyl-3-bromoindazole

To a stirred solution of *N1*-benzylindazole (21 mg, 0.10 mmol, 1.0 eq) in HFIP (2 mL) was added NBS (18 mg, 0.10 mmol, 1.0 eq) under air. The reaction mixture was stirred at 0 °C for 1h, after which a mixture of products had formed, and the experiment was halted. An ^{1}H-NMR yield of 27% was determined and the product was not purified.

4.3.4 Synthesis of *N1*-benzyl-3-bromoindazole [61]

To a solution of 3-bromoindazole (510 mg, 2.59 mmol, 1.00 eq) in anhydrous THF (20 mL) cooled at 0 °C was added potassium *tert*-butoxide (465 mg, 4.14 mmol, 1.60 eq) and the mixture was stirred for 1 h under air. Benzyl bromide (0.55 ml, 4.6 mmol, 1.8 eq) was added dropwise. The resulting mixture was stirred for 4 h at room temperature and the solvent was removed *in vacuo*. The residue was dissolved with EtOAc (50 mL), washed with water and brine, dried using $MgSO_4$, filtered and the solvent was evaporated under reduced pressure to give the product; 545 mg (73% yield) of **14** as a light-yellow oil. ^{1}H-NMR (400 MHz, Chloroform-*d*) δ 7.62 (d, J = 8.2 Hz, 1H), 7.40 – 7.26 (m, 5H), 7.24 – 7.19 (m, 3H), 5.56 (s, 2H). ^{1}H-NMR data matches that of the literature report.[61]

4.3.5 Attempted lithiation of *N1*-benzyl-3-bromoindazole using butyllithium

A 10 mL round bottomed flask equipped with a Teflon stirring bar and a rubber septum was connected to a Schlenk line. The system was flame dried and flushed with nitrogen three times. The *N*1-benzyl-3-bromoindazole (59 mg, 0.21 mmol, 1.0 eq) was added to the flask followed by dry THF (2 mL). The temperature was set as described in *table 6*. Once cooled, *t*-BuLi (0.04 mL, 1.6 M in hexane, 0.4 mmol, 2 eq) was added to the stirred solution, turning the solution bright yellow. Aliquots were taken at time intervals shown in *table 6* according to the general aliquot procedure. The major product was isolated using silica gel flash column chromatography (step gradient 0-10% EtOAc: pentane) and characterized using ^{1}H, APT, COSY, HSQC and gHMBC NMR. The product had Rf 0.3 in 5% EtOAc:pentane. ^{1}H-NMR (400 MHz, Chloroform-*d*) δ 7.41 (dd, *J* = 7.7, 1.6 Hz, 1H), 7.39 – 7.33 (m, 5H), 7.33 – 7.25 (m, 2H), 6.69 (t, *J* = 7.6 Hz, 1H), 6.64 (d, *J* = 8.5 Hz, 1H), 4.44 (s, 2H). ^{13}C-NMR (101 MHz, $CDCl_3$) δ 137.68 (CH), 134.27 (CH), 132.76 (CH), 128.86 (CH), 127.65 (CH), 127.18 (CH), 117.87 (CH), 116.92 (C), 111.11 (C), 95.98 (C), 47.49 (CH_2).

4.3.6 Attempted magnesiation of *N1*-benzyl-3-bromoindazole using Turbo Grignard

A 10 mL round bottomed flask equipped with a Teflon stirring bar and a rubber septum was connected to a Schlenk line. The system was flame dried and flushed with nitrogen three times. The flask was charged with 1-benzyl-3-bromoindazole (53 mg, 0.19 mmol, 1.0 eq) and dry THF (2 mL). The temperature was set as described in *table 6*. iPrMgCl·LiCl (0.16 mL, 1.3 M, 0.20 mmol, 1.1 eq) was added dropwise. In the case of entry 3 of *table 6*, more iPrMgCl·LiCl (0.16 mL, 1.3 M, 0.20 mmol, 1.1 eq) was added at the temperature was increased to r.t., then 50 °C. Aliquots were taken according to the general

aliquot procedure. The respective time intervals and results can be found in *table 6.* No desired product was obtained.

4.4 Attempted synthetic route 3: Stepwise lithiation

4.4.1 Synthesis of 3-acetyl-2*H*-indazole via stepwise lithiation of 3-bromoindazole [62]

A 50 mL round bottomed flask equipped with a Teflon stirring bar and a rubber septum was connected to a Schlenk line. The system was flame dried and flushed with nitrogen three times. The flask was charged with 3-bromoindazole (788 mg, 4.00 mmol, 1.00 eq) and dry THF (20 mL). The mixture was cooled -78 °C, then *n*-BuLi was added (2.8 mL, 1.42 M, 1.0 eq). A temperature of at least -65 °C was maintained. After 5 min., *t*-BuLi (5.0 mL, 1.6 M, 2.0 eq) was added dropwise and stirred for 15 min at -78 °C. Acetyl chloride (0.28 mL, 1.0 eq) was added. The mixture was stirred for 1 h at -78 °C. The reaction mixture was quenched with water and the product was extracted with EtOAc. The product was purified using silica gel flash column chromatography (step gradient 0-20% EtOAc : pentane) loaded with warm chloroform. The product was obtained; 329 mg (51% yield) of 3-acetyl-2*H*-indazole, as a white powder. In 20% EtOAc : pentane the product has Rf 0.4. ^{1}H-NMR (400 MHz, Chloroform-*d*) δ 8.41 (d, *J* = 8.5 Hz, 1H), 7.59 (t, *J* = 7.8 Hz, 3H), 7.17 (t, *J* = 7.6 Hz, 1H), 2.27 (s, 4H). ^{1}H-NMR data matches that of the literature report. LMCS: m/z 160 (M^+, 5), 118 (100). Similar MS results were found in literature.[62]

4.4.2 Synthesis of 20 via nucleophilic attack of phenyllithium on 3-acetyl-2*H*-indazole

A 10 mL round bottomed flask equipped with a Teflon stirring bar and a rubber septum was connected to a Schlenk line. The system was flame dried and flushed with nitrogen three times. To the flask, 3-acetyl-2*H*-indazole (32 mg, 0.20 mmol, 1.0 eq) and dry THF (1.5 mL) was added, and the solution was cooled to -78 °C. Once cooled, phenyllithium (0.16 mL, 1.54 M in dibutyl ether, 0.25 mmol, 1.3 eq) was added dropwise. The reaction was followed by TLC using samples taken from the reaction mixture and quenched with water. The product was purified by silica gel flash column chromatography eluded with 0-20% EtOAc : pentane. The product was obtained; 8 mg (18% yield) of **20** as a white powder. In 20% EtOAc : pentane, the product has Rf 0.5. ^{1}H-NMR (400 MHz, Chloroform-*d*) δ 8.04 (t, 2H), 7.87 (t, *J* = 7.8 Hz, 1H), 7.78 – 7.72 (m, 3H), 7.59 – 7.49 (m, 4H). HRMS: 221.10745 (M^+, 100), 222.11068 (15). Calcd. 221.10732.

4.4.3 Nucleophilic attack of lithiated indazole on 3-acetyl-2*H*-indazole

A 50 mL round bottomed flask equipped with a Teflon stirring bar and a rubber septum was connected to a Schlenk line. The system was flame dried and flushed with nitrogen three times. The flask was charged with 3-bromoindazole (788 mg, 4.00 mmol, 1.00 eq) and dry THF (20 mL). The mixture was cooled -78 °C, then *n*-BuLi was added (2.8 mL, 1.42 M, 1.0 eq). A temperature of at least -65 °C was maintained. After 5 min., *t*-BuLi (5.0 mL, 1.6 M, 2.0 eq) was added dropwise and the mixture was stirred for 15 min at -78 °C. 3-acetyl-2*H*-indazole (160 mg, 1.00 mmol, 0.250 eq) was added. The solution was stirred for 1 h at -78 °C. The reaction mixture was quenched with water and the product was extracted with EtOAc. Product ratios obtained are 3:2:2 of **22** : **9**: unknown product as shown in *figure 25*, suggesting a conversion to the desired product of approximately 43%. ^{1}H-NMR (400 MHz, DMSO-d_6) δ 7.56 (d, 4H), 7.43 (t, 2H), 7.20 (t, 2H), 3.34 (s, 3H).

4.5 Attempted synthetic route 4: N2 SEM protection for Directed *ortho*-Metalation

4.5.1 Synthesis of *N*2-SEM-indazole via SEM protection of indazole[60]

A 250 mL round bottomed flask equipped with a Teflon stirring bar and a rubber septum was connected to a Schlenk line. The system was flame dried and flushed with nitrogen three times. The flask was charged with indazole (1.12 g, 10.0 mmol, 1.00 eq) and THF (100 mL). To this was added dicyclohexylmethylamine (2.6 mL, 12 mmol, 1.2 eq), followed by SEM-Cl (2.1 mL, 12 mmol, 1.2 eq) and the mixture was stirred at room temperature for 3h. The mixture was diluted with ethyl acetate and quenched with 1 M NaOH (aq.). The organic layer was collected and washed with brine, dried over sodium sulfate, filtered, and the solvent was removed *in vacuo*. The residue was purified using silica gel flash column chromatography, eluding with a step gradient of 0-20% EtOAc : pentane, to give 1.661 g of product (66% yield). The product has an Rf of 0.4 in 10% EtOAc : pentane. ^{1}H-NMR (400 MHz, Chloroform-*d*) δ 8.11 (s, 1H), 7.73 (d, 1H), 7.68 (d, *J* = 8.4, 1.1 Hz, 1H), 7.30 (t, *J* = 8.7, 6.8 Hz, 1H), 7.10 (t, 1H), 5.73 (s, 2H), 3.63 (t, *J* = 8.2, 1.0 Hz, 2H), 0.94 (t, *J* = 8.9, 7.7 Hz, 2H), -0.03 (s, 9H). ^{1}H-NMR data matches that of the literature report.[60]

4.5.2 Synthesis of 24 via lithiation and BzCl electrophile trapping of *N*2-SEM-indazole [60]

A 25 mL round bottomed flask equipped with a Teflon stirring bar and a rubber septum was connected to a Schlenk line. The system was flame dried and flushed with nitrogen three times. The flask was charged with *N*2-SEM-indazole (248 mg, 1.00 mmol, 1.00 eq) and THF (6 mL), and was cooled to -78 °C. Once cooled, *n*-BuLi (0.78 mL, 1.42, 1.1 mmol, 1.1 eq) was added dropwise, giving a pale-yellow solution. The mixture was stirred at this temperature for 10 min., cooling was removed whilst stirring for 5 min., then the mixture was cooled to -78 °C again. Benzoyl chloride (0.13 mL, 1.1 mmol, 1.1 eq) was added and the mixture was stirred at room temperature for 30 min. The reaction was quenched with NH_4Cl (aq.). The organic layer was separated, washed with brine, dried with $MgSO_4$, filtered and the solvent was removed *in vacuo*. The crude product was analysed using ^{1}H-NMR. By this analysis, the ratio of desired product to side products is 12:7. The product has Rf 0.55 in 10% EtOAc : pentane. ^{1}H-NMR (400 MHz, Chloroform-*d*) δ 7.90 – 7.82 (m, 3H), 7.61 (t, *J* = 7.6 Hz, 1H), 7.52 (td, *J* = 7.6, 5.6 Hz, 4H), 7.49 – 7.42 (m, 2H), 7.36 – 7.29 (m, 1H), 7.14 – 7.03 (m, 2H), 6.16 (s, 2H), 3.68 – 3.61 (m, 2H), 0.92 – 0.86 (m, 2H), -0.09 (s, 9H). ^{1}H-NMR data roughly matches that of the literature report, there is significant overlap with side products and starting material.[60]

4.5.3 Attempted one-pot synthesis of BODIzy dye 2 from *N*2-SEM-indazole

A 25 mL round bottomed flask equipped with a Teflon stirring bar and a rubber septum was connected to a Schlenk line. The system was flame dried and flushed with nitrogen three times. The flask was charged with *N*2-SEM-indazole (248 mg, 1.00 mmol, 1.00 eq) and THF (6 mL), and was cooled to -78 °C. Once cooled, *n*-BuLi (0.78 mL, 1.42, 1.1 mmol, 1.1 eq) was added dropwise, giving a pale-yellow solution. The mixture was stirred at this temperature for 10 min., cooling was removed whilst stirring for 5 min., then the mixture was cooled to -78 °C again. Benzoyl chloride (0.65 mL, 0.55 mmol, 0.55 eq) was added and the mixture was stirred at room temperature for 30 min., before BF_3OEt_2 was added and the mixture was stirred for 40 h at room temperature. The reaction was quenched with NH_4Cl (aq.). The organic layer was separated, washed with brine, dried with $MgSO_4$, filtered and the solvent was removed *in vacuo*. The crude product was analysed using ^{1}H-NMR, from which no conclusions could be drawn as to the structure of the formed products.

4.5.4 Attempted synthesis of 25 via nucleophilic attack of phenyllithium on *N*2-SEM-3-benzoyl-indazole

A 25 mL round bottomed flask equipped with a Teflon stirring bar and a rubber septum was connected to a Schlenk line. The system was flame dried and flushed with nitrogen three times. The flask was charged with crude *N*2-SEM-3-benzoyl-indazole (31 mg, 0.070 mmol, 1.0 eq) and dry THF (1.5 mL), and the solution was cooled to -78 °C. Once cooled, phenyllithium (0.05 mL, 1.54 M in dibutyl ether, 0.08 mmol, 1.1 eq) was added dropwise. The reaction was tracked by TLC using samples taken from the reaction mixture and quenched with water. The product was purified by silica gel flash column chromatography eluded with 0-5% EtOAc : pentane. The obtained product was obtained; 6.0 mg (20% yield) of **25** as a white crystal. The product has Rf 0.8 in 5% EtOAc : pentane. HRMS: 283.12298 (M^+, 1), 212.11851 (100). Calcd. 283.12298.

5. References

1. Velema, W. A., Szymanski, W. & Feringa, B. L. Photopharmacology: Beyond Proof of Principle. *J. Am. Chem. Soc.* **136**, 2178–2191 (2014).

2. Hüll, K., Morstein, J. & Trauner, D. In Vivo Photopharmacology. *Chem. Rev.* **118**, 10710–10747 (2018).

3. Gautier, A. *et al.* How to control proteins with light in living systems. *Nat. Chem. Biol.* **10**, 533–541 (2014).

4. Fuchter, M. J. On the Promise of Photopharmacology Using Photoswitches: A Medicinal Chemist's Perspective. *J. Med. Chem.* **63**, 11436–11447 (2020).

5. Slanina, T. *et al.* In Search of the Perfect Photocage: Structure–Reactivity Relationships in meso -Methyl BODIPY Photoremovable Protecting Groups. *J. Am. Chem. Soc.* **139**, 15168–15175 (2017).

6. Wöll, D. *et al.* Intramolecular Sensitization of Photocleavage of the Photolabile 2-(2-Nitrophenyl)propoxycarbonyl (NPPOC) Protecting Group: Photoproducts and Photokinetics of the Release of Nucleosides. *Chem. Eur. J.* **14**, 6490–6497 (2008).

7. Zhao, H., Sterner, E. S., Coughlin, E. B. & Theato, P. o -Nitrobenzyl Alcohol Derivatives: Opportunities in Polymer and Materials Science. *Macromolecules* **45**, 1723–1736 (2012).

8. Yang, H., Zhang, X., Zhou, L. & Wang, P. Development of a Photolabile Carbonyl-Protecting Group Toolbox. *J. Org. Chem.* **76**, 2040–2048 (2011).

9. Klán, P. *et al.* Photoremovable Protecting Groups in Chemistry and Biology: Reaction Mechanisms and Efficacy. *Chem. Rev.* **113**, 119–191 (2013).

10. Holmes, C. P. Model Studies for New o -Nitrobenzyl Photolabile Linkers: Substituent Effects on the Rates of Photochemical Cleavage. *J. Org. Chem.* **62**, 2370–2380 (1997).

11. Hansen, M. J., Velema, W. A., Lerch, M. M., Szymanski, W. & Feringa, B. L. Wavelength-selective cleavage of photoprotecting groups: strategies and applications in dynamic systems. *Chem. Soc. Rev.* **44**, 3358–3377 (2015).

12. Welleman, I. M., Hoorens, M. W. H., Feringa, B. L., Boersma, H. H. & Szymański, W. Photoresponsive molecular tools for emerging applications of light in medicine. *Chem. Sci.* **11**, 11672–11691 (2020).

13. Silva, J. M., Silva, E. & Reis, R. L. Light-triggered release of photocaged therapeutics - Where are we now? *J. Control. Release* **298**, 154–176 (2019).

14. Barltrop, J. A. & Schofield, P. Photosensitive Protecting Groups. *Tetrahedron Lett.* **3**, 697–699 (1962).

15. Kaplan, J. H., Forbush, B. & Hoffman, J. F. Rapid photolytic release of adenosine 5'-triphosphate from a protected analog: utilization by the sodium:potassium pump of human red blood cell ghosts. *Biochem.* **17**, 1929–1935 (1978).

16. Engels, J. & Schlaeger, E. J. Synthesis, structure, and reactivity of adenosine cyclic 3',5'-phosphate-benzyltriesters. *J. Med. Chem.* **20**, 907–911 (1977).

17. Vorobev, A. Y. & Moskalensky, A. E. Long-wavelength photoremovable protecting groups: On the

way to in vivo application. *Comput. Struct. Biotechnol. J.* **18**, 27–34 (2020).

18. Kand, D. *et al.* Organelle-Targeted BODIPY Photocages: Visible-Light-Mediated Subcellular Photorelease. *Angew. Chem. Int. Ed.* **58**, 4659–4663 (2019).

19. Shrestha, P. *et al.* Efficient Far-Red/Near-IR Absorbing BODIPY Photocages by Blocking Unproductive Conical Intersections. *J. Am. Chem. Soc.* **142**, 15505–15512 (2020).

20. Kand, D. *et al.* Water-Soluble BODIPY Photocages with Tunable Cellular Localization. *J. Am. Chem. Soc.* **142**, 4970–4974 (2020).

21. Smith, A. M., Mancini, M. C. & Nie, S. Second window for in vivo imaging. *Nat. Nanotechnol.* **4**, 710–711 (2009).

22. Rubinstein, N., Liu, P., Miller, E. W. & Weinstain, R. meso-Methylhydroxy BODIPY: a scaffold for photo-labile protecting groups. *ChemComm* **51**, 6369–6372 (2015).

23. Jun, J. V., Chenoweth, D. M. & Petersson, E. J. Rational design of small molecule fluorescent probes for biological applications. *Org. Biomol. Chem.* **18**, 5747–5763 (2020).

24. Braslavsky, S. E. Glossary of terms used in photochemistry, 3rd edition (IUPAC Recommendations 2006). *Pure Appl. Chem.* **79**, 293–465 (2007).

25. Givens, R. S., Rubina, M. & Wirz, J. Applications of p-hydroxyphenacyl (pHP) and coumarin-4-ylmethyl photoremovable protecting groups. *Photochem. Photobiol.* **11**, 472 (2012).

26. Chaudhuri, A., Venkatesh, Y., Behara, K. K. & Singh, N. D. P. Bimane: A Visible Light Induced Fluorescent Photoremovable Protecting Group for the Single and Dual Release of Carboxylic and Amino Acids. *Org.* **19**, 1598–1601 (2017).

27. Truong, V. X., Li, F. & Forsythe, J. S. Visible Light Activation of Nucleophilic Thiol-X Addition via Thioether Bimane Photocleavage for Polymer Cross-Linking. *Biomacromolecules* **19**, 4277–4285 (2018).

28. Walton, D. P. & Dougherty, D. A. A general strategy for visible-light decaging based on the quinone cis -alkenyl lock. *ChemComm* **55**, 4965–4968 (2019).

29. Dcona, M. M., Mitra, K. & Hartman, Matthew, C. T. Photocontrolled activation of small molecule cancer therapeutics. *RSC Med. Chem.* **9**, 982–1002 (2020).

30. Singh, P. K., Majumdar, P. & Singh, S. P. Advances in BODIPY photocleavable protecting groups. *Coord. Chem. Rev.* **449**, 214193 (2021).

31. Weinstain, R., Slanina, T., Kand, D. & Klán, P. Visible-to-NIR-Light Activated Release: From Small Molecules to Nanomaterials. *Chem. Rev.* **120**, 13135–13272 (2020).

32. Nani, R. R., Gorka, A. P., Nagaya, T., Kobayashi, H. & Schnermann, M. J. Near-IR Light-Mediated Cleavage of Antibody-Drug Conjugates Using Cyanine Photocages. *Angew. Chem. Int. Ed.* **54**, 13635–13638 (2015).

33. Palao, E. *et al.* Transition-Metal-Free CO-Releasing BODIPY Derivatives Activatable by Visible to NIR Light as Promising Bioactive Molecules. *J. Am. Chem. Soc.* **138**, 126–133 (2016).

34. Nani, R. R. *et al.* In Vivo Activation of Duocarmycin–Antibody Conjugates by Near-Infrared Light. *ACS Cent. Sci.* **3**, 329–337 (2017).

35. Zhao, L. *et al.* Near-Infrared Photoregulated Drug Release in Living Tumor Tissue via Yolk-Shell Upconversion Nanocages. *Adv. Funct. Mater.* **24**, 363–371 (2014).

36. Treibs, A. & Kreuzer, F.-H. Difluorboryl-Komplexe von Di- und Tripyrrylmethenen. *Liebigs Ann.* **718**, 208–223 (1968).

37. Karolin, J., Johansson, L. B.-A., Strandberg, L. & Ny, T. Fluorescence and Absorption Spectroscopic Properties of Dipyrrometheneboron Difluoride (BODIPY) Derivatives in Liquids, Lipid Membranes, and Proteins. *J. Am. Chem. Soc.* **116**, 7801–7806 (1994).

38. Ehrenschwender, T. & Wagenknecht, H.-A. 4,4-Difluoro-4-bora-3a,4a-diaza-s-indacene as a Bright Fluorescent Label for DNA. *J. Org. Chem.* **76**, 2301–2304 (2011).

39. Zampetti, A. *et al.* Highly Efficient Solid-State Near-infrared Organic Light-Emitting Diodes incorporating A-D-A Dyes based on α,β-unsubstituted "BODIPY" Moieties. *Sci.* **7**, 1611 (2017).

40. Awuah, S. G. & You, Y. Boron dipyrromethene (BODIPY)-based photosensitizers for photodynamic therapy. *RSC Adv.* **2**, 11169 (2012).

41. Marques dos Santos, J. *et al.* BODIPY derivatives with near infra-red absorption as small molecule donors for bulk heterojunction solar cells. *RSC Adv.* **9**, 15410–15423 (2019).

42. Ortiz, A. Triarylamine-BODIPY derivatives: A promising building block as hole transporting materials for efficient perovskite solar cells. *Dye. Pigm.* **171**, 107690 (2019).

43. Çetindere, S. Photophysics of BODIPY Dyes: Recent Advances. in *Photophysics, Photochemical and Substitution Reactions - Recent Advances* (IntechOpen, 2021). doi:10.5772/intechopen.92609.

44. Tram, K., Yan, H., Jenkins, H. A., Vassiliev, S. & Bruce, D. The synthesis and crystal structure of unsubstituted 4,4-difluoro-4-bora-3a,4a-diaza-s-indacene (BODIPY). *Dye. Pigm.* **82**, 392–395 (2009).

45. Chen, Y., Zhao, J., Guo, H. & Xie, L. Geometry Relaxation-Induced Large Stokes Shift in Red-Emitting Borondipyrromethenes (BODIPY) and Applications in Fluorescent Thiol Probes. *J. Org. Chem.* **77**, 2192–2206 (2012).

46. Qu, X. *et al.* Enhancing the Stokes' shift of BODIPY dyes via through-bond energy transfer and its application for Fe3+-detection in live cell imaging. *ChemComm* **48**, 4600 (2012).

47. Loudet, A. & Burgess, K. BODIPY Dyes and Their Derivatives: Syntheses and Spectroscopic Properties. *Chem. Rev.* **107**, 4891–4932 (2007).

48. Zhou, E. Y. *et al.* Near-Infrared Photoactivatable Nitric Oxide Donors with Integrated Photoacoustic Monitoring. *J. Am. Chem. Soc.* **140**, 11686–11697 (2018).

49. Li, T. *et al.* Aza-BODIPY dyes with heterocyclic substituents and their derivatives bearing a cyanide co-ligand: NIR donor materials for vacuum-processed solar cells. *J. Mater. Chem. A* **5**, 10696–10703 (2017).

50. Basu, K., Poirier, M. & Ruck, R. T. Solution to the C 3 –Arylation of Indazoles: Development of a Scalable Method. *Org.* **18**, 3218–3221 (2016).

51. Unsinn, A. & Knochel, P. Regioselective zincation of indazoles using TMP2Zn and Negishi cross-

coupling with aryl and heteroaryl iodides. *ChemComm* **48**, 2680 (2012).

52. Murphy, L. R., Meek, T. L., Allred, A. L. & Allen, L. C. Evaluation and Test of Pauling's Electronegativity Scale. *J. Phys. Chem.* **104**, 5867–5871 (2000).

53. Zhang, L. *et al.* Rh(iii)-catalyzed, hydrazine-directed C–H functionalization with 1-alkynylcyclobutanols: a new strategy for 1H-indazoles. *ChemComm* **56**, 7415–7418 (2020).

54. Wunderlich, S. H. & Knochel, P. (TMP)2Zn·2 MgCl2·2 LiCl: A Chemoselective Base for the Directed Zincation of Sensitive Arenes and Heteroarenes. *Angew. Chem. Int. Ed.* **46**, 7685–7688 (2007).

55. Kienle, M., Dunst, C. & Knochel, P. Oxidative Amination of Heteroaromatic Zinc Reagents Mediated by PhI(OAc) 2. *Org.* **11**, 5158–5161 (2009).

56. Boens, N., Verbelen, B., Ortiz, M. J., Jiao, L. & Dehaen, W. Synthesis of BODIPY dyes through postfunctionalization of the boron dipyrromethene core. *Coord. Chem. Rev.* **399**, 213024 (2019).

57. Metzger, A., Bernhardt, S., Manolikakes, G. & Knochel, P. MgCl2-Accelerated Addition of Functionalized Organozinc Reagents to Aldehydes, Ketones, and Carbon Dioxide. *Angew. Chem. Int. Ed.* **49**, 4665–4668 (2010).

58. Tang, R.-J., Milcent, T. & Crousse, B. Regioselective Halogenation of Arenes and Heterocycles in Hexafluoroisopropanol. *J. Org. Chem.* **83**, 930–938 (2018).

59. Alam, R. M. & Keating, J. J. Regioselective N -alkylation of the 1 H -indazole scaffold; ring substituent and N -alkylating reagent effects on regioisomeric distribution. *Beilstein J. Org. Chem.* **17**, 1939–1951 (2021).

60. Luo, G., Chen, L. & Dubowchik, G. Regioselective Protection at N -2 and Derivatization at C -3 of Indazoles. *J. Org. Chem.* **71**, 5392–5395 (2006).

61. Xiao, J. *et al.* The design, synthesis, and biological evaluation of novel YC-1 derivatives as potent anti-hepatic fibrosis agents. *Org. Biomol. Chem.* **13**, 7257–7264 (2015).

62. Welch, W. M., Hanau, C. E. & Whalen, W. M. A Novel Synthesis of 3-Substituted Indazole Derivatives. *Synthesis* **1992**, 937–939 (1992).

63. Bunnell, A., O'Yang, C., Petrica, A. & Soth, M. J. Convenient Method for the 3-Functionalization of Isoindazoles. *Synth. Commun.* **36**, 285–293 (2006).

64. Casey, M. L., Kemp, D. S., Paul, K. G. & Cox, D. D. Physical organic chemistry of benzisoxazoles. I. Mechanism of the base-catalyzed decomposition of benzisoxazoles. *J. Org. Chem.* **38**, 2294–2301 (1973).

65. Muchowski, J. M. & Solas, D. R. Protecting groups for the pyrrole and indole nitrogen atom. The [2-(trimethylsilyl)ethoxy]methyl moiety. Lithiation of 1-[[2-(trimethylsilyl)ethoxy]methyl]pyrrole. *J. Org. Chem.* **49**, 203–205 (1984).

66. Ye, Y., Kevlishvili, I., Feng, S., Liu, P. & Buchwald, S. L. Highly Enantioselective Synthesis of Indazoles with a C3-Quaternary Chiral Center Using CuH Catalysis. *J. Am. Chem. Soc.* **142**, 10550–10556 (2020).

67. Whitten, J. P., Matthews, D. P. & McCarthy, J. R. [2-(Trimethylsilyl)ethoxy]methyl (SEM) as a novel and effective imidazole and fused aromatic imidazole protecting group. *J. Org. Chem.* **51**,

1891–1894 (1986).

68. Reich, H. J. Role of Organolithium Aggregates and Mixed Aggregates in Organolithium Mechanisms. *Chem. Rev.* **113**, 7130–7178 (2013).

69. Rohbogner, C. J., Wagner, A. J., Giuliano, C. C. & Knochel, P. Magnesation of Weakly Activated Arenes Using TMP2Mg·2LiCl: Synthesis of tert-Butyl Ethyl Phthalate. *Org. Synth.* **86**, 374 (2009).

6. Appendix

6.1 Straightforward lithiations and magnesations.

6.1.1 Compound 8: 3-bromoindazole

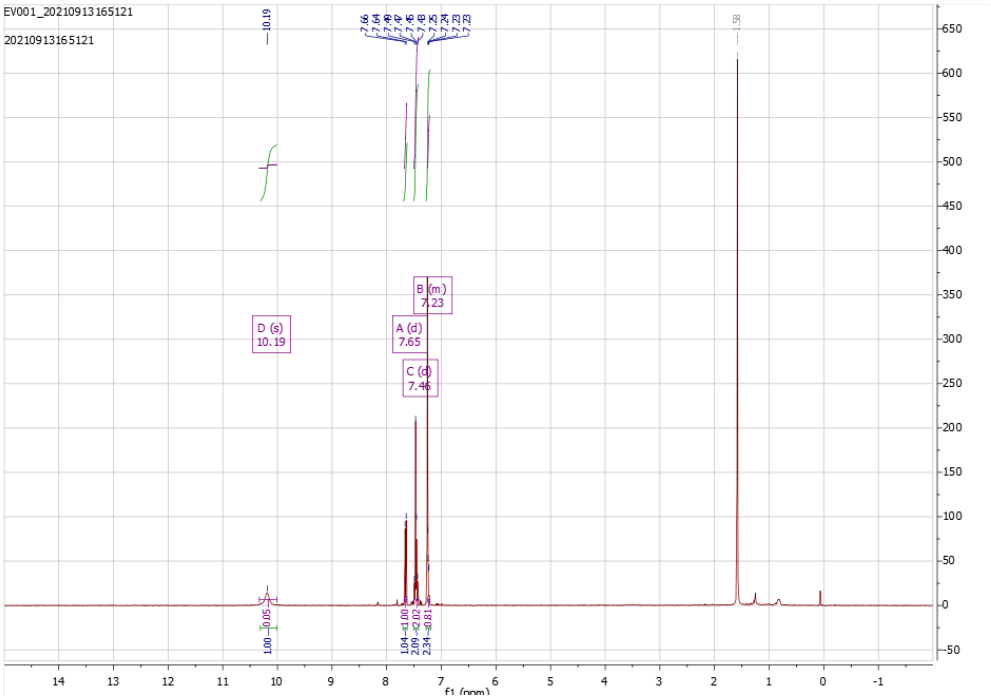

Figure 33: ^{1}H-NMR of the product of the bromination of indazole in $CDCl_3$.

6.1.2 Lithium/halogen exchange deuteration studies with entry 1 crude product

Figure 34: ^{1}H-NMR of the product of deuteration studies entry 1 in $CDCl_3$.

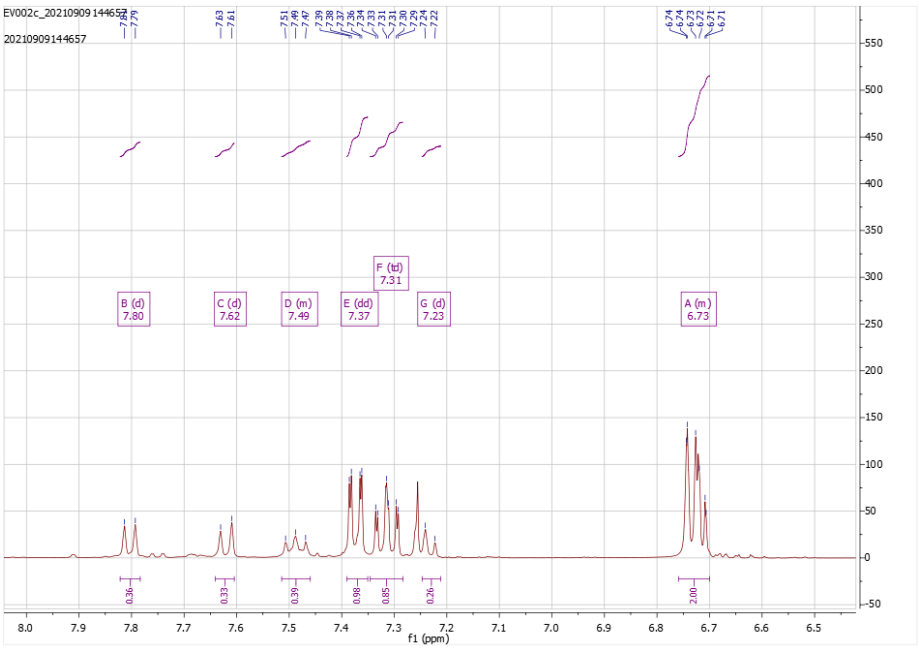

Figure 35: Expansion of ^{1}H-NMR spectrum of the crude product of deuteration studies entry 1. The multiplet around 6.73 ppm corresponds to formation of the ring opening product (see NMRs of 10 also).

6.1.3 Deuteration studies entry 2 aliquot

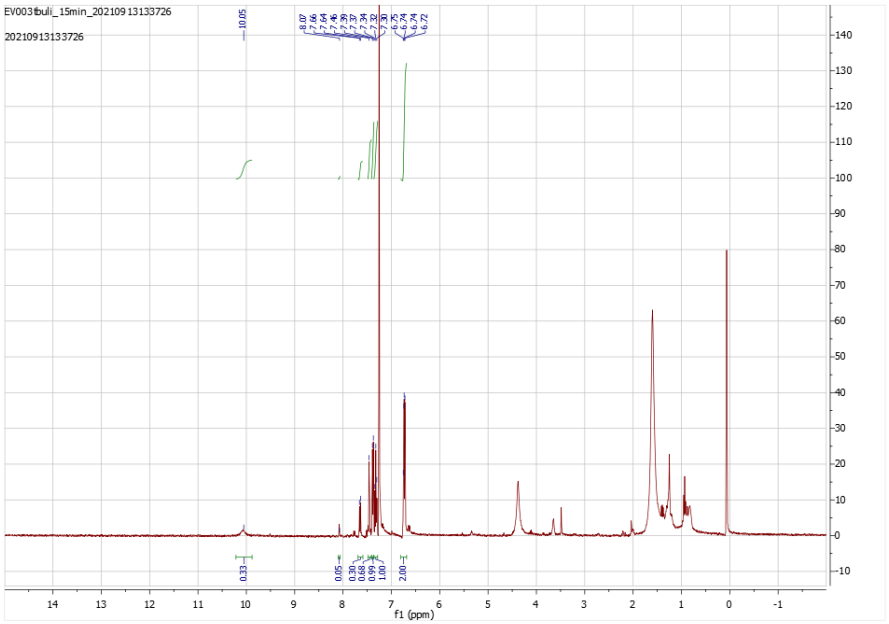

Figure 36: ^{1}H-NMR spectrum of an aliquot of the reaction mixture of deuteration studies entry 2 in $CDCl_3$.

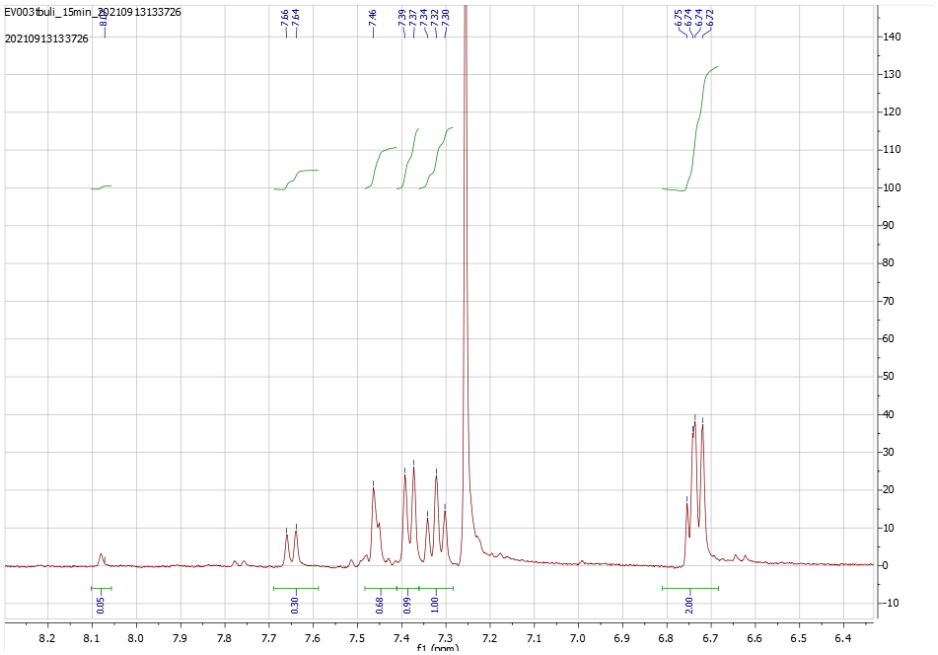

Figure 37: Expansion of previous ^{1}H-NMR spectrum 2. Note the NH signal around 10 ppm, C3H signal around 8.1 ppm and the ring opening multiplet around 6.7 ppm.

6.1.4 Deuteration studies entry 3 crude product:

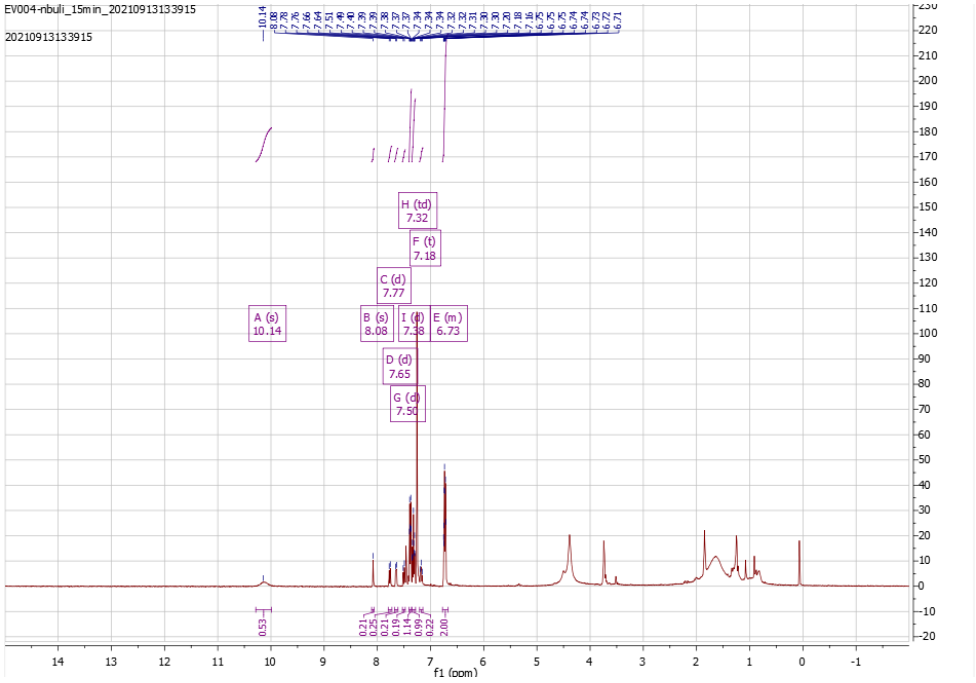

Figure 38: ^{1}H-NMR spectrum of an aliquot the reaction mixture of deuteration studies entry 3 in $CDCl_3$.

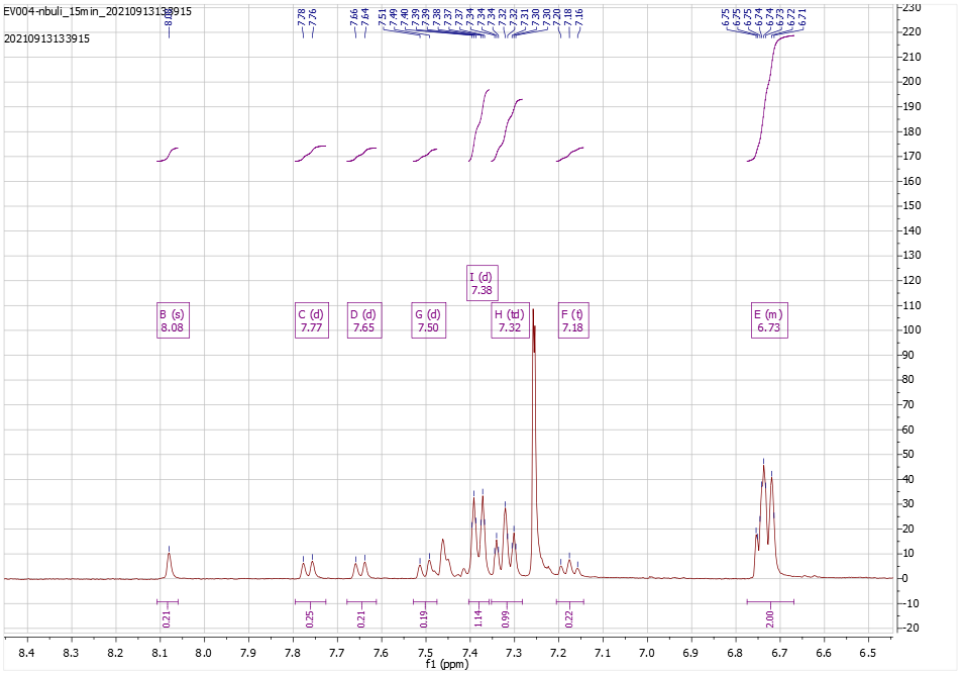

Figure 39: Expansion of the previous ^{1}H-NMR spectrum.

6.1.5 Deuteration studies entry 4 crude product

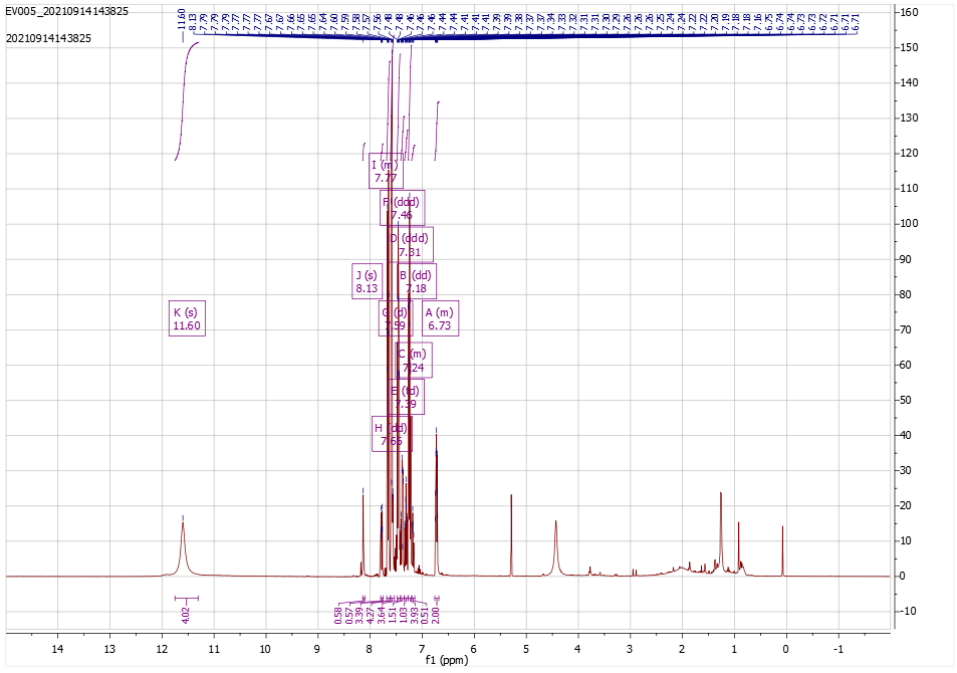

Figure 40: ^{1}H-NMR spectrum of the crude product of deuteration studies entry 4 in $CDCl_3$.

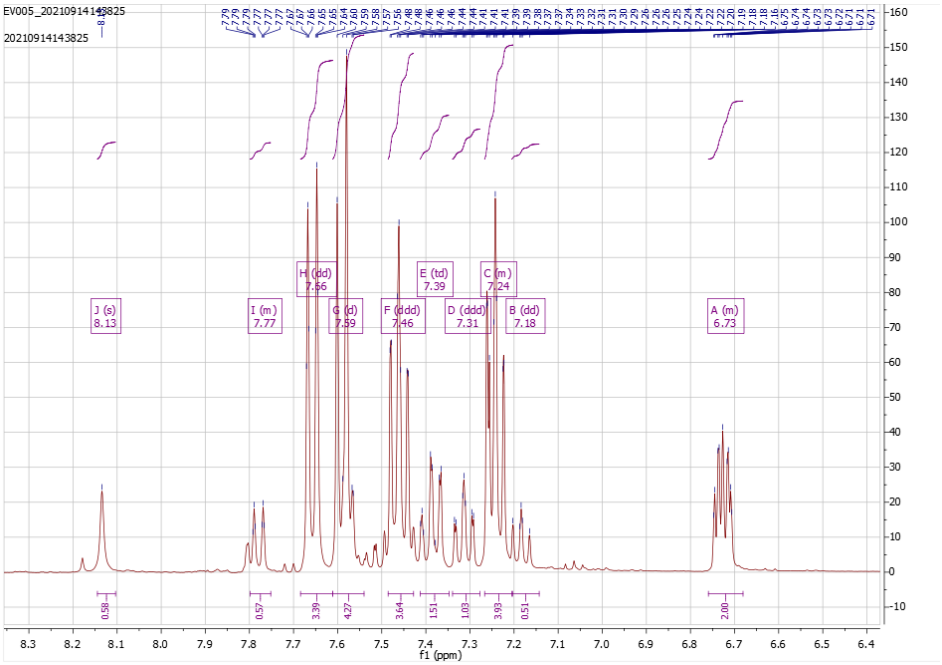

Figure 41: Expansion of the previous ^{1}H-NMR spectrum

6.1.6 Deuteration studies entry 5 crude product

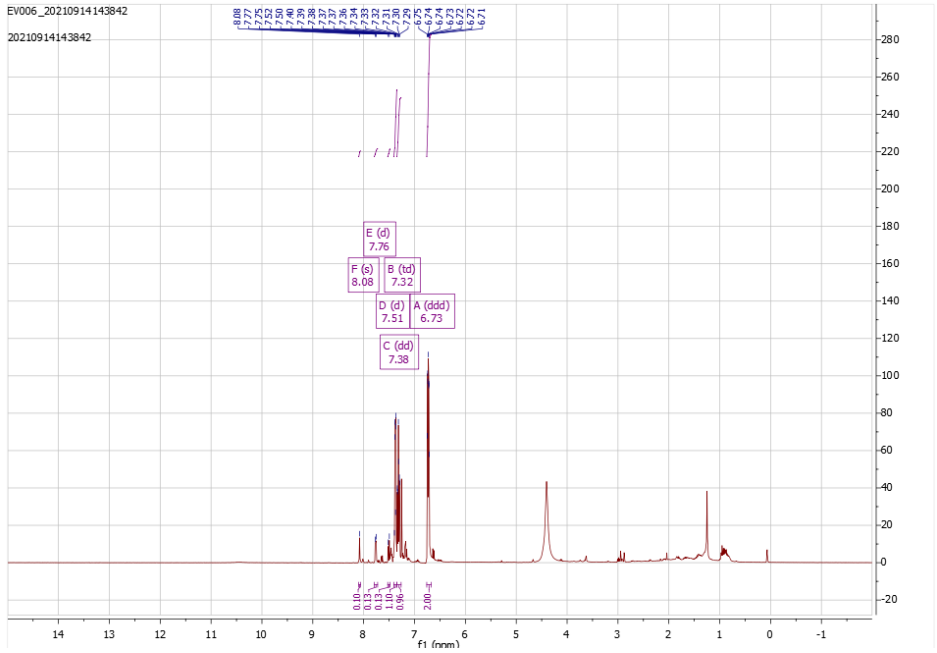

Figure 42: ^{1}H-NMR spectrum of the crude product of deuteration studies entry 5 in $CDCl_3$.

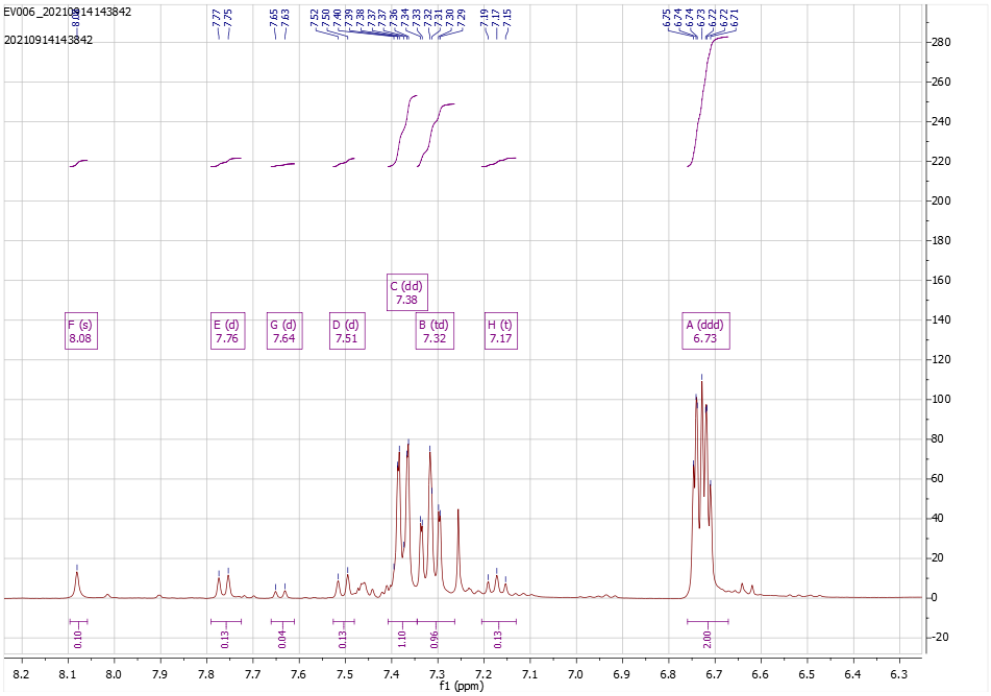

Figure 43: Expansion of the previous ^{1}H-NMR spectrum.

6.1.7 Deuteration studies entry 6 crude product

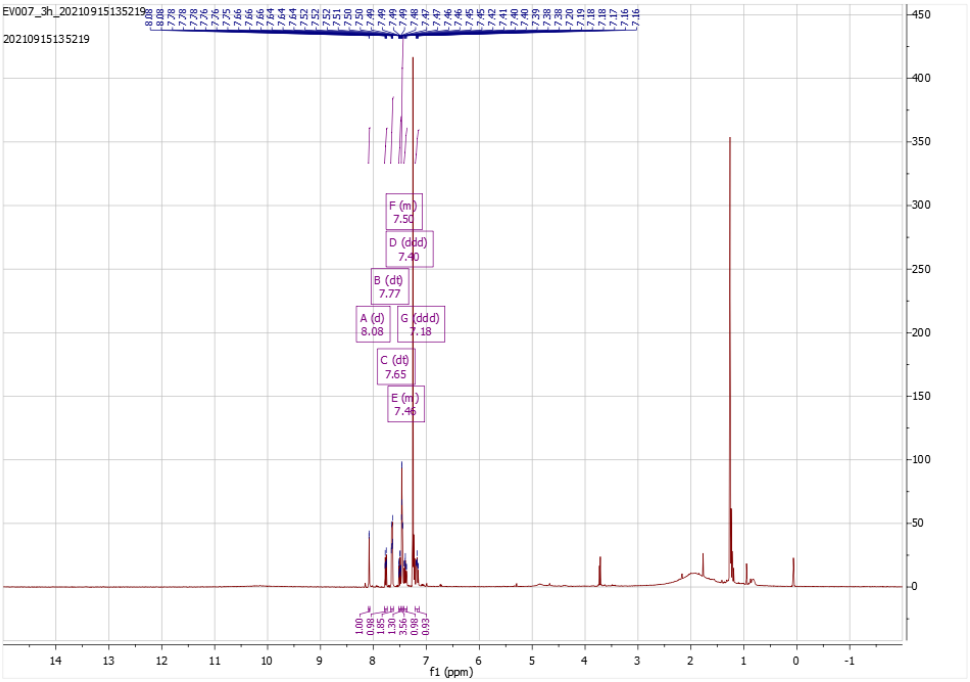

Figure 44: ^{1}H-NMR spectrum of an aliquot of the reaction mixture of deuteration studies entry 6 in $CDCl_3$.

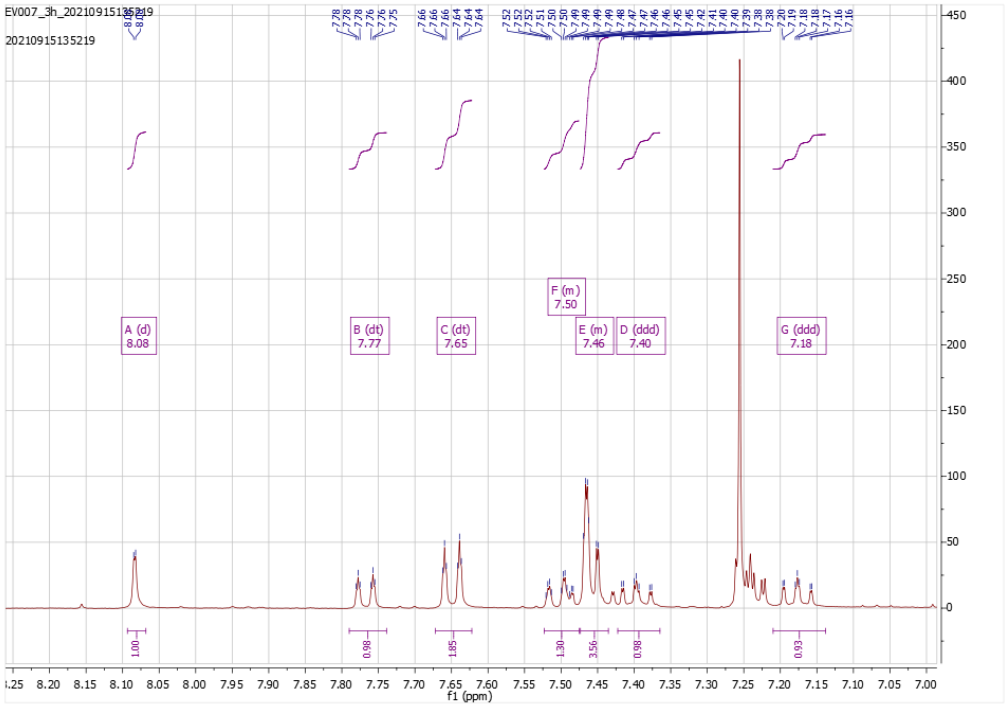

Figure 45: Expansion of the previous ^{1}H-NMR spectrum.

6.1.8 Compound 14: *N1*-benzyl-3-bromoindazole batch 1

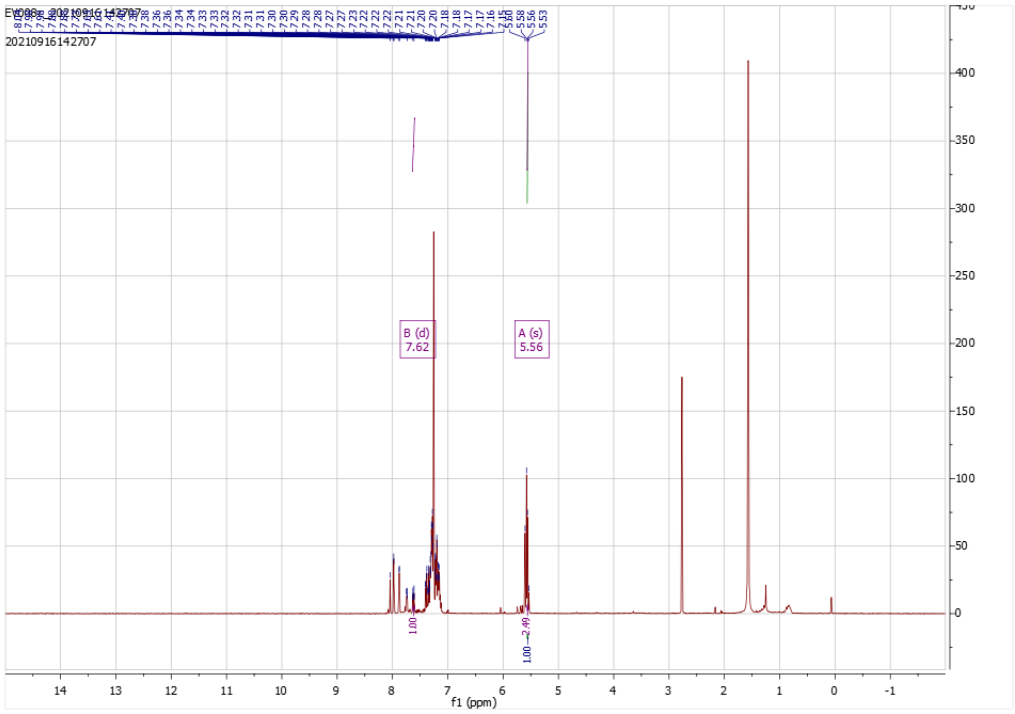

Figure 46: ^{1}H-NMR spectrum of batch 1 of N1*-benzyl-3-bromoindazole in $CDCl_3$. Characteristic signal of the desired products are integrated, see also the ^{1}H-NMR of compound **14** batch 2, which is the same product, only of higher purity.*

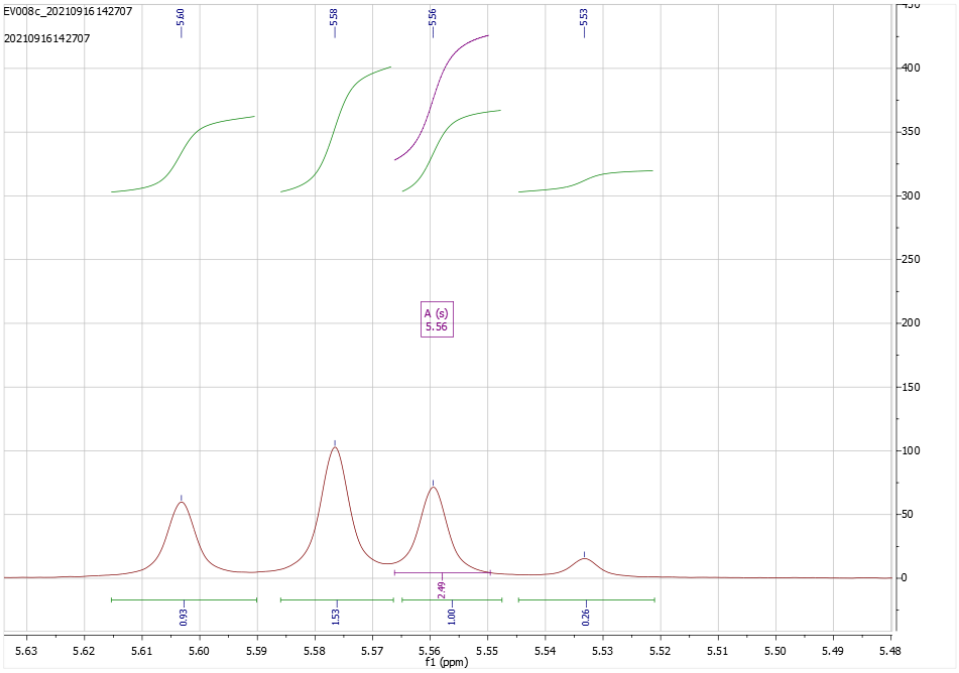

Figure 47: Expansion of the previous ^{1}H-NMR spectrum. The characteristic CH_2 benzyl signal of the product (5.56 ppm) compared to those of side products.

Compound **14:** *N1*-benzyl-3-bromoindazole batch 2

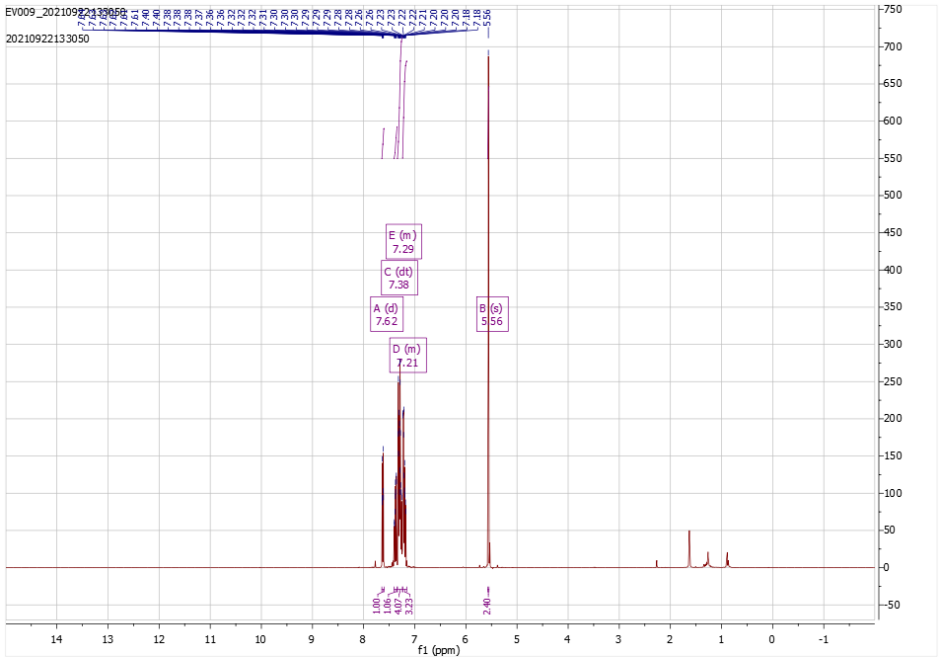

Figure 48: ^{1}H-NMR spectrum of batch 2 of N1-benzyl-3-bromoindazole in $CDCl_3$, corresponding to what is reported in literature. [61]

6.1.9 Ring opening product resulting from *N1*-benzyl-3-bromoindazole metalation isolated from attempted metalation of *N1*-benzyl-3-bromoindazole entry 1

6.1.10

Figure 49: ^{1}H-NMR spectrum of the ring opening product of N1*-benzyl-3-bromoindazole metalation.*

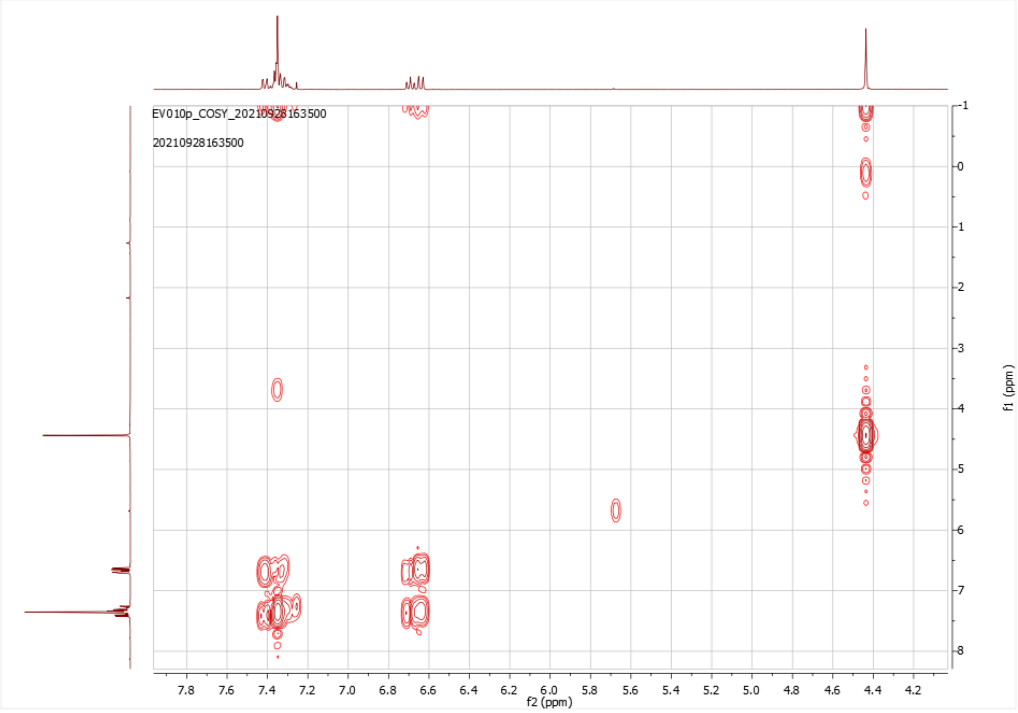

Figure 50: COSY NMR of the ring opening product of N1*-benzyl-3-bromoindazole metalation.*

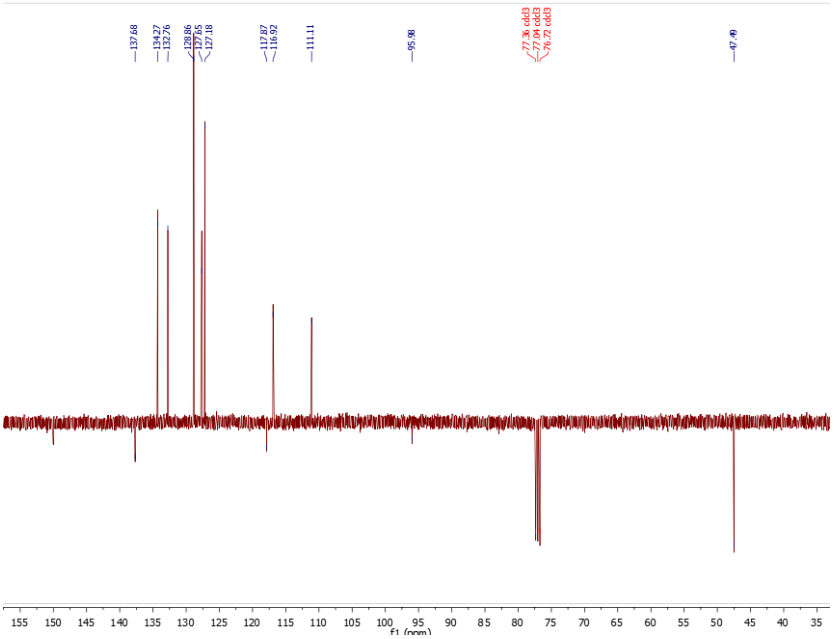

Figure 51: C APT NMR of the ring opening product of N1*-benzyl-3-bromoindazole metalation.*

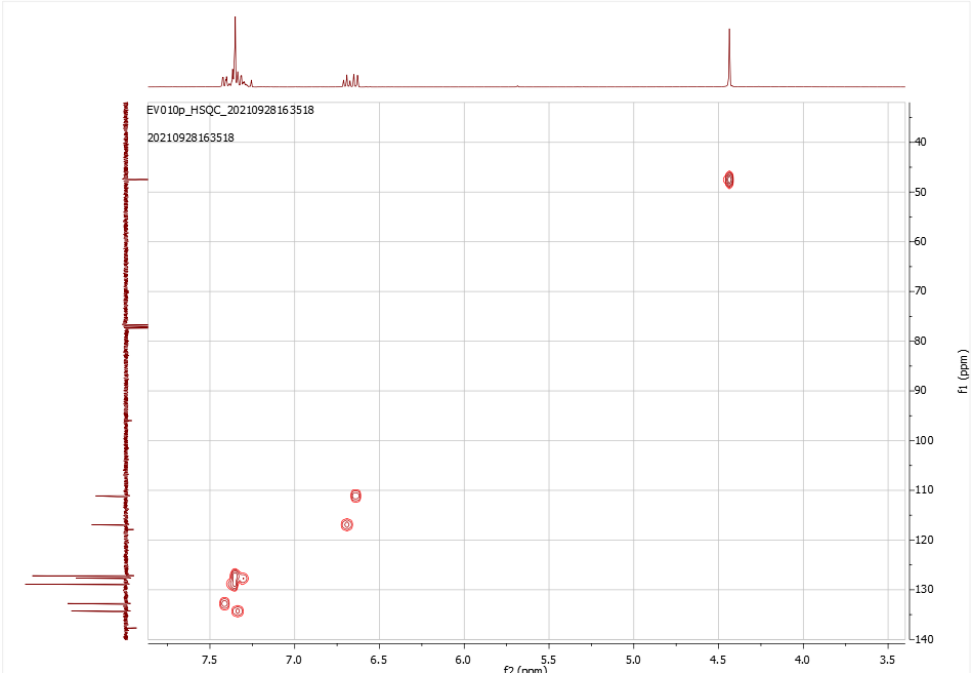

Figure 52: HSQC NMR of the ring opening product of N1*-benzyl-3-bromoindazole metalation.*

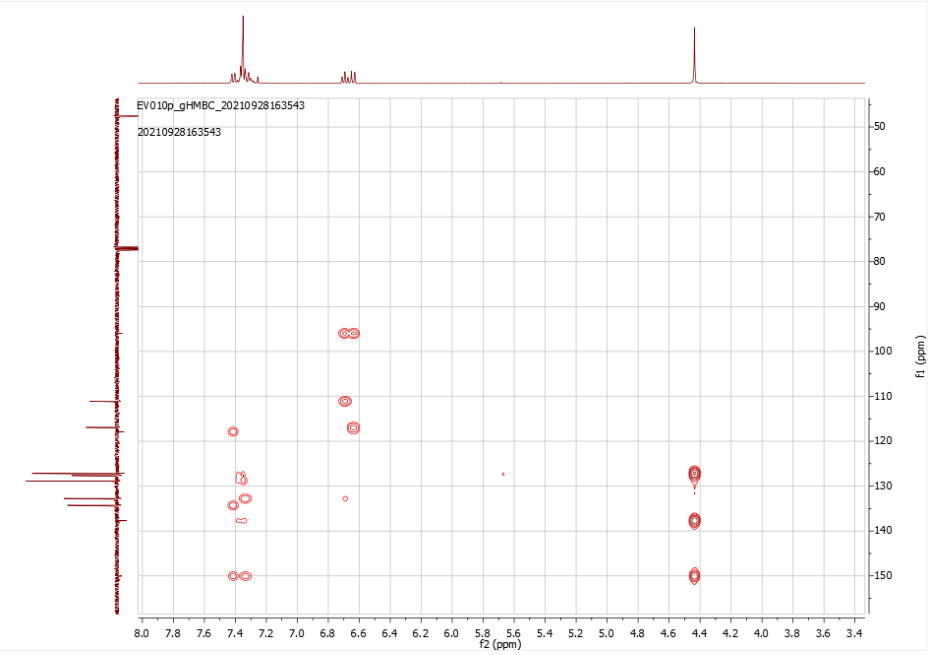

Figure 53: gHMBC NMR of the ring opening product of N1*-benzyl-3-bromoindazole metalation.*

Compound **14:** *N1*-benzyl-3-bromoindazole batch 3

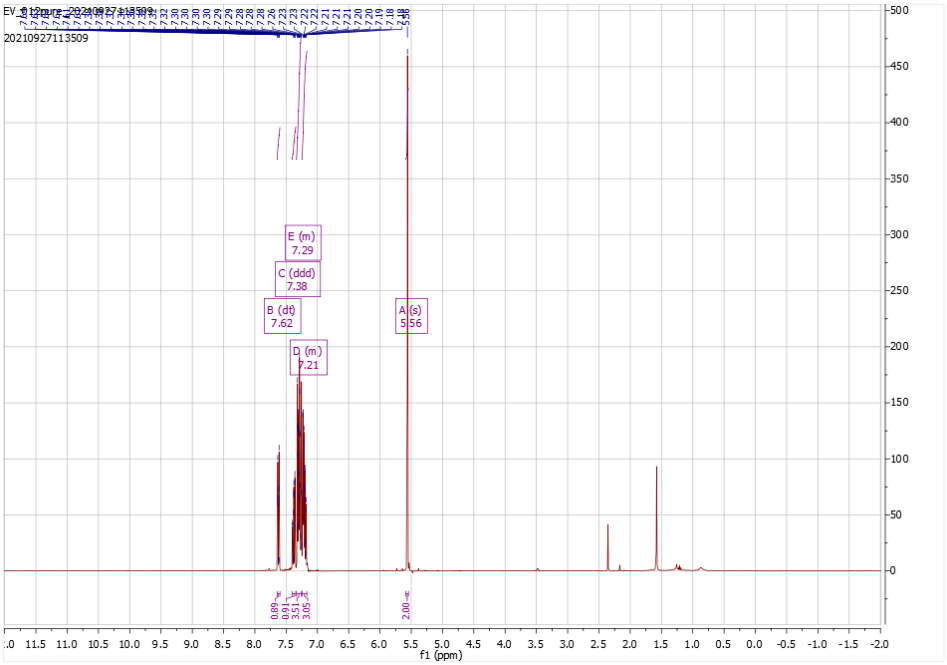

Figure 54: ^{1}H-NMR spectrum of batch 3 of N1*-benzyl-3-bromoindazole in $CDCl_3$.*

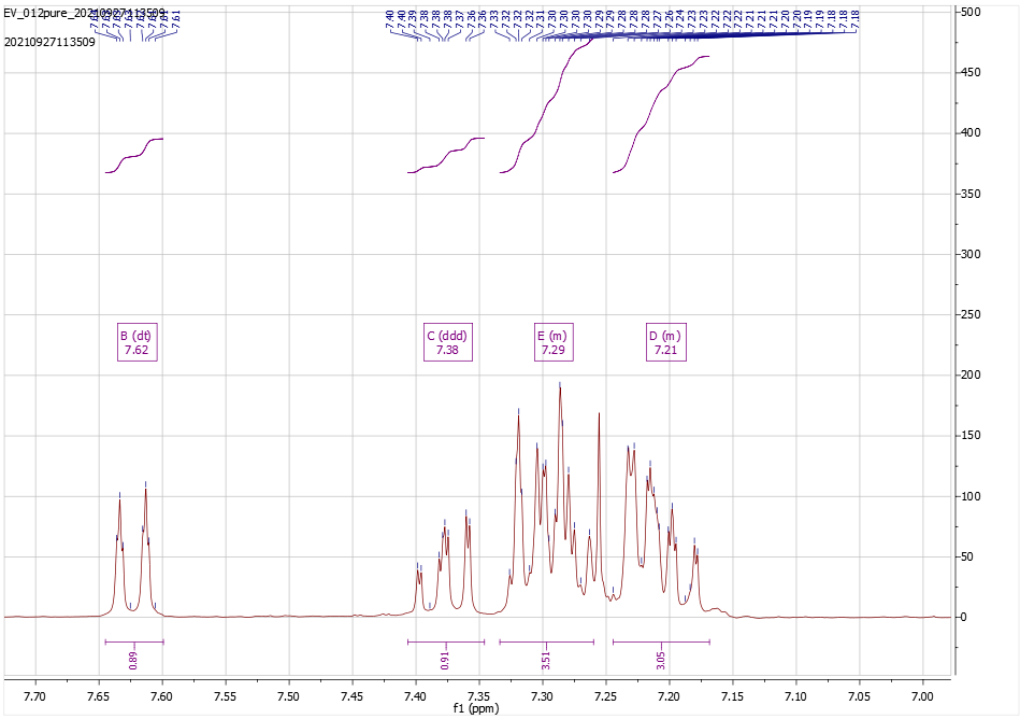

Figure 55: Expansion of the previous ^{1}H-NMR spectrum.

6.1.11 Attempted metalation of *N1*-benzyl-3-bromoindazole entry 2 aliquot

Figure 56: ^{1}H-NMR spectrum of the 30 min. aliquot of the reaction mixture in $CDCl_3$., note the triplet and doublet characteristic of ring opening around 6.57 ppm and the C3H signals around 8.1 ppm.

6.1.13 Attempted metalation of *N1*-benzyl-3-bromoindazole entry 3 aliquot

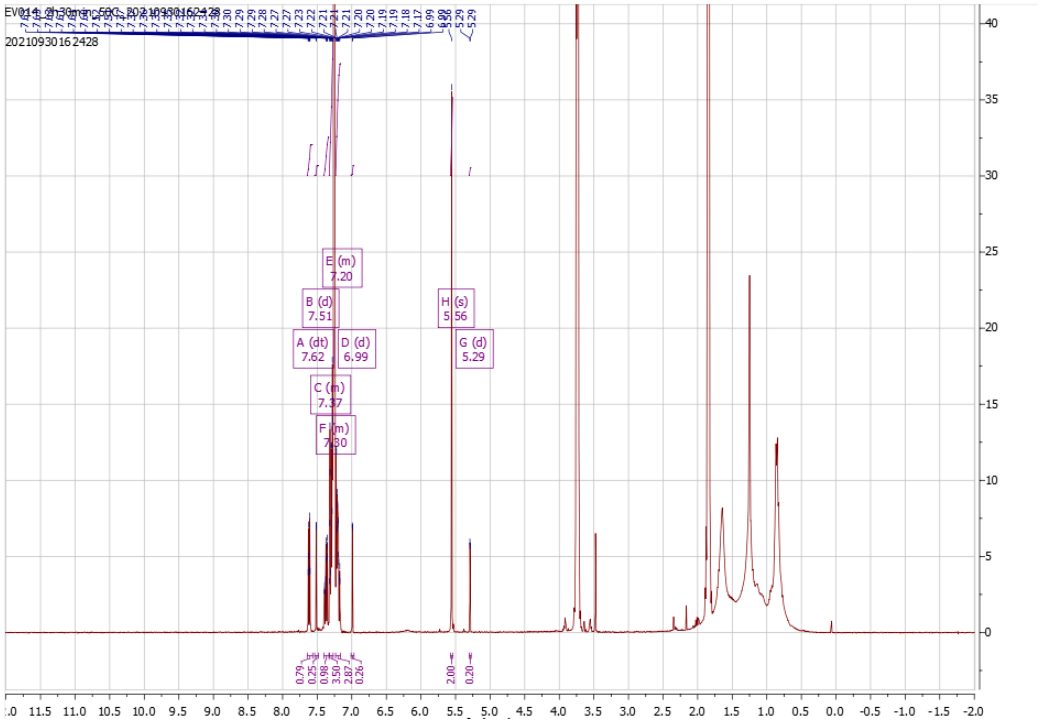

Figure 57: [1]H-NMR spectrum of an aliquot of the reaction mixture in $CDCl_3$ after at the end of the reaction as described in results and discussion. Upfield there is significant THF contamination.

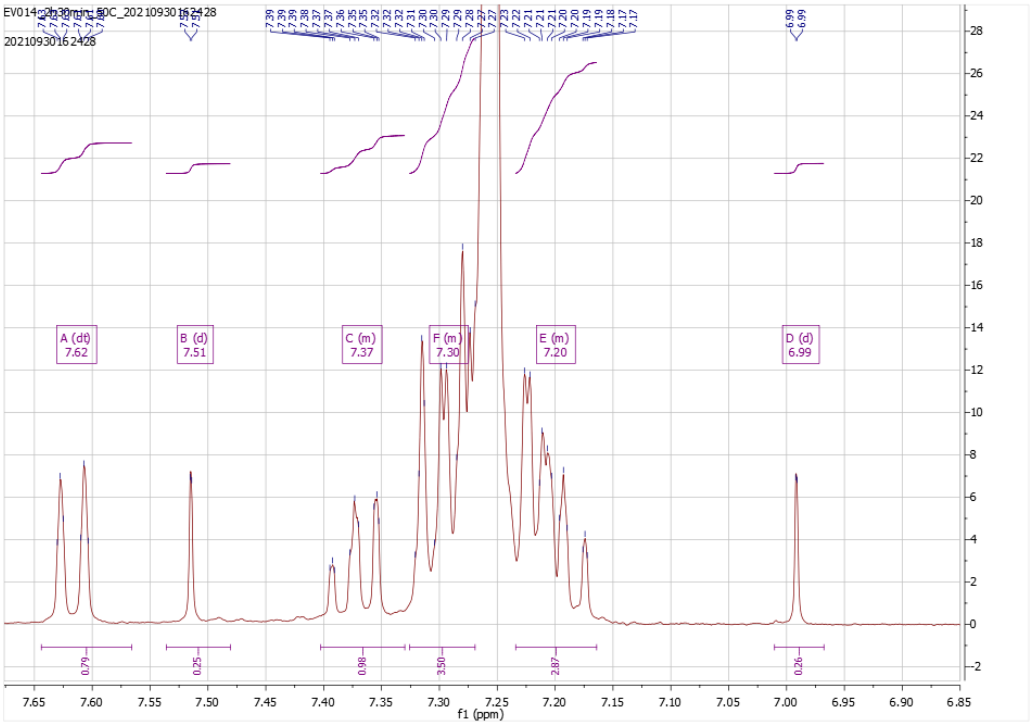

Figure 58: Expansion of [1]H-NMR spectrum of the previous spectrum.

6.1.14 Attempted metalation of *N1*-benzyl-3-bromoindazole entry 4

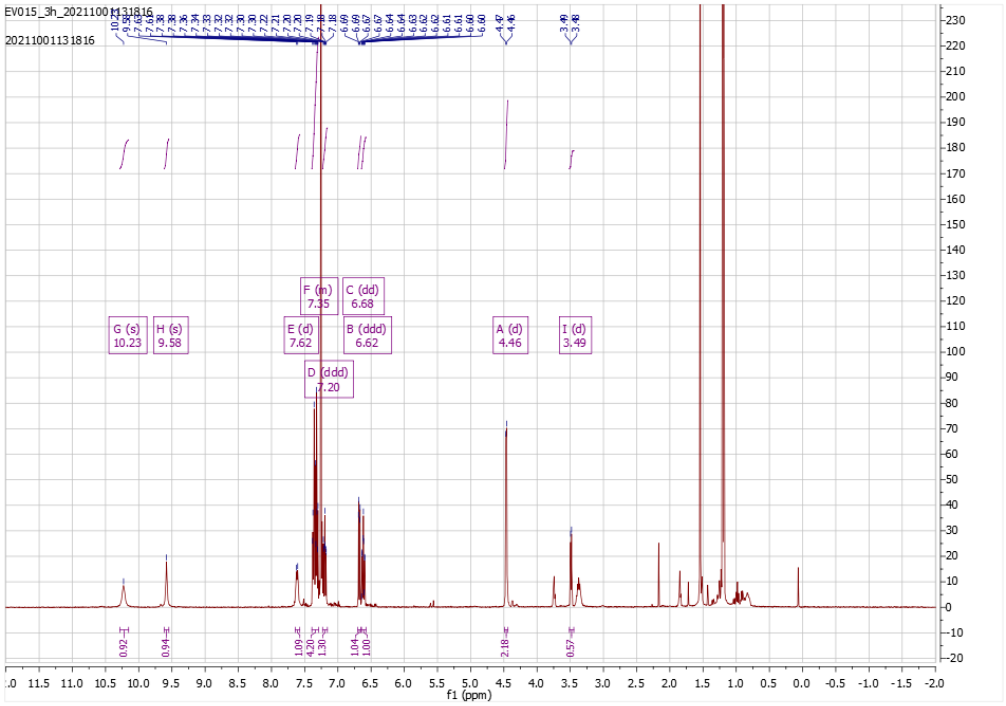

Figure 59: [1]H-NMR spectrum of the 3 h aliquot of the reaction mixture in $CDCl_3$. Note the NH signal around 9.6 and 10.4 ppm.

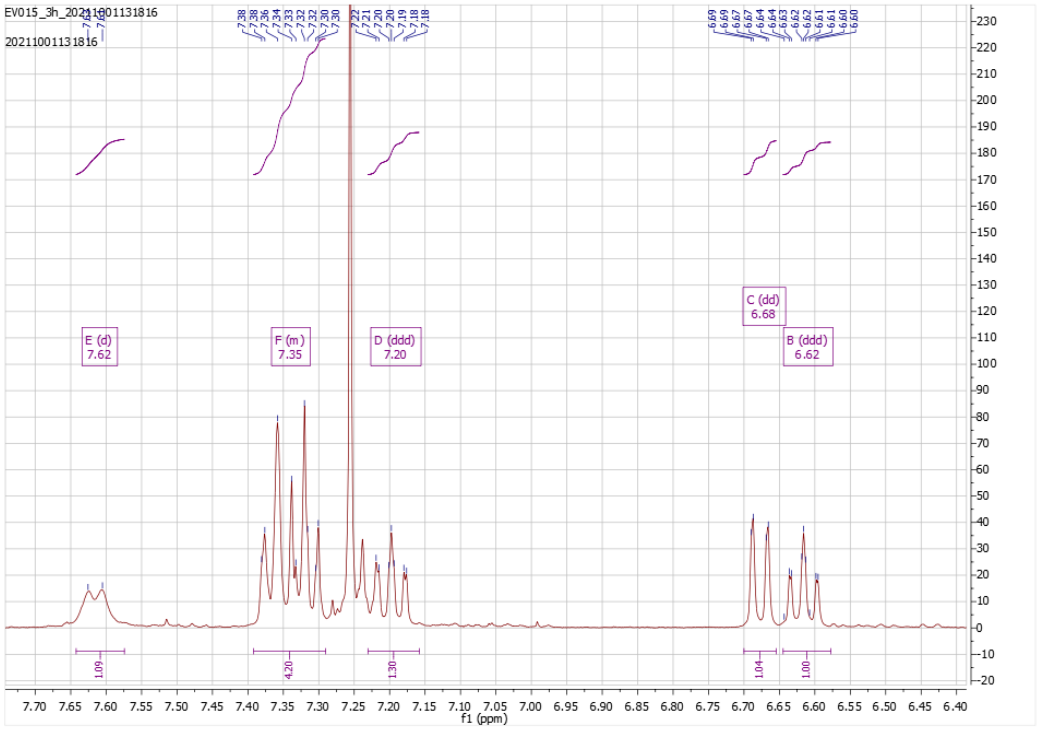

Figure 60: Expansion of the previous [1]H-NMR spectrum. Note the triplet and doublet characteristic of ring opening have moved, suggesting a different major product has formed.

6.2 Stepwise lithiations

6.2.1 Compound 9 via stepwise lithiation entry 1

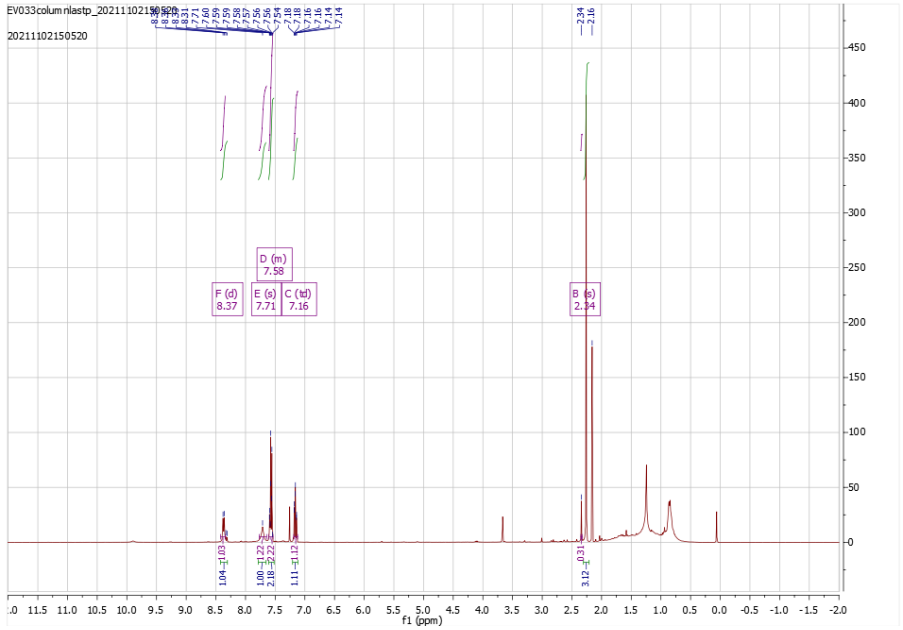

Figure 61: ^{1}H-NMR spectrum of 3-acetyl-2H-indazole in $CDCl_3$.

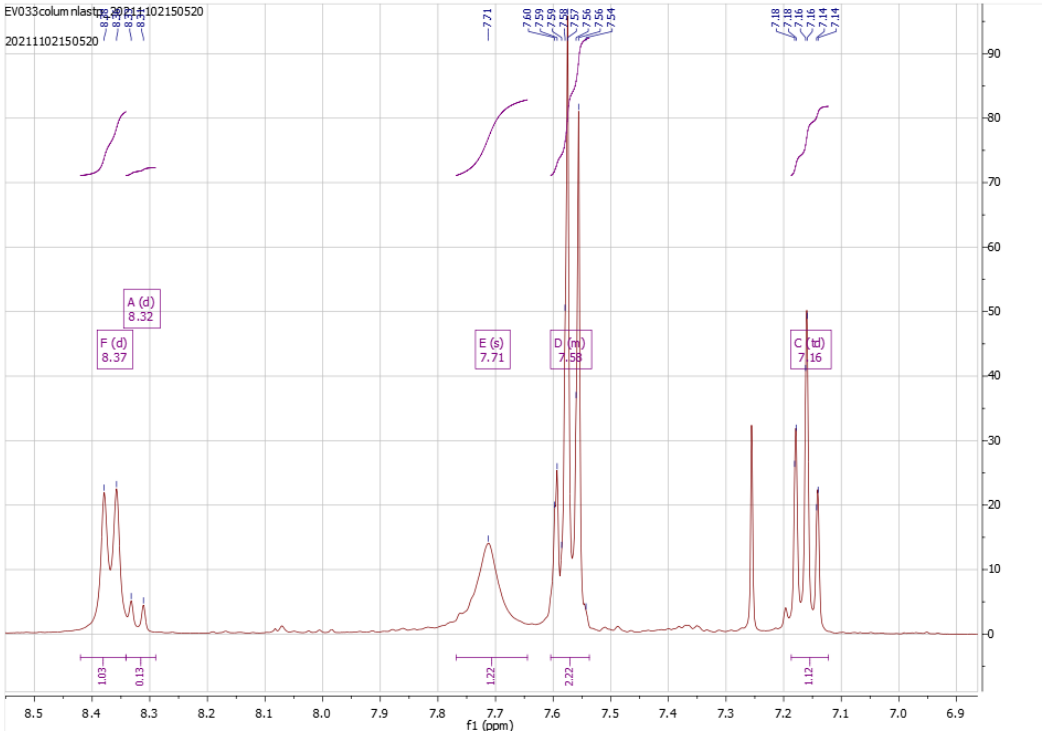

Figure 62: Expansion of previous ^{1}H-NMR. The doublet at 8.37 is not product but has been integrated to indicate there is an impurity in the sample 1:10 ratio with the desired product.

6.2.2 Compound 9 via stepwise lithiation entry 2

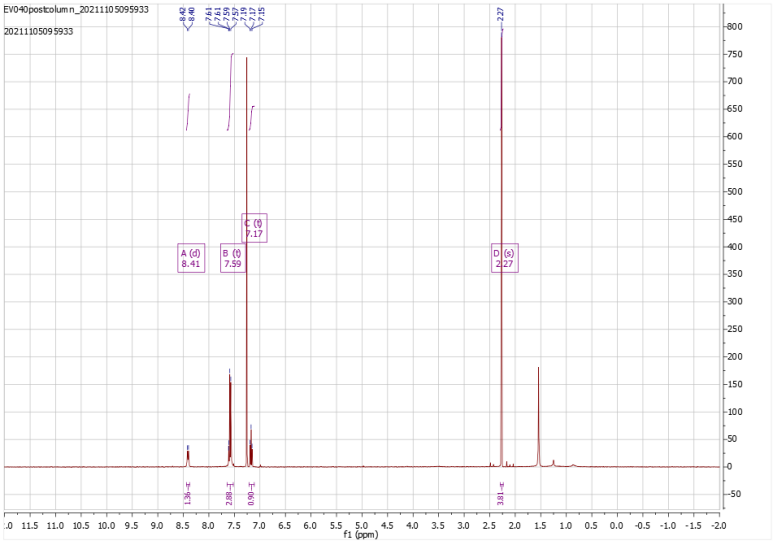

Figure 64: ^{1}H-NMR spectrum of 3-acetyl-indazole in $CDCl_3$.

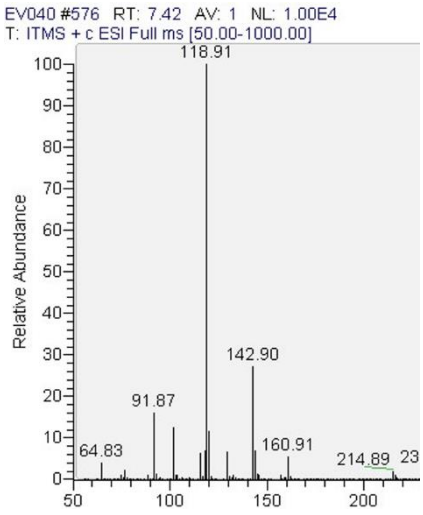

Figure 63: MS spectrum of synthesized 3-acetyl-indazole, showing the masses of 3-acetyl-indazole and indazole in a 5:100 ratio.

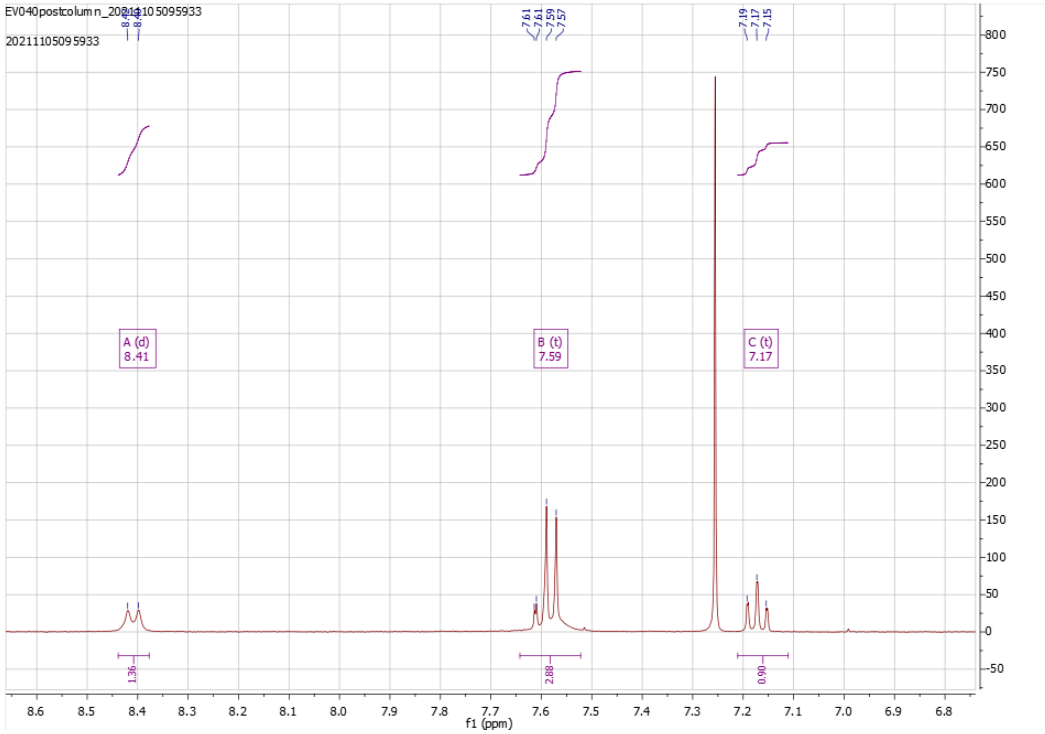

Figure 65: Expansion of the previous ^{1}H-NMR spectrum showing the aromatic region.

6.2.3 Compound 20: product of nucleophilic attack of phennyllithium on 9

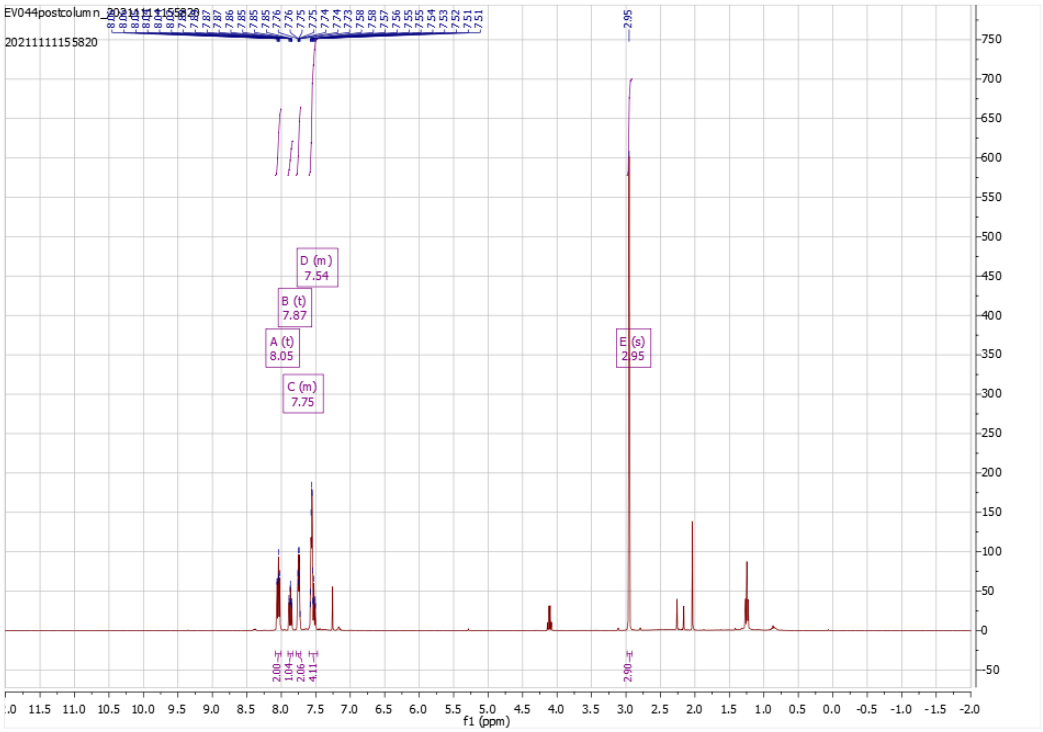

*Figure 66: ^{1}H-NMR spectrum of **20** in $CDCl_3$. Note the ratio between aromatic signals and the CH_3 singlet upfield.*

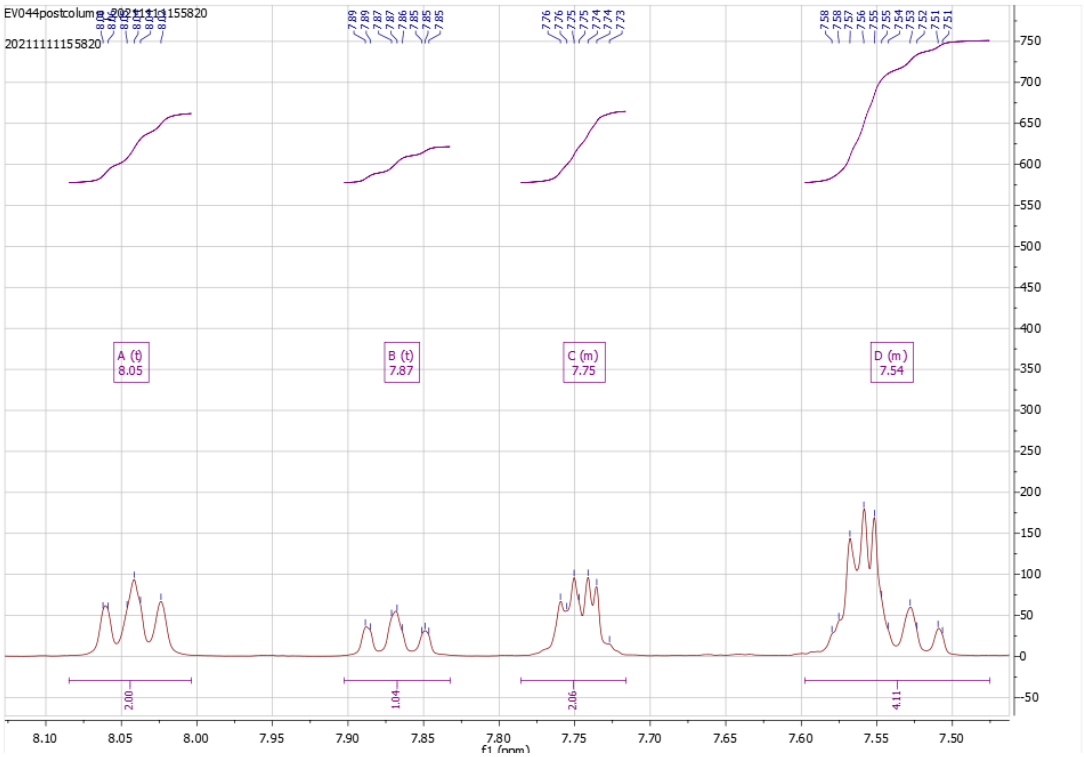

Figure 67: Expansion of the aromatic region of the previous ^{1}H-NMR spectrum. Overlap makes precise signal appointing impossible, but no impurities can be observed in this region and the integration corresponds nicely to the proposed bis(indazole).

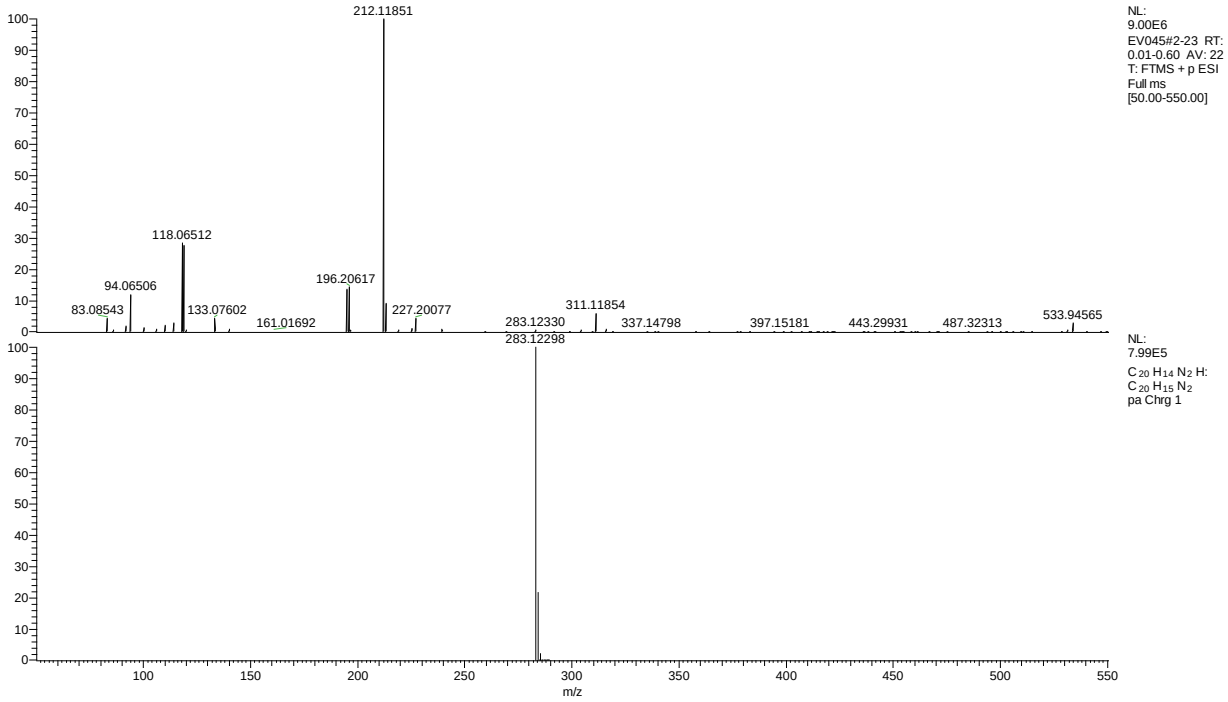

*Figure 68: Full HRMS spectrum **20**. Top: measured results. Bottom: calculated results of structure **20**.*

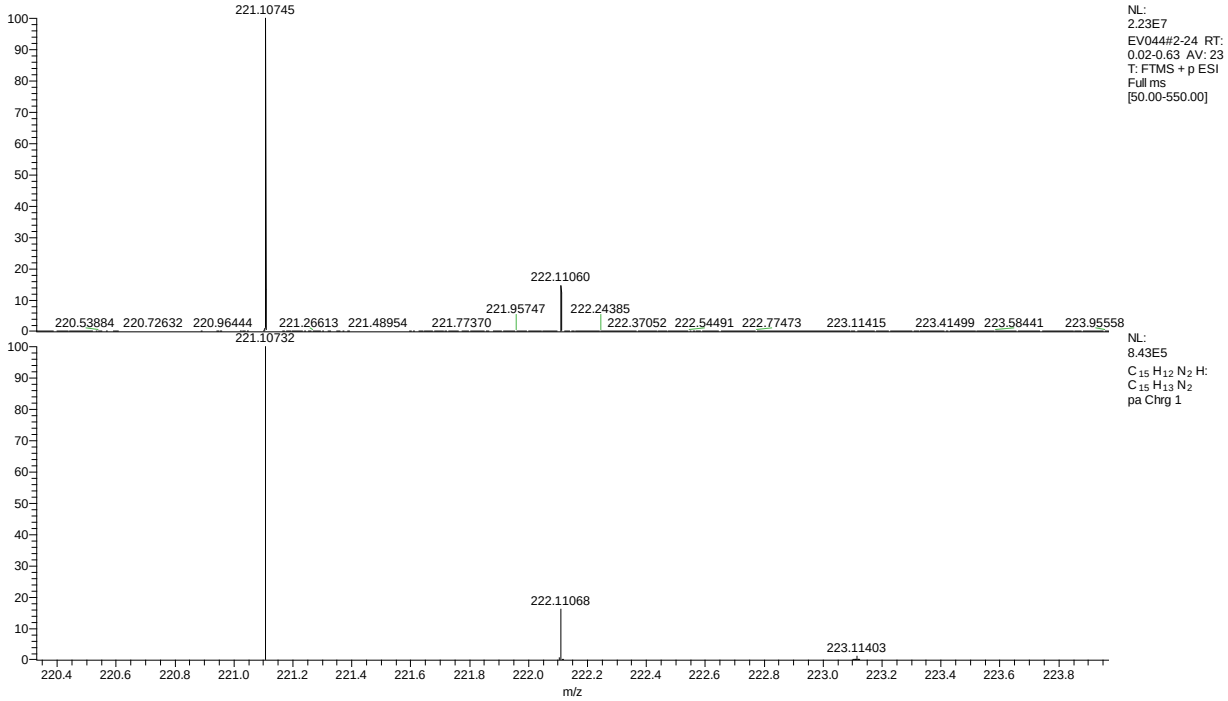

*Figure 69: Zoomed in HRMS results of **20**. Top: measured results, bottom: calculated results based on the structure of **20.***

6.2.4 Compound 22: Nucleophilic attack of lithated indazole on 9

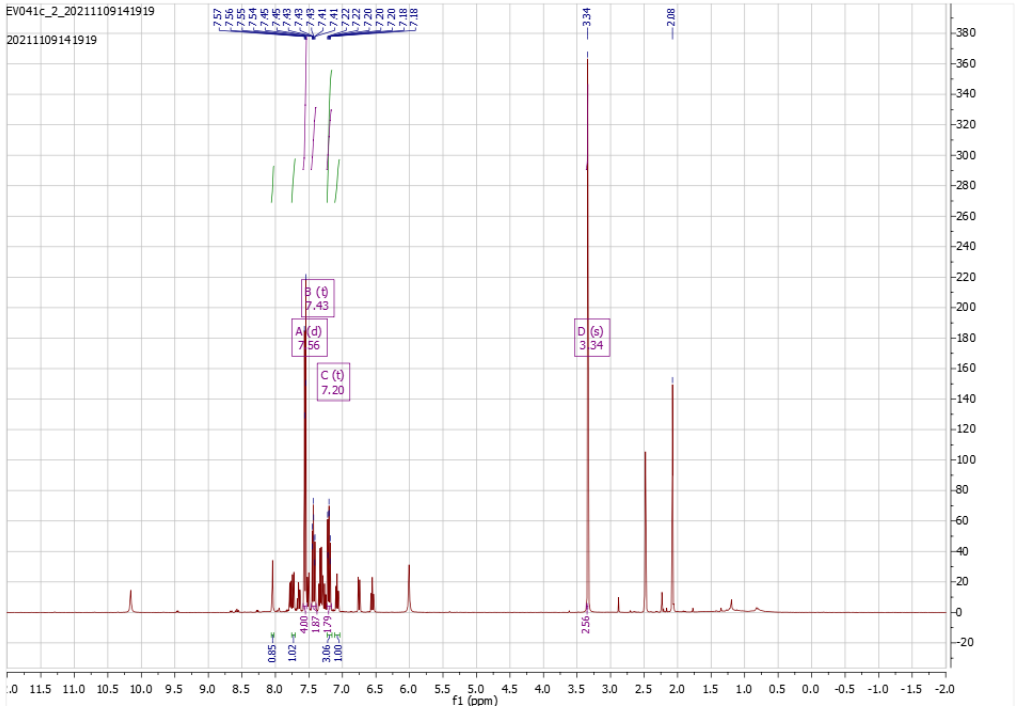

*Figure 70: [1]H-NMR spectrum of **22** in DMSO. Note the ratio between the aromatic signals and the CH_3 singlet. Also note the singlet at 2.08 ppm, likely acetic acid from the starting material, possibility a cause for a lower yield.*

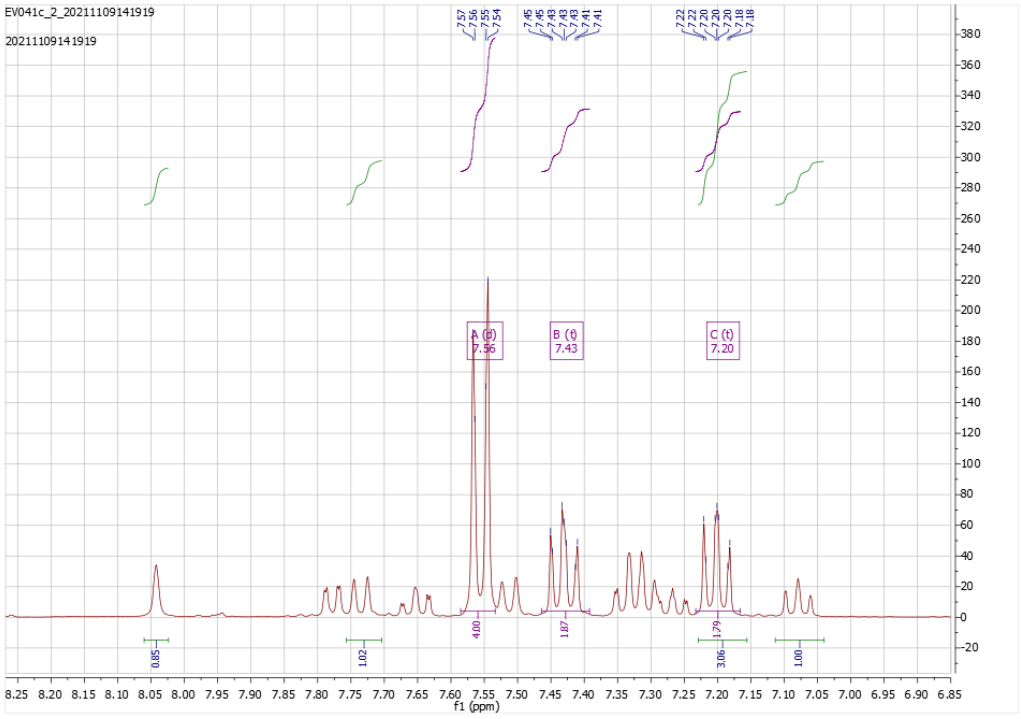

Figure 71: Expansion of the previous [1]H-NMR spectrum showing the aromatic region. Note the ratio between (t, 7.20 ppm, product) (t, 7.07 ppm and s, 8.05, indazole) and (d, 7.73, a side product).

6.3 Regioselective zincation

6.3.1 Compound 1: 1-(methoxymethyl)-indazole batch 1

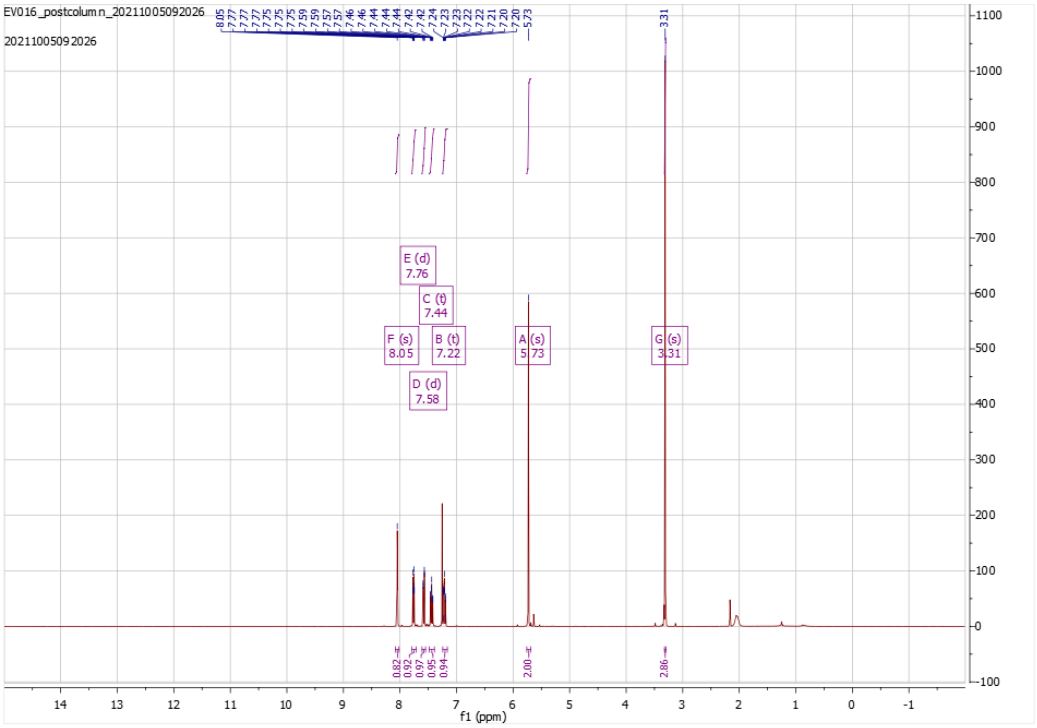

Figure 72: ^{1}H-NMR spectrum of the product of 1-MOM-indazole in $CDCl_3$, showing the MOM CH_2 CH_3 signals and the aromatic signals.

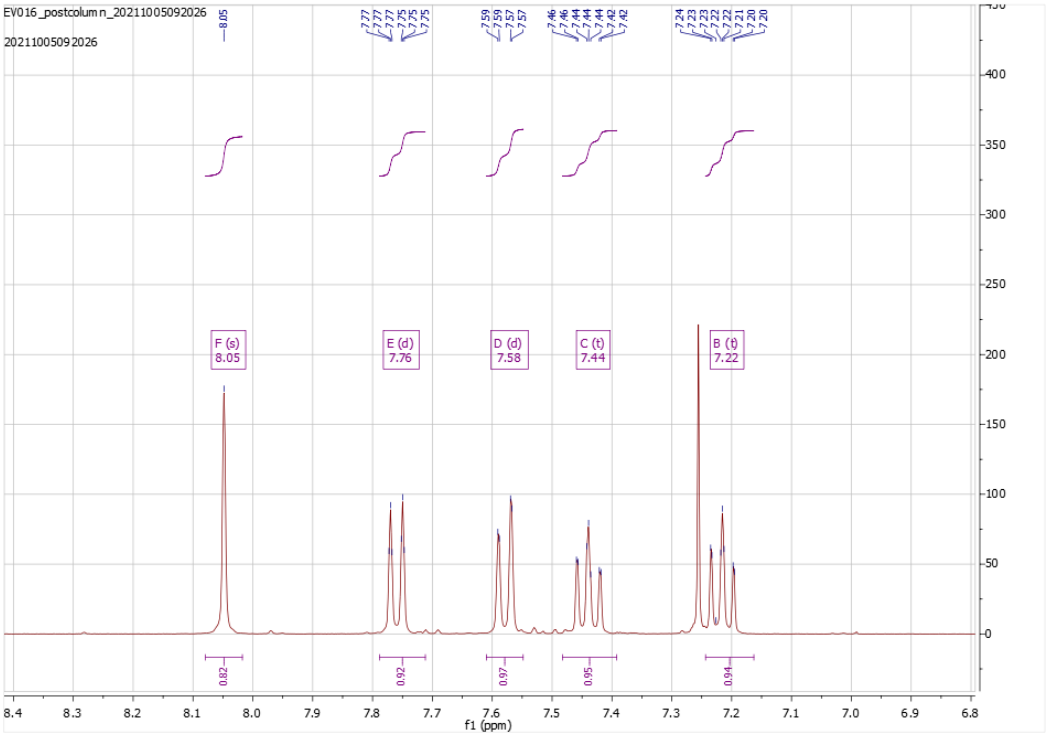

Figure 73: Expansion of the previous [1]H-NMR spectrum, clearly showing the aromatic signals of MOM-indazole, corresponding to literature.[51]

6.3.2 Deuteration study: zincation of MOM-indazole

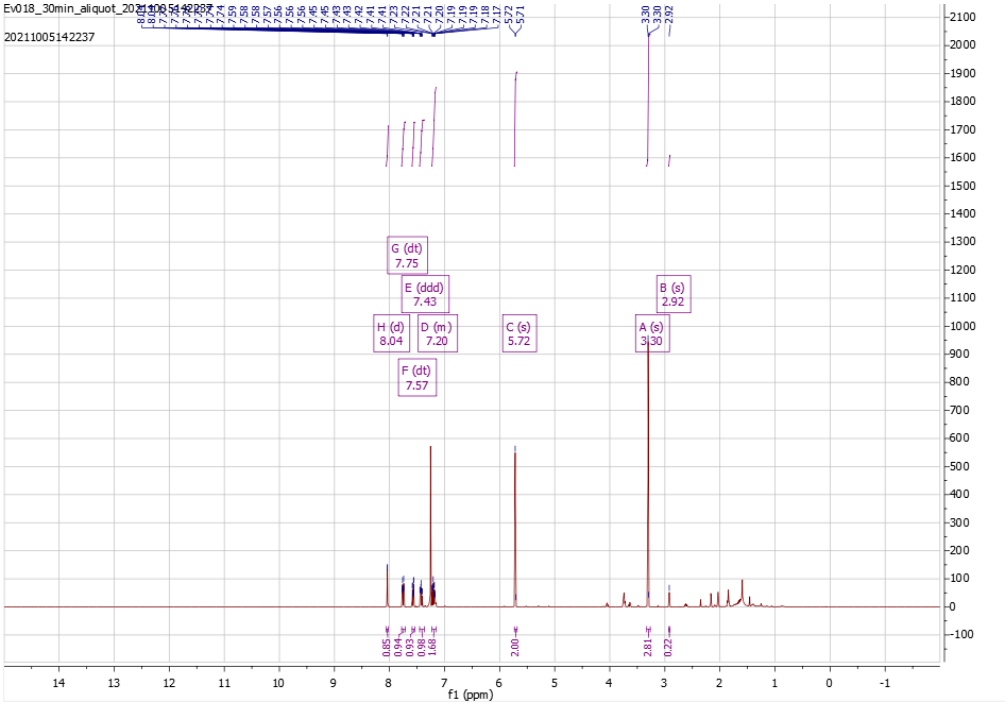

Figure 74: [1]H-NMR spectrum of deuteration MOM-indazole using TMP_2Zn in $CDCl_3$. Bar from a few impurities, it is clear is this MOM-indazole with mediocre metalation at best.

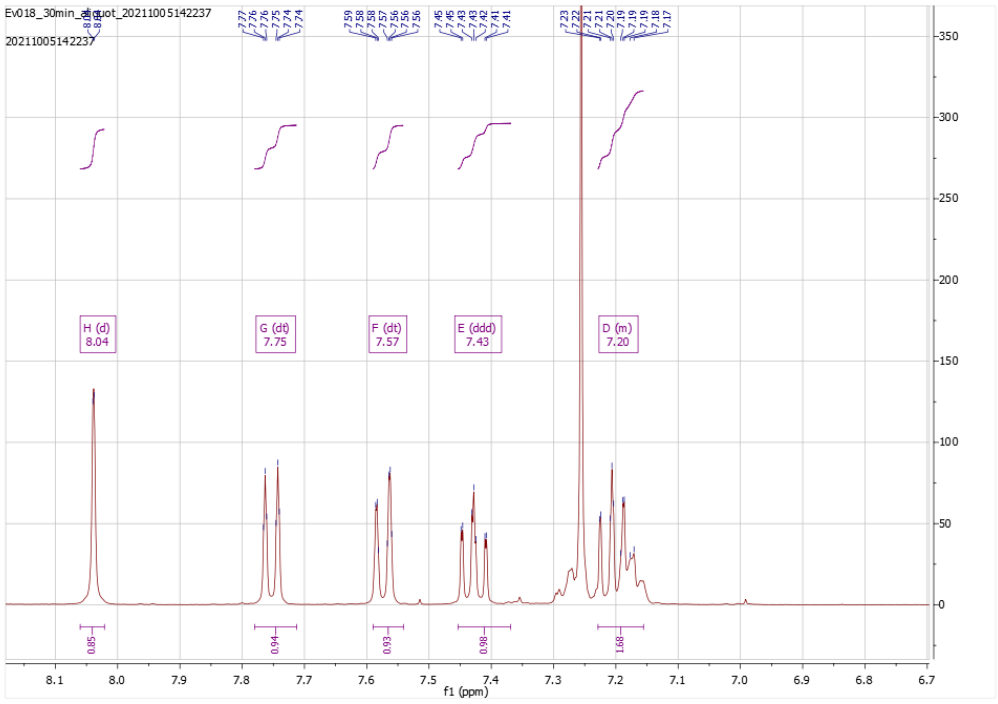

Figure 75: Expansion of the previous ^{1}H-NMR spectrum.

6.3.3 Compound 1: 1-(methoxymethyl)-indazole

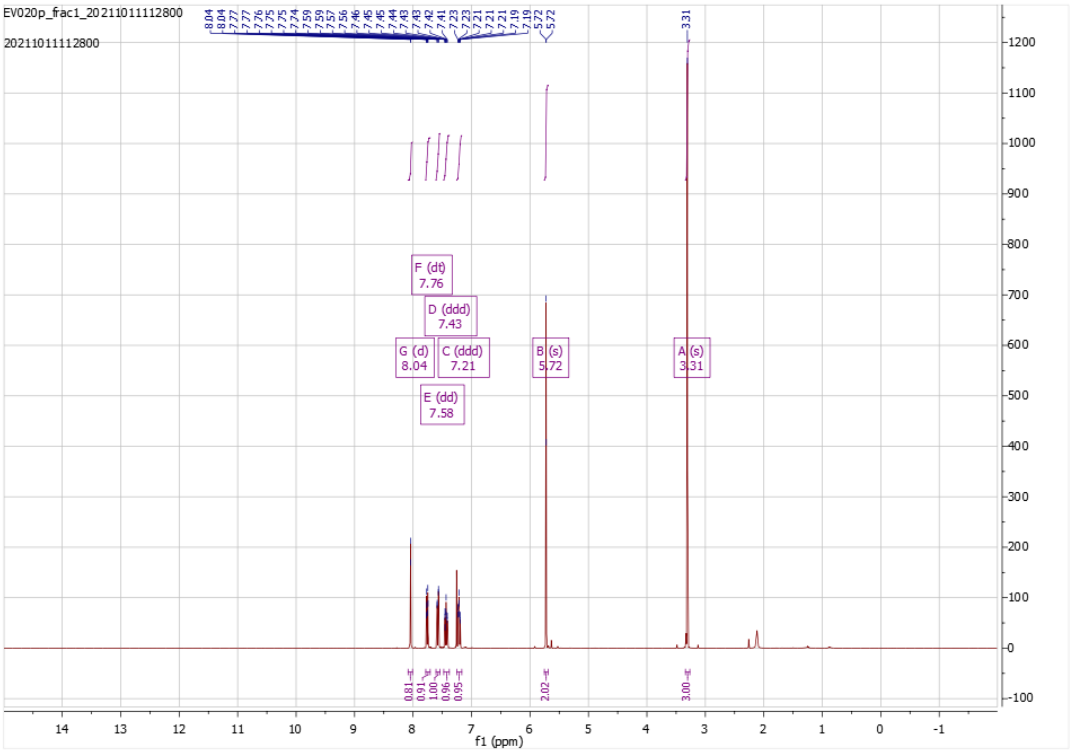

Figure 76: ^{1}H-NMR spectrum of MOM-indazole batch 2 in $CDCl_3$.

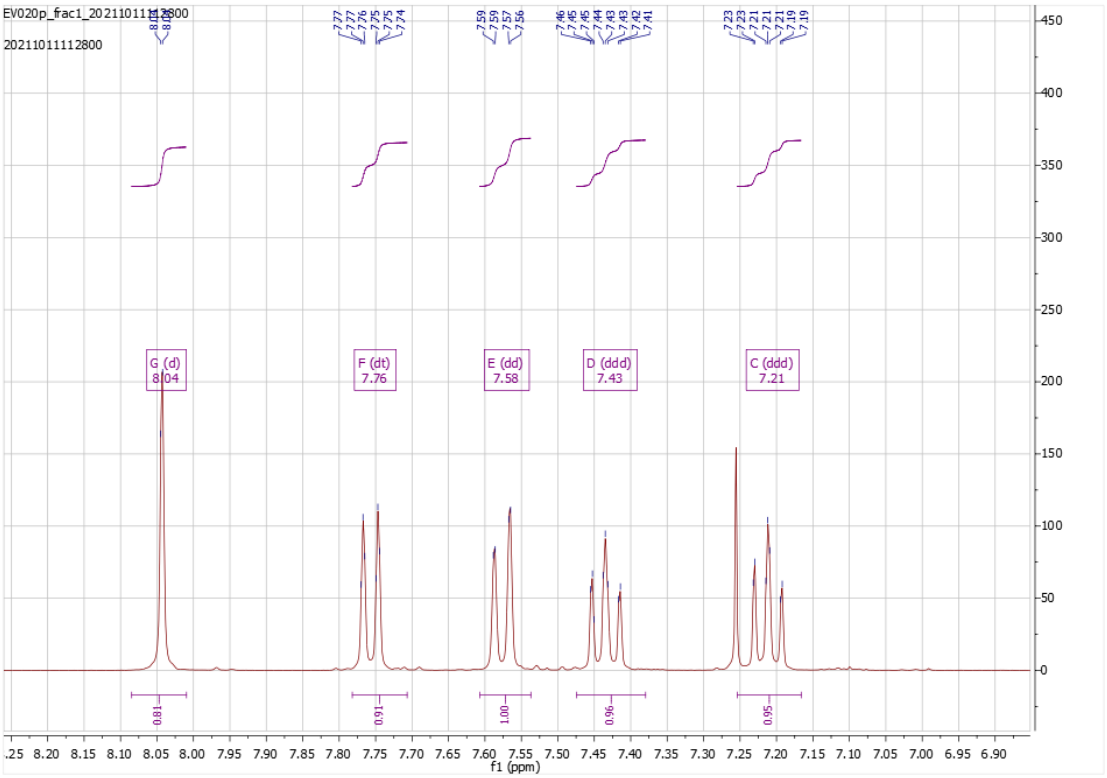

Figure 77: Expansion of the previous ^{1}H-NMR spectrum.

6.3.4 Aliquot of attempted synthesis of 2: Attempted zincation and electrophile trapping of MOM-indazole entry 1

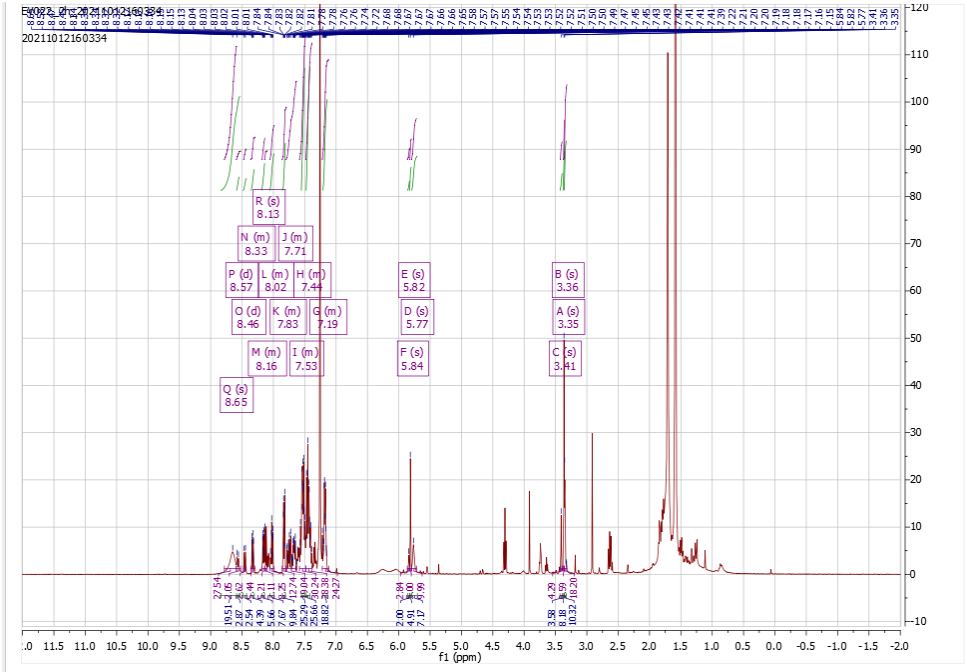

Figure 78: ^{1}H-NMR spectrum of an aliquot of the attempted zincation and electrophile trapping of MOM-indazole entry 1 in $CDCl_3$.

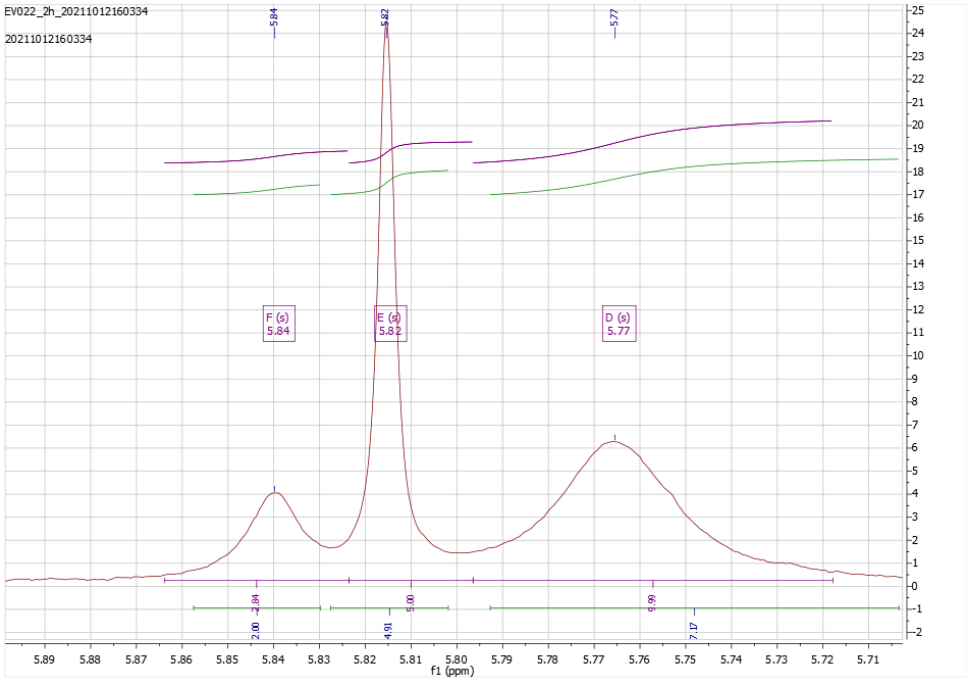

Figure 79: Expansion of previous ^{1}H-NMR spectrum highlighting the 3 different CH_2 MOM signals.

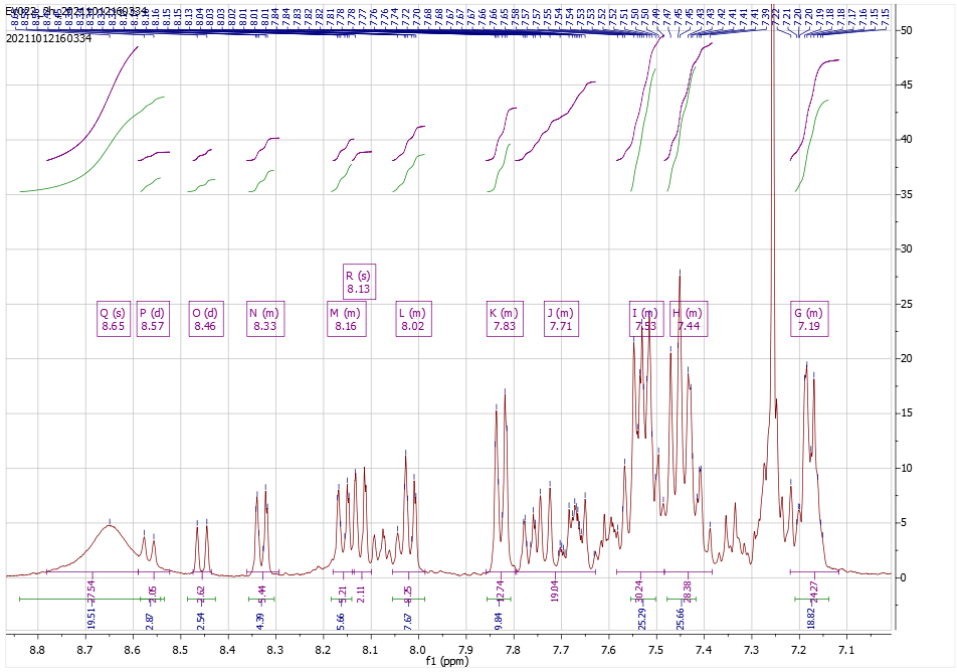

Figure 80: Expansion of ^{1}H-NMR spectrum of the previous spectrum showing the complex aromatic region.

6.3.5 Aliquot of attempted synthesis of 2: Attempted zincation and electrophile trapping of MOM-indazole entry 2

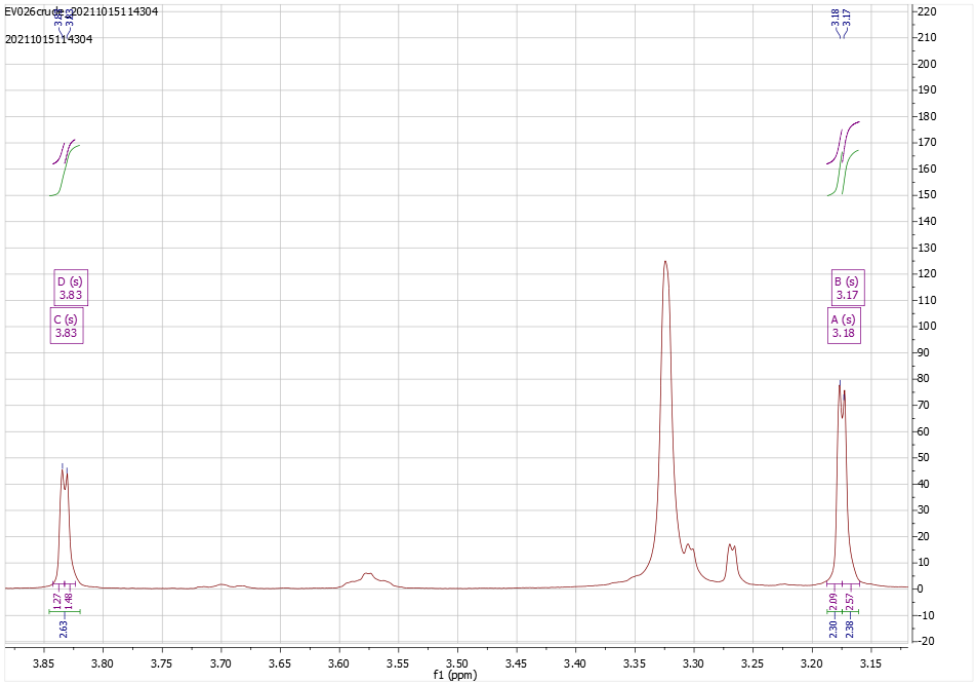

Figure 81: Expansion of the ^{1}H-NMR spectrum of the product of the attempted zincation and electrophile trapping of MOM-indazole entry 2 highlighting the overlapping singlets upfield, suggesting 2 products in 1:1 ratio.

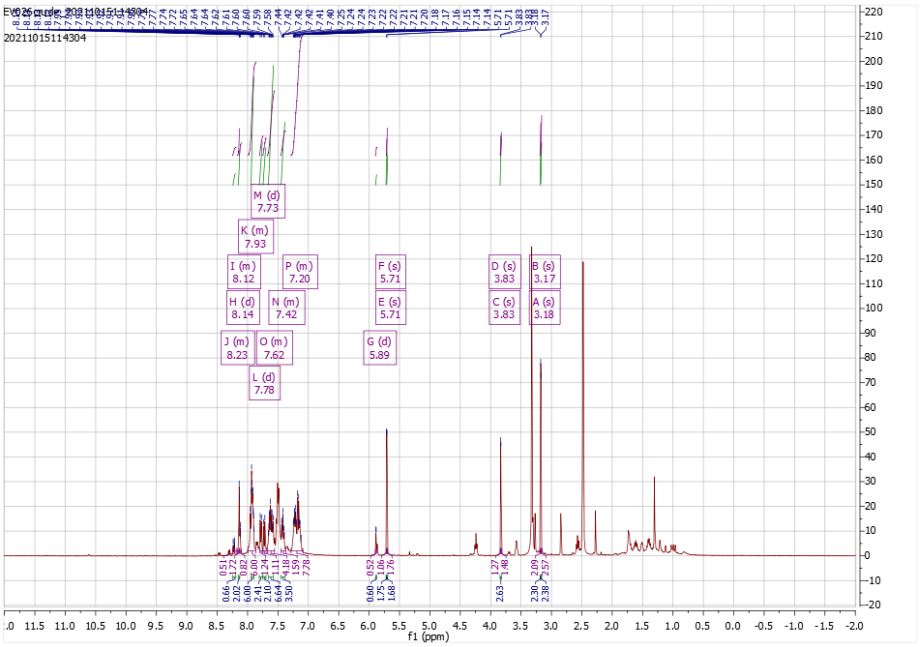

Figure 82: Full ^{1}H-NMR spectrum and aliquot of the attempted zincation and electrophile trapping of MOM-indazole entry 2 in DMSO.

6.3.6 Isolated unknown product from attempted synthesis of 2: Attempted zincation and electrophile trapping of MOM-indazole entry 2

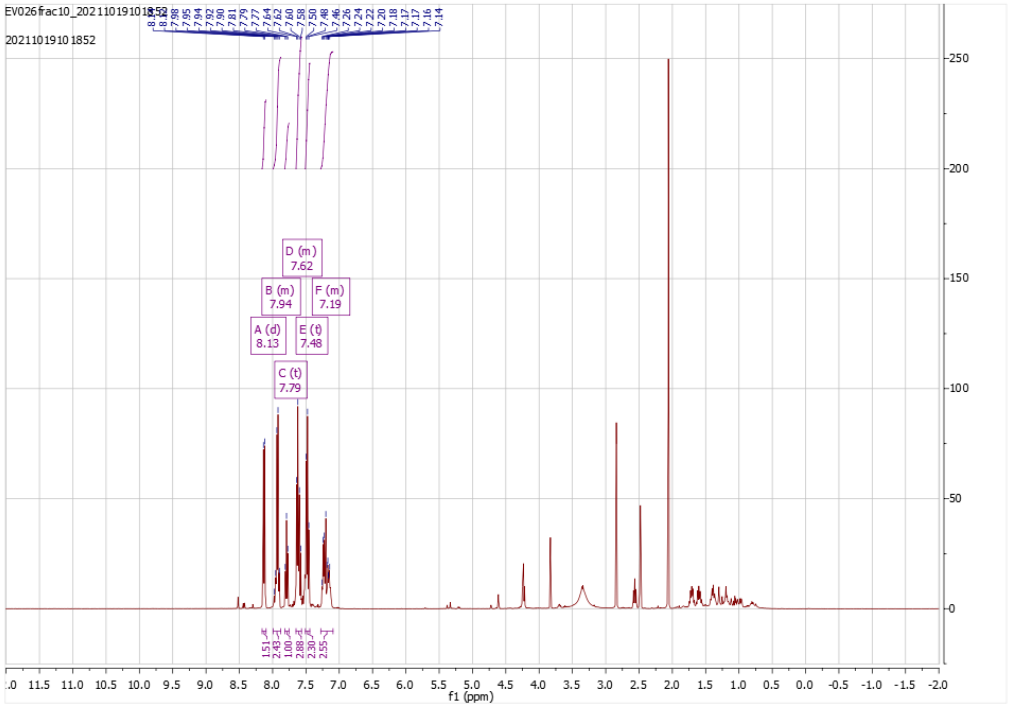

Figure 83: ^{1}H-NMR spectrum of the isolated product in DMSO, with some impurities upfield, but clearly no CH_2 MOM signal and thereofore it is unlikely any of the upfield singlets correspond to the MOM CH_3.

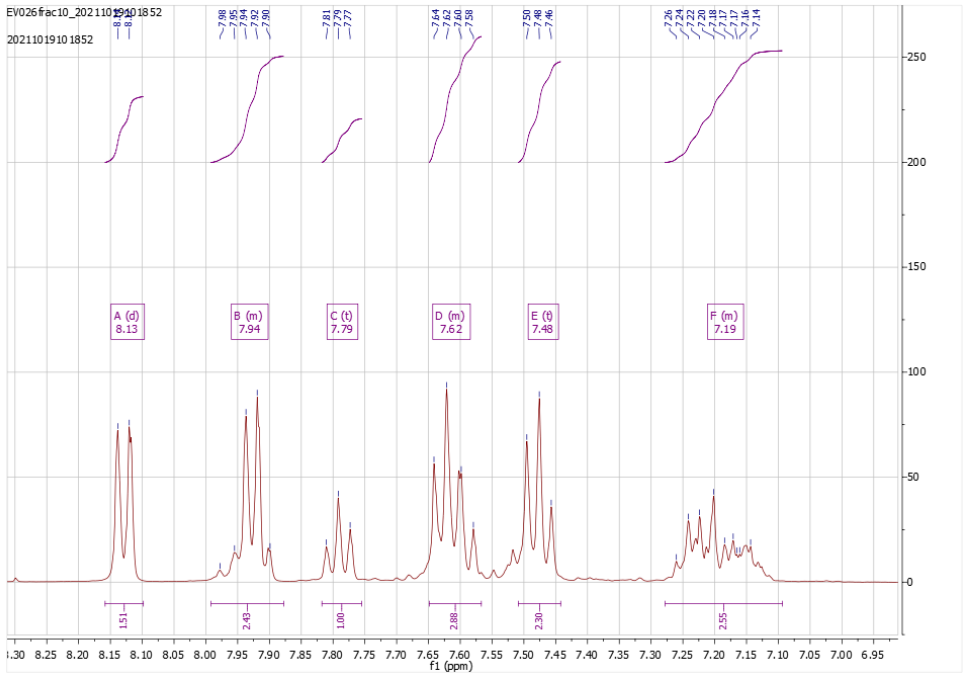

Figure 84: Expansion of the aromatic region of the previous ^{1}H-NMR spectrum, containing all signals thought correspond to the the unknown product.

6.3.7 Aliquot of attempted synthesis of 2: Attempted zincation and electrophile trapping of MOM-indazole entry 3

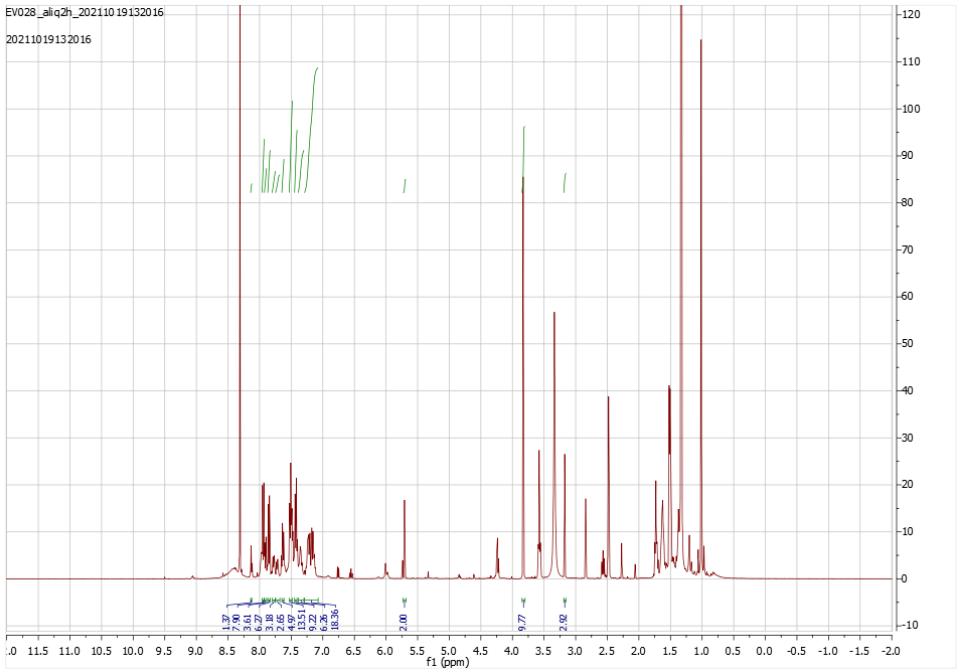

Figure 85: ^{1}H-NMR spectrum of an aliquot of the attempted zincation and electrophile trapping of MOM-indazole entry 3 reaction mixture in DMSO. There are many impurities including THF, water and EtOAc upfield and $CHCl_3$ downfield.

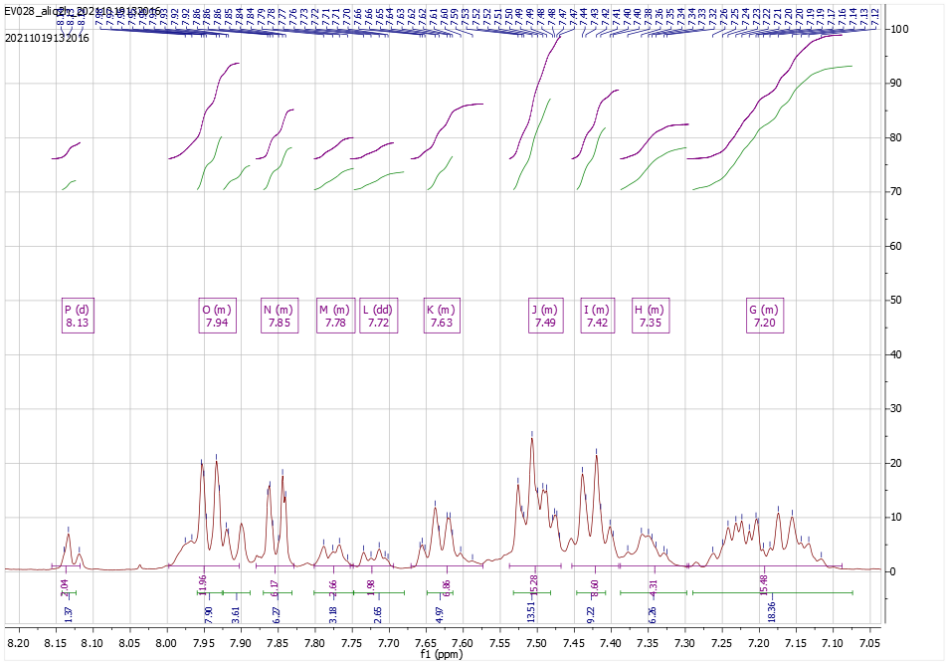

Figure 86: Expansion of the aromatic region of the previous ^{1}H-NMR spectrum.

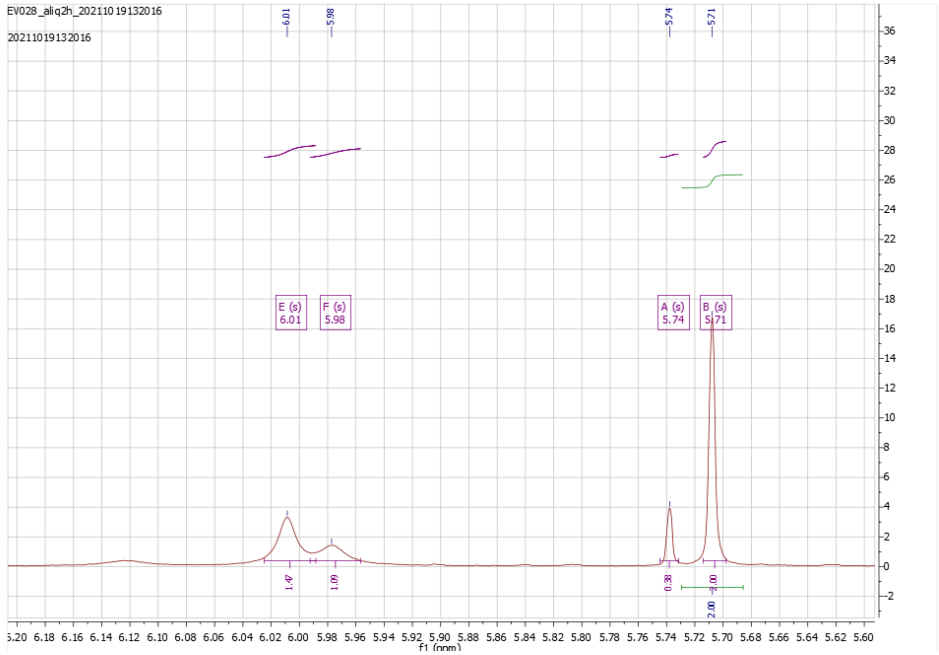

Figure 87: Expansion of the previous ^{1}H-NMR showing the singlets around the region where the MOM CH_2 singlet is expected.

6.3.8 Aliquot of attempted synthesis of 2: Attempted zincation and electrophile trapping of MOM-indazole entry 4

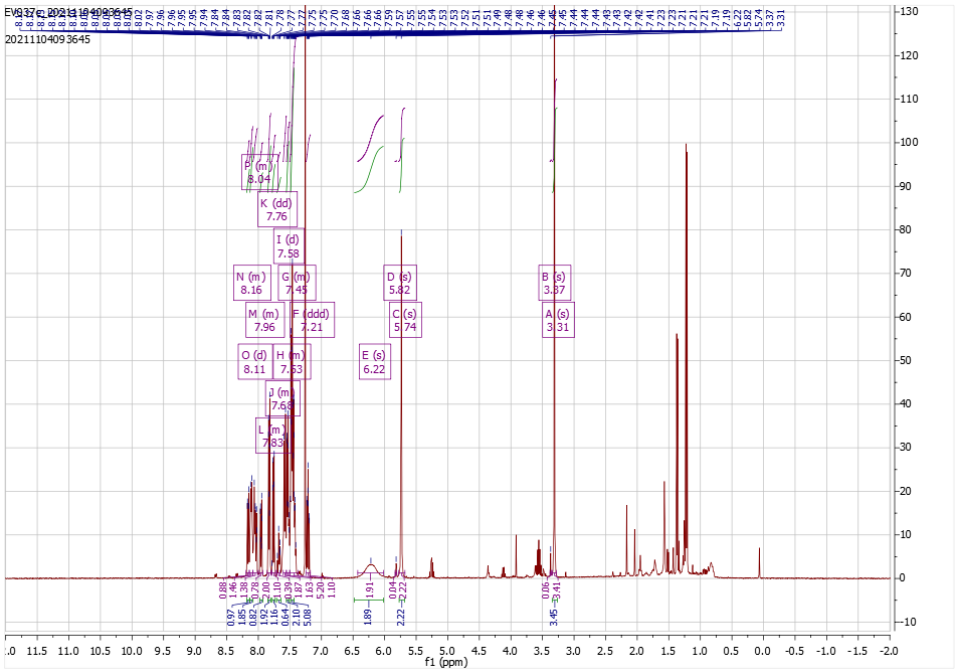

Figure 88: ^{1}H-NMR spectrum of an aliquot of the reaction mixture of attempted zincation and electrophile trapping of MOM-indazole entry 4 in $CDCl_3$.

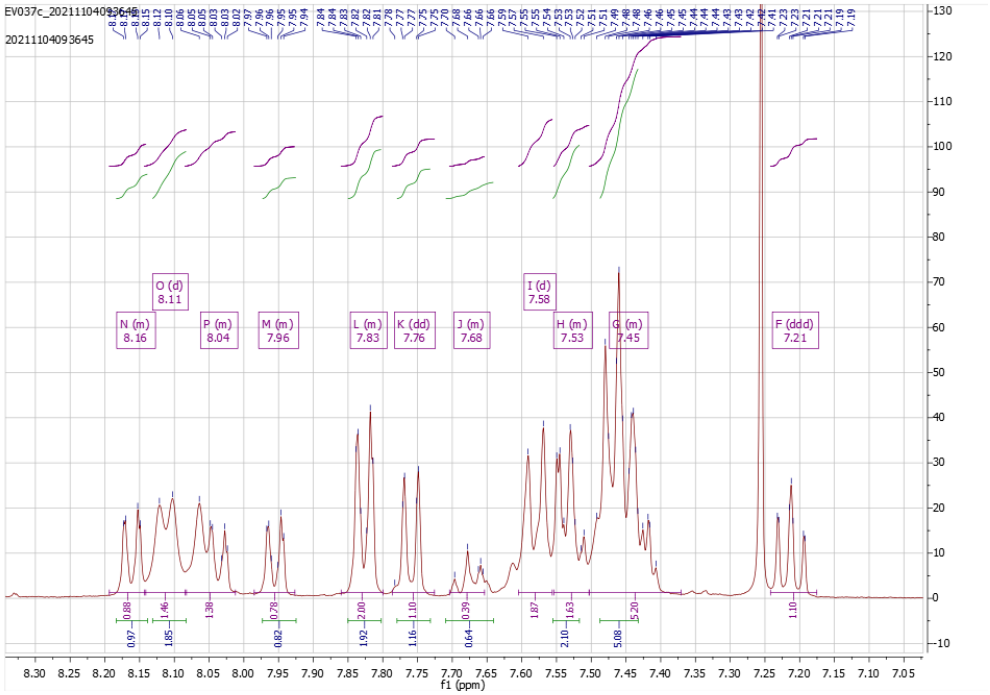

Figure 89: Expansion of the previous [1]H-NMR spectrum. Note the triplet at 7.22 ppm, characteristic of the starting material, integrating perfectly with the major MOM CH_2 and CH_3 signals.

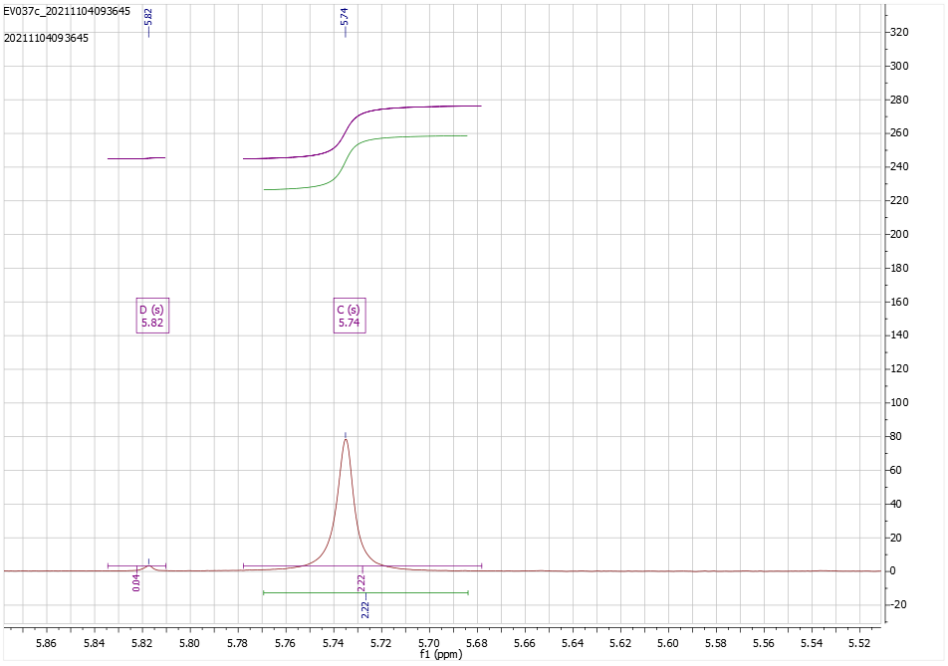

Figure 90: Expansion of the [1]H-NMR spectrum of 6 highlighting the ratio between CH_2 MOM signals.

6.4 N2 SEM protection for Directed *ortho*-Metalation

6.4.1 Compound 23: *N2*-SEM-indazole

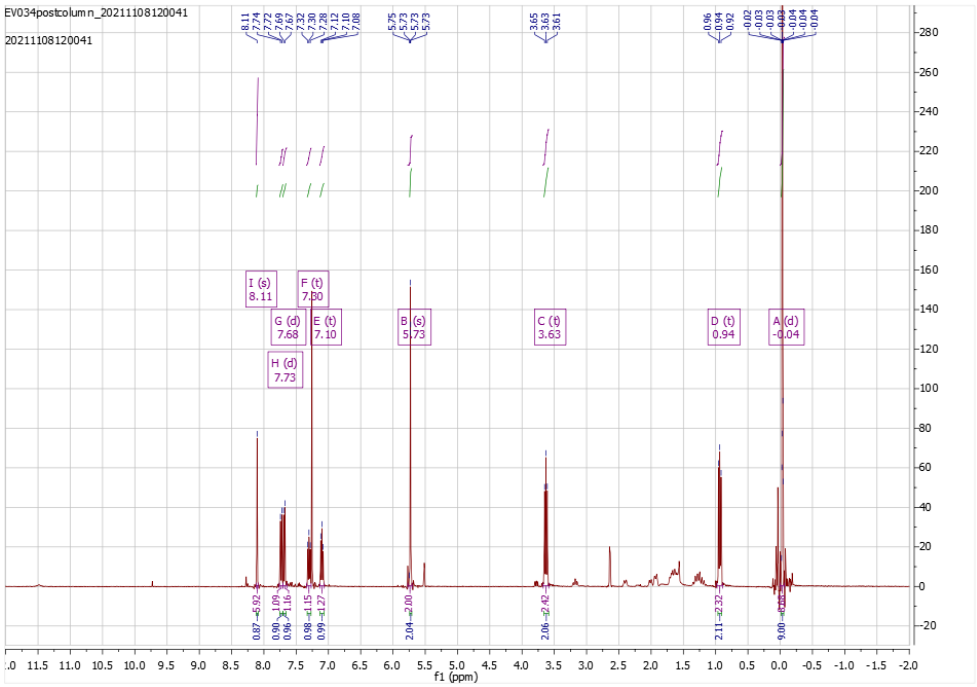

Figure 91: ^{1}H-NMR spectrum of N2-SEM-indazole in $CDCl_3$. Note the SEM $(CH_3)_3$ singlet, 2 CH_2 triplets and CH_2 singlet and the indazoles two doublets, two triplets and one singlet, all in perfect integration ratios. (Multiplet analysis integration (purple) is showing software issues, green integration is correct.)

6.4.2 Crude 24: lithiation and BzCl electrophile trapping of *N2*-SEM-indazole

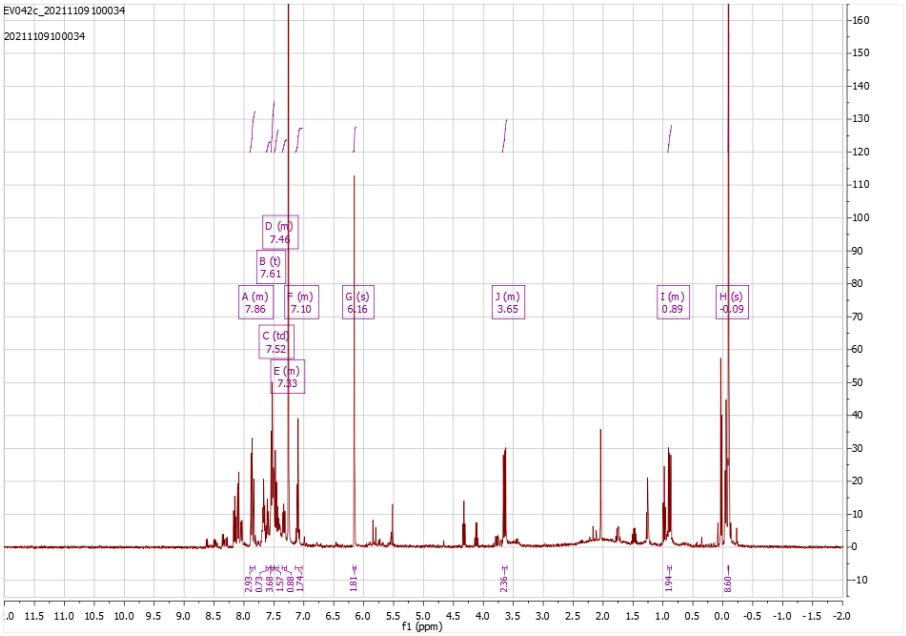

*Figure 92: ^{1}H-NMR spectrum crude **24** in $CDCl_3$. The regions that are analysed are based on what was reported in literature. The integrations are higher than reported in the aromatic region due to significant signal overlap with side product signals.*

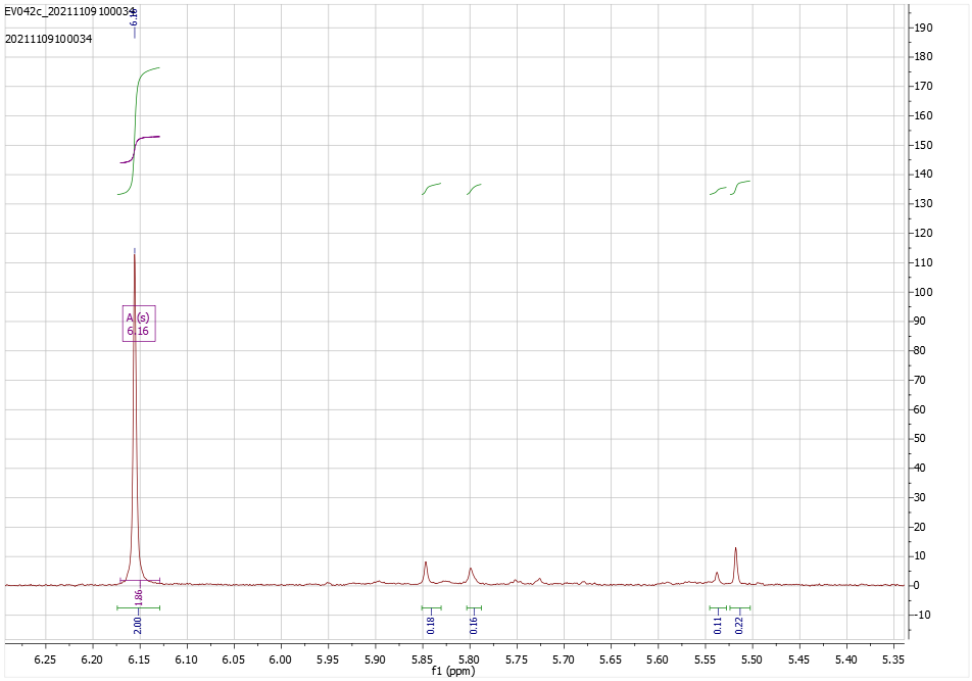

Figure 93: Expansion of previous ^{1}H-NMR spectrum highlighting the ratio between CH_2 MOM signals and therefore major product : minor products.

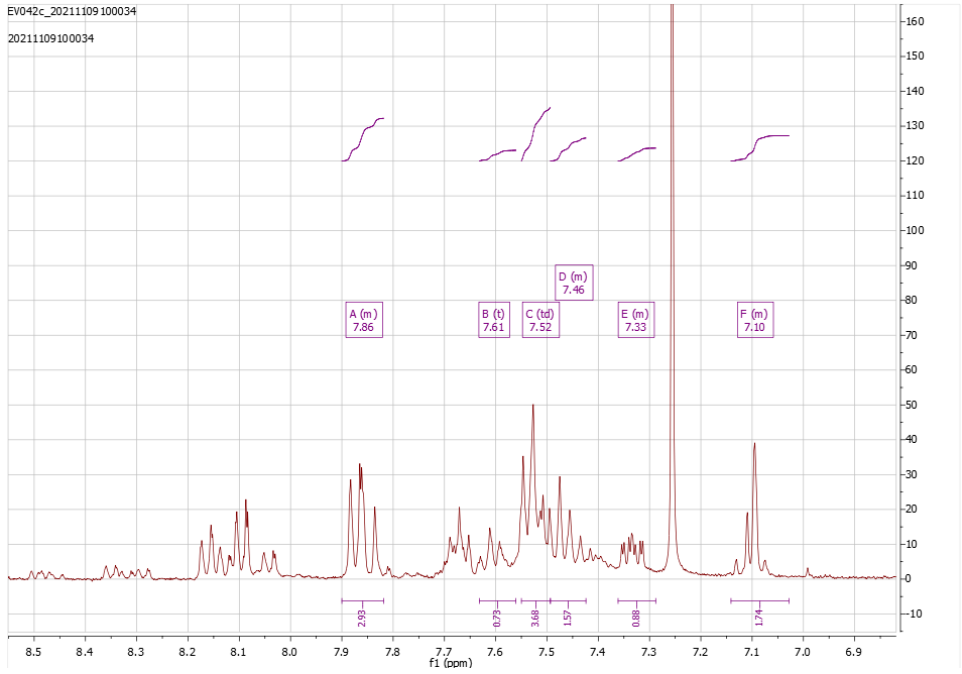

*Figure 94: Expansion of ^{1}H-NMR spectrum of crude **24** showing the aromatic region in $CDCl_3$.*

6.4.3 Product of attempted one-pot synthesis of BODIzy dye 2 from *N*2-SEM-indazole

*Figure 95: [1]H-NMR spectrum of the crude product the attempted one-pot synthesis of **BODIzy dye 2** from N2-SEM-indazole in $CDCl_3$.*

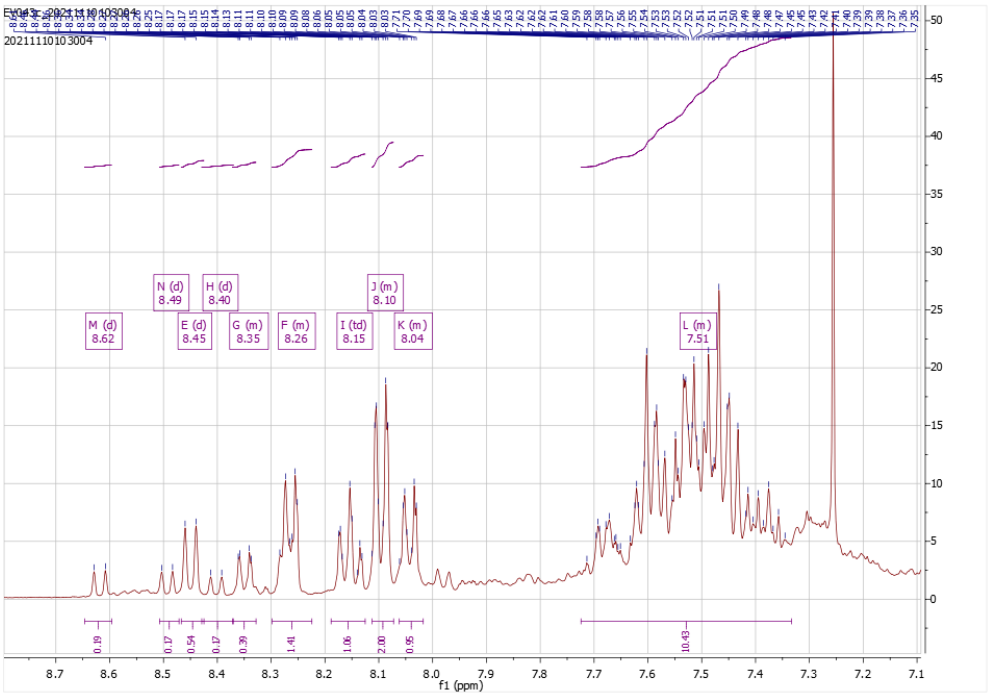

Figure 96: Expansion of the aromatic region of the previous [1]H-NMR spectrum.

6.4.4 Crude product of attempted synthesis of 25: Nucleophilic attack of phenyllithium on *N*2-SEM-3-benzoyl-indazole

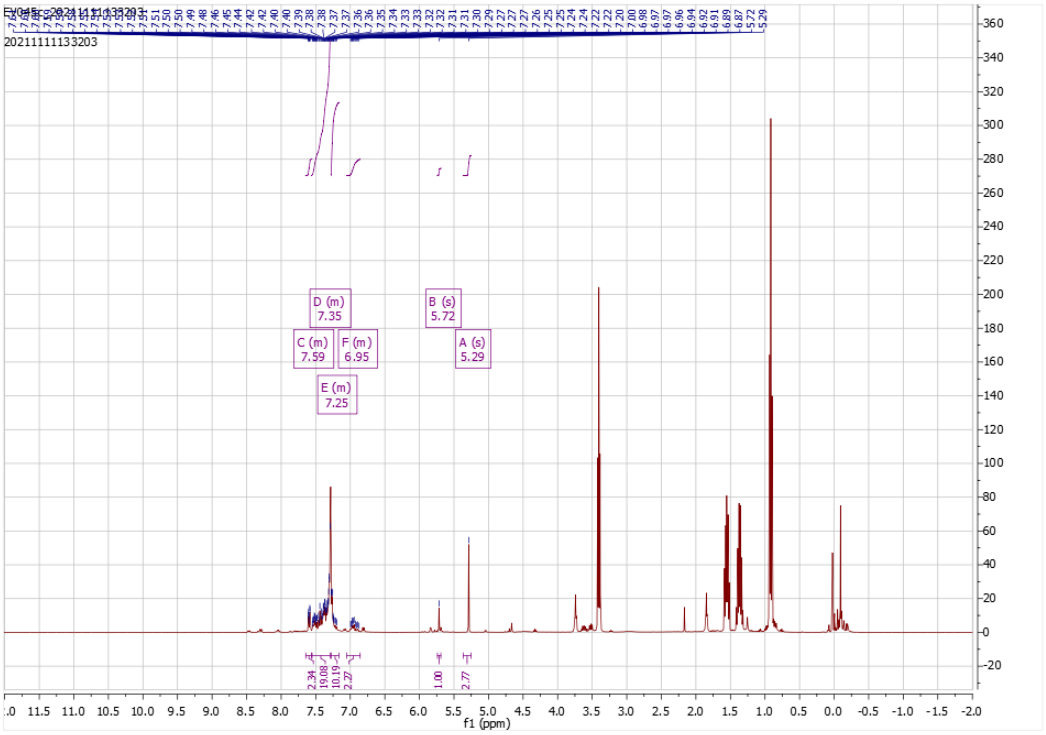

*Figure 97: ^{1}H-NMR spectrum of the crude product of the attempted synthesis of **25** in $CDCl_3$. Note the presence of dibutyl ether between 3.5-0.8 ppm.*

6.4.5 Product of attempted synthesis of 25: Nucleophilic attack of phenyllithium on *N*2-SEM-3-benzoyl-indazole

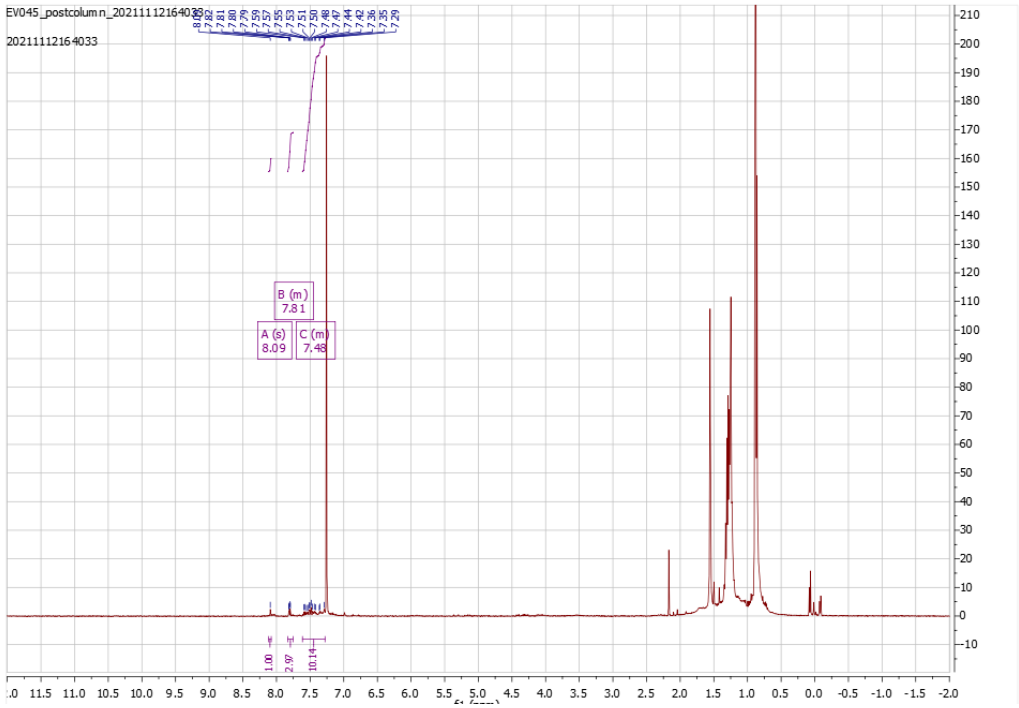

*Figure 98: ^{1}H-NMR spectrum of the product of the attempted synthesis of **25** in $CDCl_3$ after purification. The concentration is too low to extract much information.*

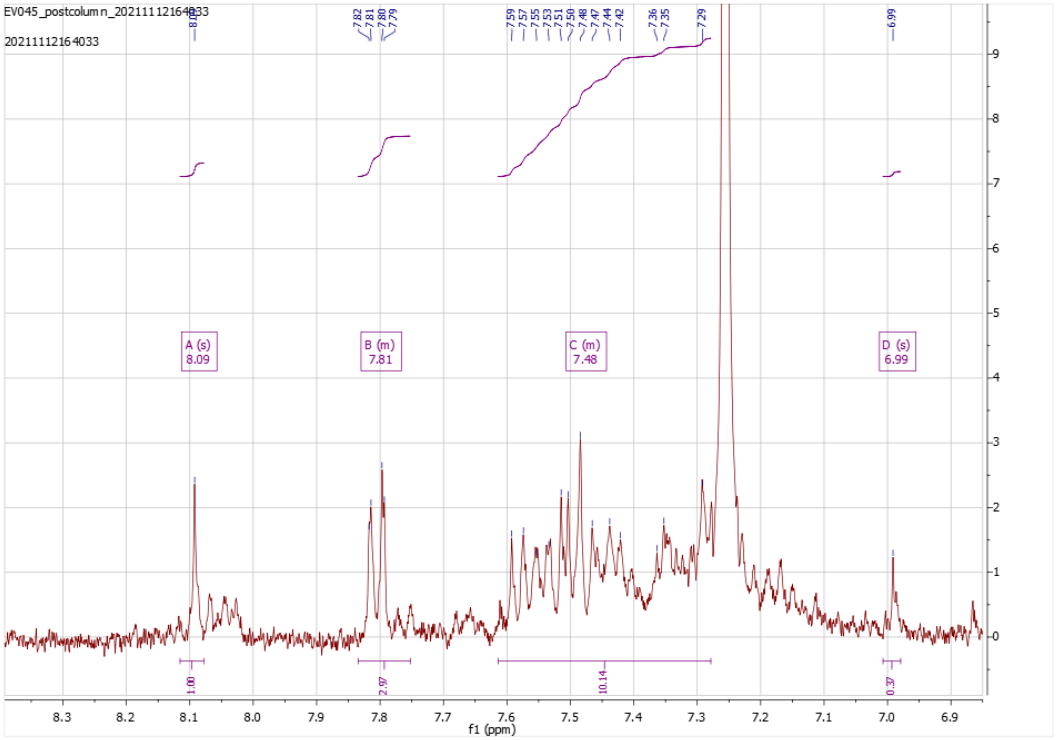

Figure 99: Expansion of the previous ^{1}H-NMR spectrum.